# Design of Multi-story hotel in Carlsbad, California, USA

**Capstone project II**

**Bachelor of Science**
**Civil and Environmental Engineering**


**Alikhan Serikbekov**
**Zhaksylyk Olzhabekov**
**Darkhan Serikbay**
**Aruzhan Sibekova**
**Aidos Bolat**
**Damir Kiyashov**
**Diara Gazezova**

**2023**

**DECLARATION**

We hereby declare that this report entitled "*Design of Multi-story hotel in Carlsbad, California, USA"* is the result of our own project work except for quotations and citations which have been duly acknowledged. We also declare that it has not been previously or concurrently submitted for any other degree at Nazarbayev University.

Alikhan Serikbekov

Zhaksylyk Olzhabekov

Darkhan Serikbay

Aruzhan Sibekova

Aidos Bolat

Damir Kiyashov

Diara Gazezova

## ABSTRACT

This Capstone project's goal is to create a seven-story hotel in Carlsbad, California, that complies with building, safety, and sustainability standards while taking into account the area's moderate seismic activity. There is a demand for an excellent hotel that will start making money soon because the chosen area has good tourism potential but is undersupplied with hotels. This report also includes a sustainable greywater treatment system in addition to preliminary structural, geotechnical, and architectural designs.

The structure will have a rectangle building space of 40.7x20.5 m2 and 80 rooms, and it will be built on Carlsbad's west side close to the Pacific Ocean. The structure's architectural design was completed, and subsequently, technical drawings were given. To gather the data for each component and provide the theoretical foundation, secondary data analysis was used. Overall, the report details the need for a parking zone, a 3D view, an elevation view, a parking zone, and any relevant technical drawings in compliance with ASCE 7-10 and IBC standards.

Given that Carlsbad is in a seismic zone, reinforced concrete was used for structural members. The structural segment finished estimating member size, choosing materials and structural types, and computing live and dead loads. The soil investigation and liquefaction potential of the soil were evaluated in the geotechnical section, and it was determined that the soil is not liquefiable. It was decided to use precast concrete pile foundations with square cross sections. Given the rising demand for water, it was decided to implement the Greywater Treatment System (GTS) in the environmental section of the water supply analysis.

Overall, all project sections, as well as the initial design, calculations, and drawings, have made great progress.

**List of Tables**

**List of Figures**

# 1. INTRODUCTION

## 1.1 Project Overview

The project's primary goal is to construct a multi-story hotel in Carlsbad, California, in the United States. Setting the requirements, techniques, and potential results are all included in the project scope. Three disciplines are arranged according to their distinct scopes and requirements. The architectural component includes site investigation, architectural design, and 3D modeling of the future building with interior and exterior architectural drawings. The scope of structural parts includes initial structural analysis and design. Foundation design and soil analysis are examples of geotechnical components. The environmental section was implemented to create an effective environmental system.

## 1.2 Project challenges

The project's main difficulties are related to thick layers of sand and clay soil, moderate risk seismic activity, and precipitation-heavy weather. To ensure the safety and durability of the project, the proper foundation type must be chosen for the available soil types. Additionally, using the right materials and architectural elements should guarantee that the structure will withstand earthquakes.

## 1.3 Methodology

A thorough literature study, designs and calculations for the architectural, structural, geotechnical, environmental, and construction management aspects are among the major deliverables of this project. The newly built structure is anticipated to last at least 50 years and be structurally sound. Architectural and structural components were designed in accordance with specialized building norms and regulations. The design team's goals include conducting a site investigation, developing a geotechnical and structural design that takes into account the site's seismic characteristics, developing an architectural design that complements the city's landscape, designing a workable greywater harvesting system, and creating all necessary construction management plans and documents.

# 2. ARCHITECTURAL DESIGN

## 2.1 Design codes

The multi-story hotel was designed in accordance with American Concrete Institute, American Society of Civil Engineers, and International Building Code. The codes that were used are as follows: ACI 318-9, ACI 318-14, ASCE 7-10, IBC-2009.

## 2.2 Site selection and site analysis

Carlsbad is a city located along the coast of California, United States. Since Carlsbad is becoming a popular tourist destination and has a high tourism potential in the future, a seven-story hotel is to be constructed in this area. Total area that is to be occupied with hotel facilities is 13 000 $m^2$.

Carlsbad averages about 263 sunny days per year, a rainfall period usually lasting from October to April. Summer is almost rainless in the region. Carlsbad mostly has high temperatures and is not exposed to heavy snow and strong winds. Earthquakes happen near Carlsbad with a magnitude of 2.9. Figure 2-1 demonstrates the site layout of the building.

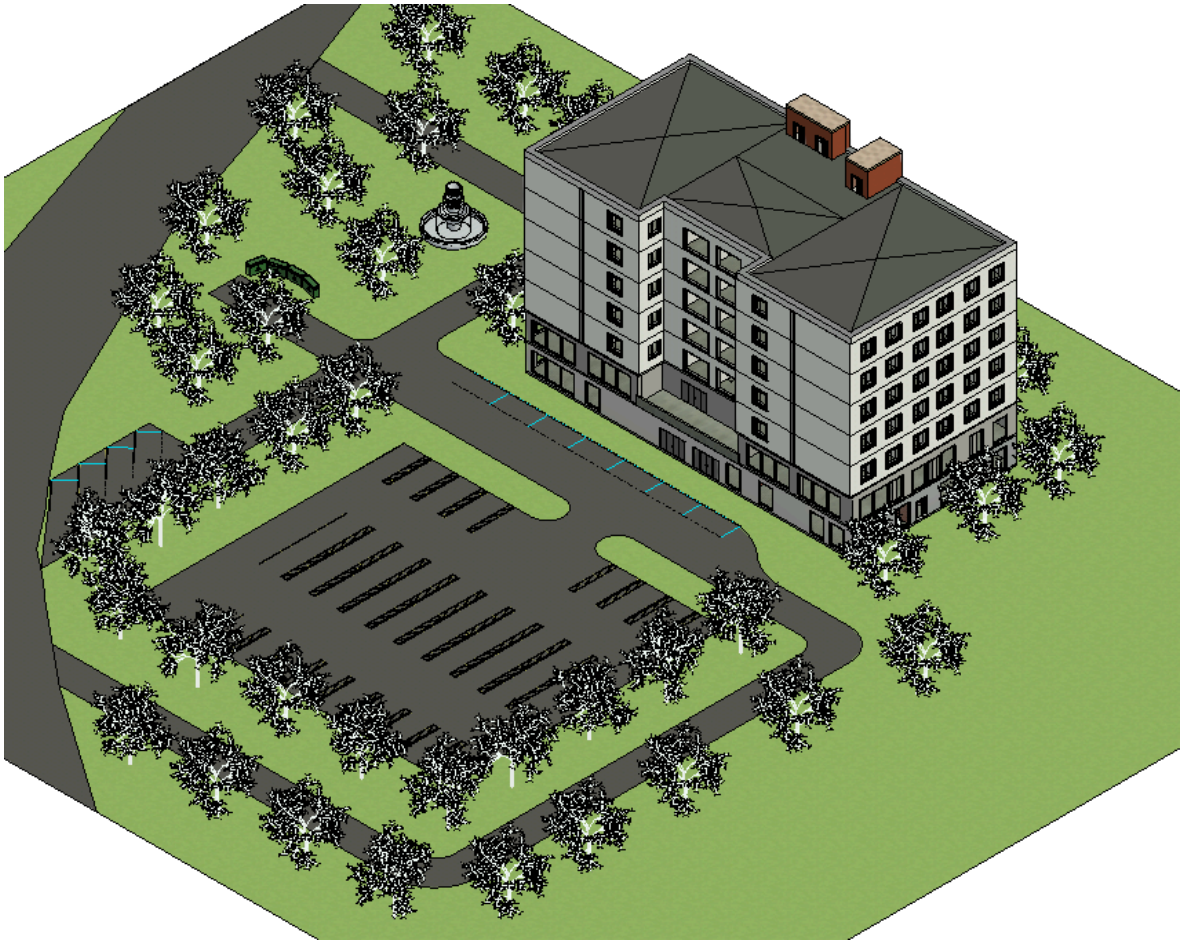

Figure 2-1. Parking of the hotel.

### 2.3 Fire protection System

The construction is created with the use of International building Code (2009). All of the required fire alarm systems are projected and aimed to prevent any accidents in the hotel. Moreover, IBC 2009 suggested using the system with the high fire resistance and emergency doors were established.

### 2.4 Elevators

There are two elevators in the building that connect the basement and the roof. It meets the requirements of International Building Code (2009).

### 2.5 Parking lot

To determine the required parking space for the building, it was necessary to understand the demand for parking lots. Total number of residents of the hotel is 340 people. Total number of living rooms in the building is 80, therefore 40 parking spaces are required. Parking slot dimension is 4.5 m x 7 m. Figure 2-2. Demonstrates the parking space for the hotel.

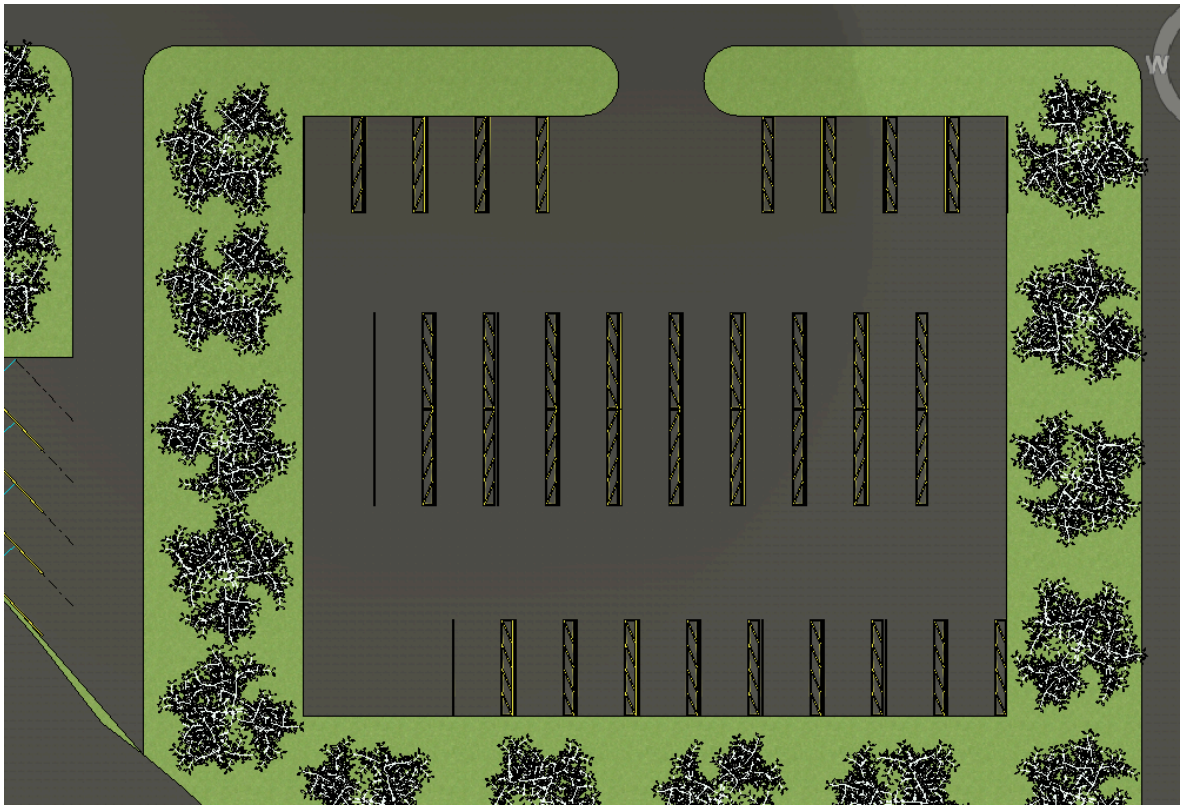

Figure 2-2. Parking of the hotel.

### 2.6 Life Cycle Cost Analysis Using Life-365 Software

Life cycle cost analysis provided was done for beams, columns and slab. Figures 2-3, 2-4 and 2-5 show life cycle cost analysis for columns, beams and slaves respectively.

## Life-365 v2.2 - Life-Cycle Costs

Project: New Project

Description: Default settings for a new project

Analyst: Analyst

Date: 04/16/2023

### Life-Cycle Costs

| Name | Construction Cost | Barrier Cost | Repair Cost | Life-Cycle Cost |
|---|---|---|---|---|
| Base case | $48.31 per m | $0.00 per m | $1,031.34 per m | $1,079.65 per m |

### Graphs

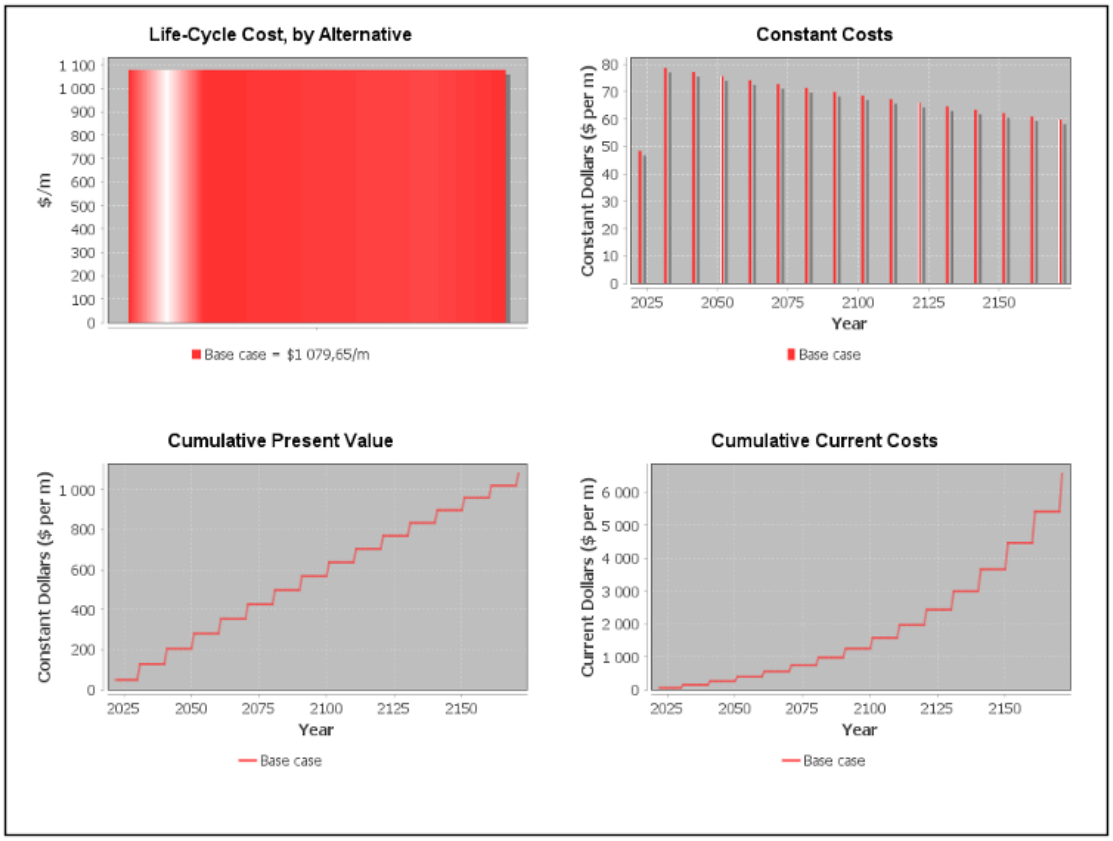


Figure 2-3. Life cycle cost of column

## Life-Cycle Costs

| Name | Construction Cost | Barrier Cost | Repair Cost | Life-Cycle Cost |
|---|---|---|---|---|
| Base case | $17.39 per m | $0.00 per m | $618.80 per m | $636.20 per m |

## Graphs

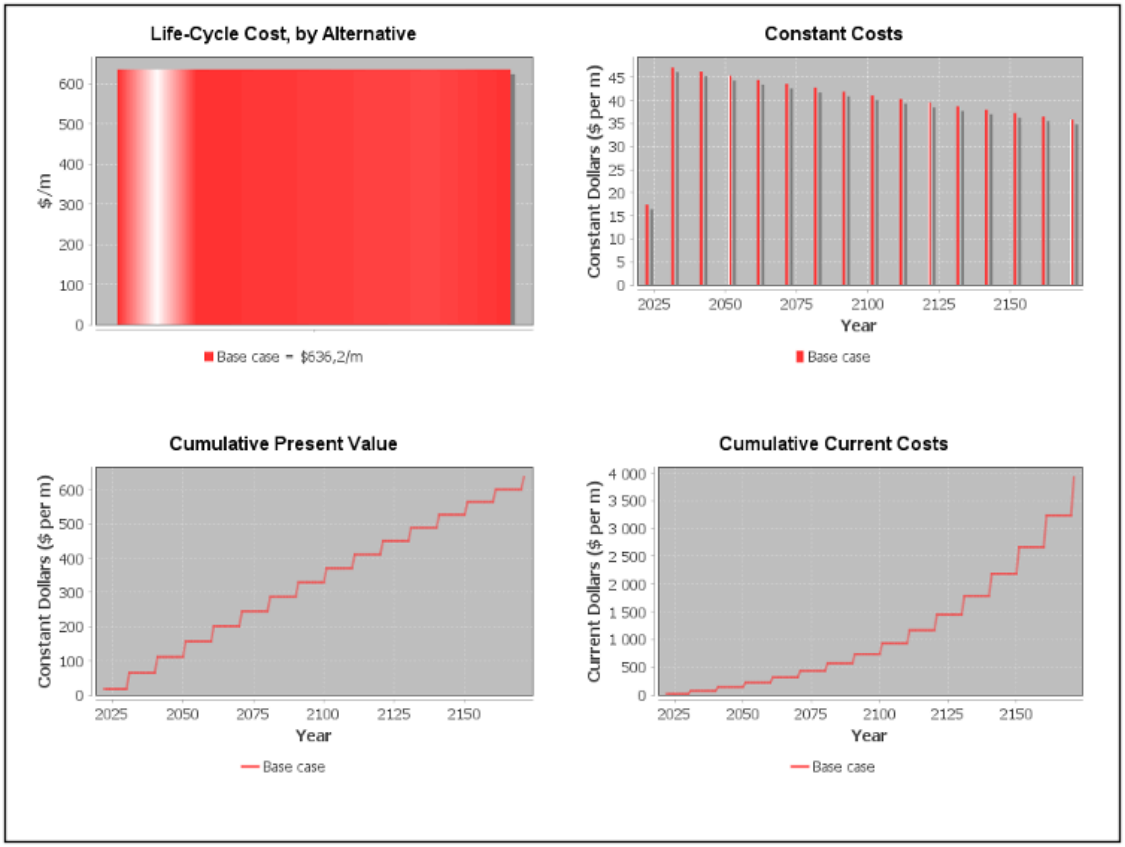


Figure 2-4. Life cycle cost of beam

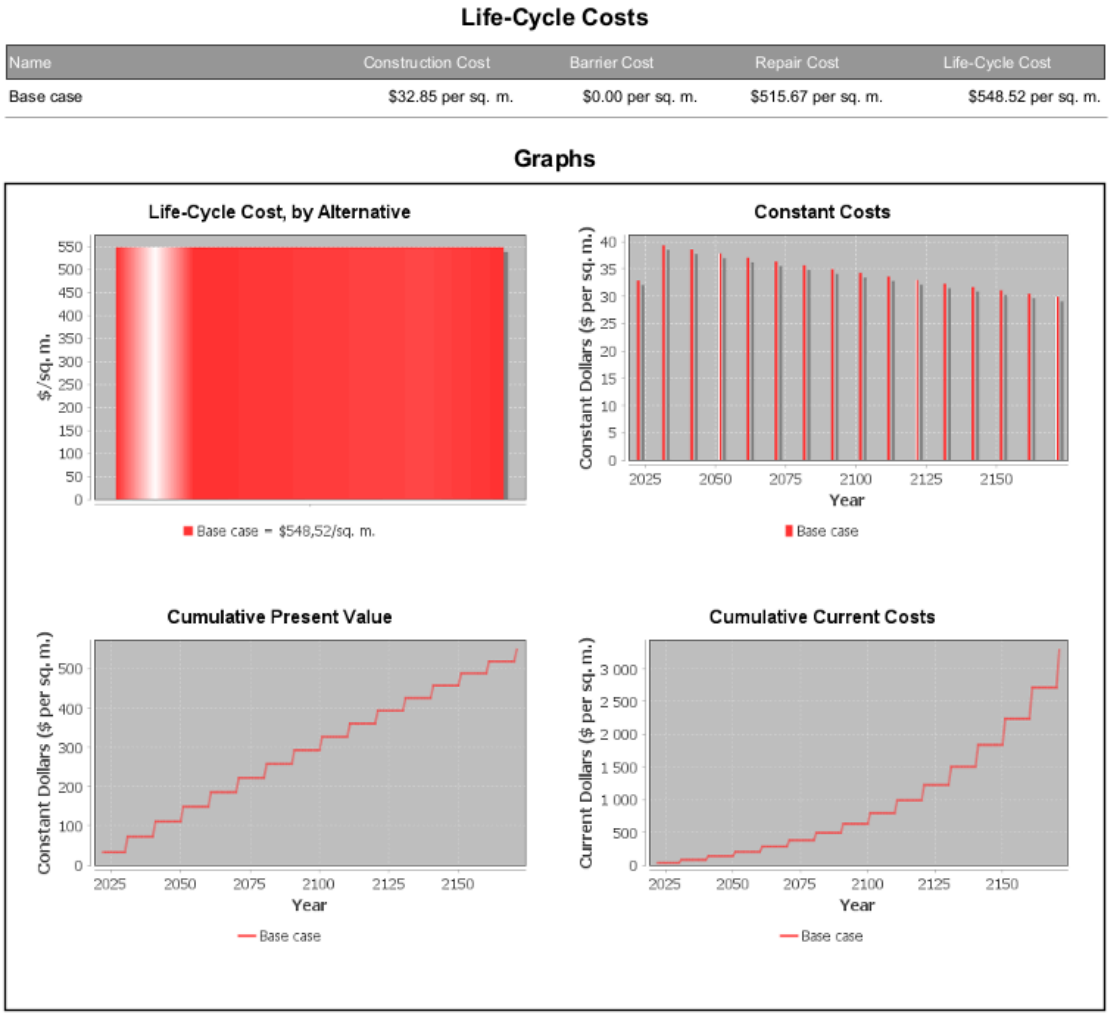


Figure 2-5. Life cycle cost of beam

## 2.7 LEED for green building design

Leadership in Energy and Environmental design (LEED) is a voluntary certification program used for sustainable, and green building.

Table 2-1. LEED certification

| LEED for Building Design and Construction (BD+C) | | | | |
|---|---|---|---|---|
| New Construction | | | | |
| # | Scoring | Requirement | Credits | Points |
| Integrative process | | | 1 | 1 |

| | | | | |
|---|---|---|---|---|
| 1 | Credit | Integrative Process | 1 | 1 |
| Location and Transportation | | | 32 | 12 |
| | | LEED for neighborhood development | | |
| 2 | Credit | Location | 16 | 1 |
| 3 | Credit | Sensitive Land Protection | 1 | 1 |
| 4 | Credit | High-Priority Site and Equitable development | 2 | 0 |
| 5 | Credit | Surrounding Density and Diverse Uses | 5 | 3 |
| 6 | Credit | Access to Quality Transit | 5 | 4 |
| 7 | Credit | Bicycle Facilities | 1 | 1 |
| 8 | Credit | Reduced Parking Footprint | 1 | 1 |
| 9 | Credit | Electric Vehicles | 1 | 1 |
| Sustainable sites | | | 10 | 5 |
| | | Construction activity pollution | | |
| 10 | Prerequisite | Prevention | P | P |
| 11 | Credit | Site Assessment | 1 | 1 |
| 12 | Credit | Protect or Restore Habitat | 2 | 0 |
| 13 | Credit | Open Space | 1 | 1 |
| 14 | Credit | Rainwater Management | 3 | 3 |
| 15 | Credit | Heat Island Reduction | 2 | 0 |
| 16 | Credit | Light Pollution Reduction | 1 | 0 |
| Water efficiency | | | 11 | 7 |
| 17 | Prerequisite | Outdoor Water Use Reduction | P | P |
| 18 | Prerequisite | Indoor Water Use Reduction | P | P |
| 19 | Prerequisite | Building-Level Water Metering | P | P |
| 20 | Credit | Outdoor Water Use Reduction | 2 | 2 |
| 21 | Credit | Indoor Water Use Reduction | 6 | 2 |
| 22 | Credit | Optimize Process Water Use | 2 | 2 |
| 23 | Credit | Water Metering | 1 | 1 |
| Energy and atmosphere | | | 33 | 19 |
| 24 | Prerequisite | Fundamental Commissioning and Verification | P | P |
| 25 | Prerequisite | Minimum Energy Performance | P | P |
| 26 | Prerequisite | Building -Level Energy Metering | P | P |
| 27 | Prerequisite | Fundamental Refrigerant Management | P | P |
| 28 | Credit | Enhanced Commissioning | 6 | 0 |
| 29 | Credit | Optimize Energy Performance | 18 | 14 |
| 30 | Credit | Advanced Energy Metering | 1 | 0 |
| 31 | Credit | Grid Harmonization | 2 | 1 |
| 32 | Credit | Renewable Energy | 5 | 4 |
| 33 | Credit | Enhanced Refrigerant Management | 1 | 0 |

| | | | | |
|---|---|---|---|---|
| Materials and resources | | | 13 | 4 |
| | | Storage and Collection of Recyclables | | |
| 34 | Prerequisite | Construction and Demolition | P | P |
| 35 | Prerequisite | Waste Management Planning | P | P |
| 36 | Credit | Building Life -Cycle Impact Reduction | 5 | 0 |
| 37 | Credit | Building Product Disclosure and Optimization – EPD | 2 | 2 |
| 38 | Credit | Building Product Disclosure and Optimization – Sourcing of Raw Materials | 2 | 1 |
| 39 | Credit | Building Product Disclosure and Optimization – Material Ingredients | 2 | 1 |
| 40 | Credit | Waste Management | 2 | 0 |
| Indoor environmental quality | | | 16 | 12 |
| | | Minimum Indoor Air Quality | | |
| 41 | Prerequisite | Environmental Tobacco Smoke Control | P | P |
| 42 | Prerequisite | Minimum Acoustic Performance | P | P |
| 43 | Credit | Enhanced Indoor Air Quality Strategies | 2 | 2 |
| 44 | Credit | Low -Emitting Materials | 3 | 3 |
| 45 | Credit | Indoor Air Quality Management Plan | 1 | 0 |
| 46 | Credit | Indoor Air Quality Assessment | 2 | 2 |
| 47 | Credit | Thermal Comfort | 1 | 1 |
| 48 | Credit | Interior Lighting | 2 | 1 |
| 49 | Credit | Daylight | 3 | 3 |
| 50 | Credit | Quality Views | 1 | 0 |
| 51 | Credit | Acoustic Performance | 1 | 0 |
| Innovation | | | 6 | 3 |
| 52 | Credit | Innovation | 5 | 2 |
| 53 | Credit | LEED Accredited Professional | 1 | 1 |
| Regional priority | | | 4 | 0 |
| 54 | Credit | Regional priority | 4 | 0 |
| Total | | | 110 | 67 |

The project gains 67 points out of the total credits, and as a result, achieves the “Gold” level of LEED certification.

# 3. STRUCTURAL DESIGN

## 3.1 Selection of Structural Materials

In Capstone I, it was decided to use reinforced concrete as a primary material. It was decided to choose reinforced concrete as the main structural material due to its properties. Due to the high seismic activity of the region, moment-resisting frames would be used. To prevent corrosion of structural materials, it is suggested to use admixtures during the concrete preparation. ACI 222 R-10 suggests to use appropriate water cement ratio, or use admixtures like Calcium Nitrite. Another way to avoid corrosion is to use galvanized or epoxy coated steel. In this building, epoxy coated steel is used

For finishing materials ceramic tiles, linoleum, vinyl were chosen for floor finishing. Ceramic tiles were used in the restaurant and spa zone, while linoleum flooring were used in the rooms and gym zone.

Table 3-1. Material properties of concrete

| Concrete grade | Compressive strength $f_c'$ psi (MPa) | Modulus of Elasticity $E_c$ ksi (GPa) | Modulus of rupture $f_r$ psi (MPa) | Unit weight of concrete kN/m^3 |
|---|---|---|---|---|
| 6 000 | 6 000 ( 40) | 3645 (25) | 474 (4) | 2500 |

Table 3-2. Material properties of steel bar

| Steel bar grade | Yield strength $f_y$ psi (MPa) | Tensile strength, GPa | Elongation, % | Normal weight steel bar density kN/m^3 |
|---|---|---|---|---|
| A615 GR60 | 60 000 (420) | 620 | 8 | 7890 |

## 3.2 Structural system

Two-way slab systems with simply supported beams were used, the ratio of longer span (6.7 m) to shorter span (5 m) is less than 2, therefore a given system can be used. Moreover, slab is supported by beams on all sides. Load transfer mechanism is provided in such a way: Two-Way Slab →Major Beams → Minor Beams → Column →Foundation. Structural layout of the building is represented in figure 3-1.

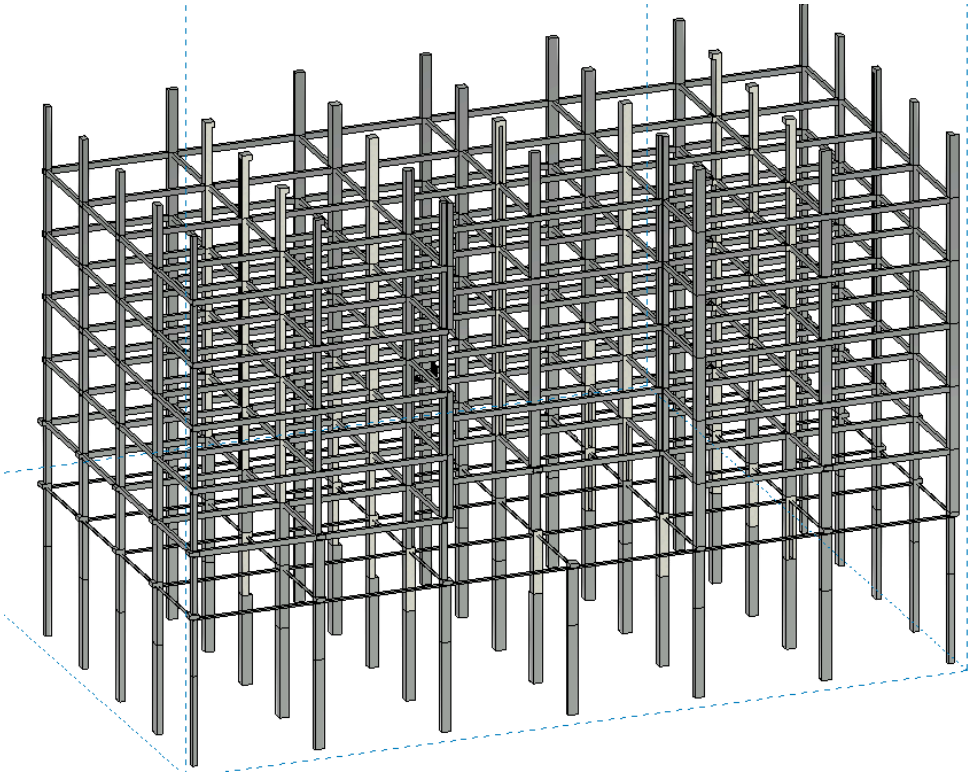

Figure 3-1. Structural layout of the building

### 3.3 Dead load

Dead loads are calculated as a combination of the weight of structural materials, structural slab and non-structural materials. Material selection for insulation is dense-packed cellulose because of its high fire resistance. Load design values of materials were retrieved from ASCE 7-10. Moreover, to make rooms more comfortable, mineral wool insulation is used due its soundproof properties.

Table 3-3. Floor Dead load of the basement.

| Element | Material | | Thickness, mm | Load, kPa | Area, m2 | load, kN |
|---|---|---|---|---|---|---|
| | Cover | ceramic tiles | 10 | 0.72 | 834 | 600 |
| | Levelling | concrete screed | 50 | 0.02 | 834 | 16 |
| | Waterproofing | chip seal | | 0.07 | 834 | 58, |

| | | | | | | |
|---|---|---|---|---|---|---|
| Finishing | Insulation | Dense-Packed Cellulose | 45 | 0 | 834 | 0 |
| Structural slab | Slab | reinforced concrete | 210 | 3.75 | 834 | 3127 |
| Ceiling | Acoustical fiber board | | | 0.05 | 834 | 41 |
| | Gypsum board | | 9.5 | 0.2 | 834 | 166 |
| | Mechanical duct allowance | | | 0.19 | 834 | 158 |
| Total | Combined load | | | | | 4170 |
| Combined load | Non-structure | | | | | 1750 |
| Total Load | | | | | | 5920 |

Table 3-4. Wall dead load of the basement

| Element | Material | Thickness, mm | Load, kPa | Area, m2 | load, kN |
|---|---|---|---|---|---|
| Interior walls | Aerated concrete blocks | 160 | 0.37 | 18.78 | 6.9486 |
| Exterior walls | Aerated concrete blocks | 120 | 0.28 | 720 | 201.6 |
| | Concrete screed | 40 | 0.09 | 720 | 64.8 |
| | Mineral wool insulation | 40 | 0.88 | 720 | 633.6 |
| | Windows glass frame | | 0.38 | 82 | 31.16 |
| | Aluminum finishing | 20 | 0.54 | 720 | 388.8 |
| Structural wall | Reinforced concrete | 200 | 5 | 1.2 | 6 |
| Total | Combined load | | | | 1332.9086 |
| Combined load | Non-structure | | | | 49 |
| Total load | | | | | 1381.9086 |

Table 3-5. Floor dead load of the first floor.

| Element | Material | | Thickness, mm | Load, kPa | Area, m2 | load, kN |
|---|---|---|---|---|---|---|
| Finishing | Cover | ceramic tiles | 10 | 0.72 | 834 | 576 |
| | Levelling | concrete screed | 50 | 0.02 | 834 | 16 |
| | Waterproofing | chip seal | | 0.07 | 834 | 56 |
| | Insulation | Dense-Packed Cellulose | 45 | 0 | 834 | 0 |
| Structural slab | Slab | reinforced concrete | 170 | 4.96 | 834 | 3968 |
| Ceiling | Acoustical fiber board | | | 0.05 | 834 | 40 |
| | Gypsum board | | 9.5 | 0.2 | 834 | 160 |
| | Mechanical duct allowance | | | 0.19 | 834 | 152 |
| Total | Combined load | | | | | 4968 |
| Combined load | Non-structure | | | | | 1819 |
| Total load | | | | | | 6787 |

Table 3-6. Wall dead load of the first floor

| Element | Material | Thickness, mm | Load, kPa | Area, m2 | load, kN |
|---|---|---|---|---|---|
| Interior walls | Aerated concrete blocks | 160 | 0.37 | 18.78 | 6.9486 |
| Exterior walls | Aerated concrete blocks | 120 | 0.28 | 720 | 201.6 |
| | Concrete screed | 40 | 0.09 | 720 | 64.8 |
| | Mineral wool insulation | 40 | 0.88 | 720 | 633.6 |

| | | | | | |
|---|---|---|---|---|---|
| | Windows glass frame | | 0.38 | 82 | 31.16 |
| | Aluminum finishing | 20 | 0.54 | 720 | 388.8 |
| Structural wall | Reinforced concrete | 200 | 5 | 1.2 | 6 |
| Total | Combined load | | | | 1332.9086 |
| Combined load | Non-structure | | | | 850 |
| Total load | | | | | 2182.9086 |

Table 3-7. Floor dead load of second floor.

| Element | Material | | Thickness, mm | Load, kPa | Area, m2 | load, kN |
|---|---|---|---|---|---|---|
| Finishing | Cover (restaurant) | ceramic tiles | 10 | 0.72 | 609 | 419.76 |
| | Cover (gym) | Linoleum tiles | 6 | 0.05 | 225 | 10.85 |
| | Levelling | concrete screed | 50 | 0.02 | 834 | 16 |
| | Waterproofing | chip seal | | 0.07 | 834 | 56 |
| | Insulation | Dense-Packed Cellulose | 45 | 0 | 834 | 0 |
| Structural slab | Slab | reinforced concrete | 210 | 4.96 | 834 | 3968 |
| Ceiling | Acoustical fiber board | | | 0.05 | 834 | 40 |
| | Gypsum board | | 9.5 | 0.2 | 834 | 160 |
| | Mechanical duct allowance | | | 0.19 | 834 | 152 |
| Total | Combined load | | | | | 4822.61 |
| Combined load | Non-structure | | | | | 1716 |
| Total load | | | | | | 6538.61 |

Table 3-8. Walls dead load of second floor.

| Element | Material | Thickness, mm | Load, kPa | Area, m2 | load, kN |
|---|---|---|---|---|---|
| Interior walls | Aerated concrete blocks | 160 | 0.37 | 18.78 | 6.9486 |
| Exterior walls | Aerated concrete blocks | 120 | 0.28 | 720 | 201.6 |
| | Concrete screed | 40 | 0.09 | 720 | 64.8 |
| | Mineral wool insulation | 40 | 0.88 | 720 | 633.6 |
| | Windows glass frame | | 0.38 | 5.12 | 1.9456 |
| | Aluminum finishing | 20 | 0.54 | 720 | 388.8 |
| Structural wall | Reinforced concrete | 200 | 5 | 1.2 | 6 |
| Total | Combined load | | | | 1303.6942 |
| Combined load | Non-structure | | | | 780 |
| Total load | | | | | 2083.6942 |

Table 3-9. Floor dead loads of third-seventh floors

| Element | Material | | Thickness, mm | Load, kPa | Area, m2 | load, kN |
|---|---|---|---|---|---|---|
| Finishing | Cover (Hall) | ceramic tiles | 10 | 0.72 | 451 | 325 |
| | Cover (Rooms) | Linoleum tiles | 6 | 0.05 | 384 | 19.15 |
| | Levelling | concrete screed | 50 | 0.02 | 834 | 16 |
| | Waterproofing | chip seal | | 0.07 | 834 | 56 |
| | Insulation | Dense-Packed Cellulose | 45 | 0 | 834 | 0 |
| Structural slab | Slab | reinforced concrete | 210 | 4.96 | 834 | 3968 |
| Ceiling | Acoustical fiber board | | | 0.05 | 834 | 40 |
| | Gypsum board | | 9.5 | 0.2 | 834 | 160 |
| | Mechanical duct allowance | | | 0.19 | 834 | 152 |

| | | | | | | |
|---|---|---|---|---|---|---|
| Total | Combined load | | | | | 4551.7137 |
| Combined load | Non-structure | | | | | 1830 |
| Total Load for one floor | | | | | | 6381.7137 |
| Total Load | | | | | | 31908.5685 |

Table 3-10. Wall dead loads of third-seventh floors

| Element | Material | Thickness, mm | Load, kPa | Area, m2 | load, kN |
|---|---|---|---|---|---|
| Interiror walls | Aerated concrete blocks | 160 | 0.37 | 18.78 | 6.9486 |
| Exteriror walls | Aerated concrete blocks | 120 | 0.28 | 720 | 201.6 |
| | Concrete screed | 40 | 0.09 | 720 | 64.8 |
| | Mineral wool insulation | 40 | 0.88 | 720 | 633.6 |
| | Windows glass frame | | 0.38 | 5.12 | 1.9456 |
| | Aluminum finishing | 20 | 0.54 | 720 | 388.8 |
| Shear wall | Reinforced concrete | 200 | 5 | 1.2 | 6 |
| Total | Combined load | | | | 1303.6942 |
| Combined load | Non-structure | | | | 1120 |
| Total Load for one floor | | | | | 2423.6942 |
| Total Load | | | | | 12118.471 |

Table 3-11. Roof dead load.

| Element | Category | Material | Thickness, mm | Load,kPa | Area,m2 | Load,kN |
|---|---|---|---|---|---|---|
| Roof | Composition | Copper | - | 0.05 | 834 | 40 |

| | | | | | | |
|---|---|---|---|---|---|---|
| | Water-proofing, air and vapor barrier | Bituminous, smooth surface | 4 | 0.07 | 834 | 56 |
| | Thermal Insulation | Polystyrene foam | 50 | 0.02 | 834 | 16 |
| Structural Slab | Slab | Reinforced concrete | 150 | 3.75 | 834 | 3000 |
| Ceiling | Acoustical fiber board | | | 0.048 | 834 | 38.4 |
| | Gypsum board | | 25-Apr | 0.203 | 834 | 162.4 |
| | Mechanical duct allowance | | | 0.192 | 834 | 153.6 |
| Total | Non-structure | | | | | 364.34 |
| | Combined load | | | | | 3830.74 |

**3.4 Live load**

Live load was calculated according to the International Building Code.

Live load reduction

$L = L_0(0.25 + \frac{4.57}{\sqrt{K_{LL}A_T}})$

where

$L$ = reduced live load per m2 of area supported by the member

$L_0$ = unreduced live load

$K_{LL}$ = live load element factor

$A_T$ = tributary area in m2

- $L > 0.50L_0$ (for members supporting one floor)
- $L > 0.40L_0$ (for members supporting two or more floors)
- $K_{LL} = 4$ (for interior and exterior columns)

Live load reduction factor was determined according to the residential building. According to ASCE 7-10, it is suggested to use a reduction factor of 0.6 for residential buildings.

Table 3-12. Live load

| Floor | Area | Live load kn/m2 | Live load reduction factor | Total live load in the room |
|---|---|---|---|---|
| Floor 1 | | | | |
| Restaurant | 800 | 4.79 | 0.6 | 751.8863 |
| Store | 45.42 | 4.79 | 0.6 | 217.5618 |
| Kitchen | 48.39 | 4.79 | 0.6 | 231.7881 |
| Hall | 173.84 | 4.79 | 0.6 | 832.6936 |
| Lobby | 19.61 | 4.79 | 0.6 | 93.9319 |
| Reception | 30.62 | 4.79 | 0.6 | 146.6698 |
| Yoga room | 43.14 | 4.79 | 0.6 | 206.6406 |
| Locker female | 7.16 | 4.79 | 0.6 | 34.2964 |
| Locker male | 7.16 | 4.79 | 0.6 | 34.2964 |
| Jacuzzi | 18.78 | 4.79 | 0.6 | 89.9562 |
| Massage | 17.08 | 4.79 | 0.6 | 81.8132 |
| Floor total | | | | 2721.5343 |
| Floor 2 | | | | |
| Restaurant | 254.79 | 4.79 | 0.6 | 1220.4441 |
| Café | 42.47 | 4.79 | 0.6 | 203.4313 |
| Gym | 214.36 | 4.79 | 0.6 | 1026.7844 |
| Floor total | | | | 2450.6598 |
| Floor 3-7 | | | | |
| King room | 207.68 | 1.916 | 0.6 | 397.91488 |
| Queen Suite | 129.4 | 1.916 | 0.6 | 247.9304 |
| King suite | 68.22 | 1.916 | 0.6 | 130.70952 |
| Total live load on the floor | | | | 776.5548 |
| Live load in 3-7 floors | | | | 3882.774 |
| Total live load | | | | 9054.9681 |

### 3.5 Wind Load

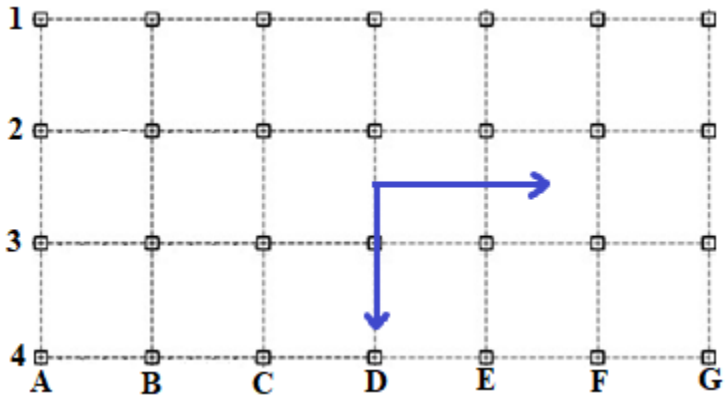


Figure 3-2. Frames and direction of wind

It was mentioned above that the Risk Category of the building is II, thus, the first step is to identify basic wind speed.

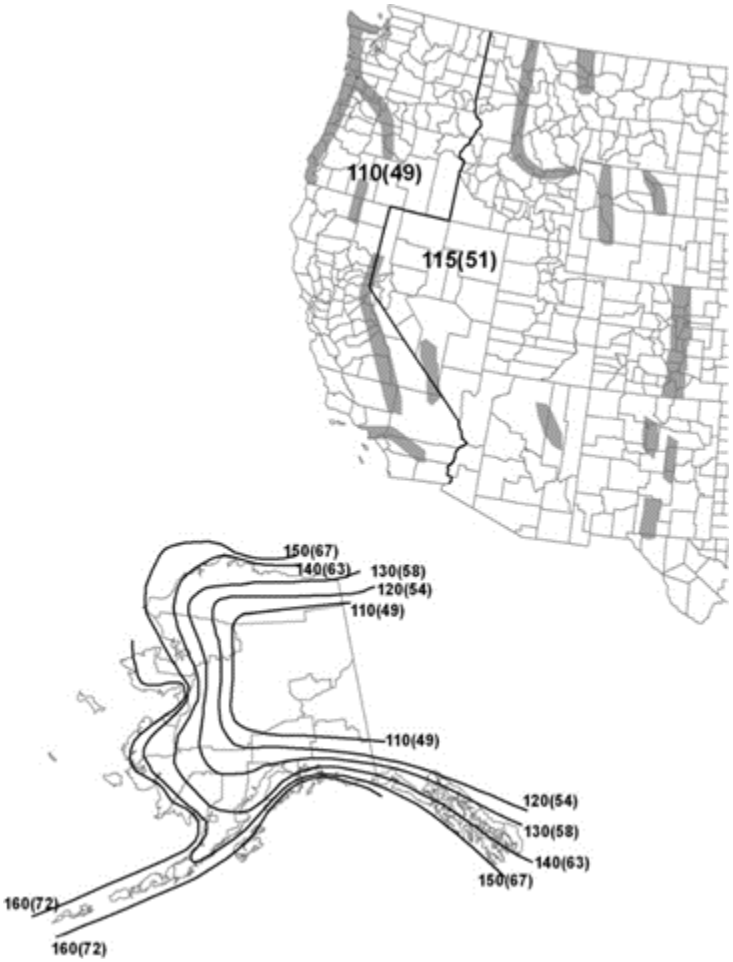


Figure 3-3. Basic Wind Speeds Map for Occupancy Category II buildings and other structures (ASCE 7-10)

The hotel building is located in Carlsbad, CA, USA, therefore, according to the map above:
$V(Basic\ wind\ speed) = 41\ m/s$
According to ASCE 7-10, the Exposure Category of the building is identified as B. Other wind load parameters were determined from ASCE 7-10 and summarized in Table below:

Table 3-13. Wind load coefficients

| | | |
|---|---|---|
| Wind directionality factor | $K_d$ | 0.85 |
| Topographic factor | $K_{zt}$ | 1 |
| Gust Effect Factor | $G_f$ | 0.89 |

According to basic information:
h = 24.1 m
B = 40.7 m
L = 20.5 m
Gust Effect Calculations:

$$n_a = 43.5/h^{0.9}$$

$$n_a = 43.5/75^{0.9} = 0.8847 < 1\ (flexible\ building)$$

Figure 3-4. Terrain Exposure Constants (ASCE 7-10)

*In metric*

| Exposure | α | $z_g$ (m) | $\hat{\alpha}$ | $\hat{b}$ | $\bar{\alpha}$ | $\bar{b}$ | c | $\ell$ (m) | $\bar{\epsilon}$ | $z_{min}$ (m)* |
|---|---|---|---|---|---|---|---|---|---|---|
| B | 7.0 | 365.76 | 1/7 | 0.84 | 1/4.0 | 0.45 | 0.30 | 97.54 | 1/3.0 | 9.14 |
| C | 9.5 | 274.32 | 1/9.5 | 1.00 | 1/6.5 | 0.65 | 0.20 | 152.4 | 1/5.0 | 4.57 |
| D | 11.5 | 213.36 | 1/11.5 | 1.07 | 1/9.0 | 0.80 | 0.15 | 198.12 | 1/8.0 | 2.13 |

*$z_{min}$ = minimum height used to ensure that the equivalent height $\bar{z}$ is greater of $0.6h$ or $z_{min}$.
For buildings with $h \le z_{min}$, $\bar{z}$ shall be taken as $z_{min}$.

For flexible buildings, the gust effect according to ASCE 7-10 should be calculated by:

$$G_f = 0.925\left(\frac{1+1.7I_z\sqrt{g_Q^2Q^2+g_R^2R^2}}{1+1.7g_vI_z}\right),$$

where $g_Q = 3.4$ *and* $g_V = 3.4$

and $g_R$ is given by the formula below:

$$g_R = \sqrt{2\ln(3{,}600n_1)} + \frac{0.577}{\sqrt{2\ln(3{,}600n_1)}}$$

Formulas for $I_{\bar{z}}$, Q, $L_{\bar{z}}$ are presented below:

In SI: $I_{\bar{z}} = c\left(\frac{10}{\bar{z}}\right)^{1/6}$

where $I_{\bar{z}}$ is the intensity of turbulence at height $\bar{z}$ where $\bar{z}$ is the equivalent height of the structure defined as $0.6h$, but not less than $z_{min}$ for all building heights $h$. $z_{min}$ and $c$ are listed for each exposure in Table 26.9-1; $g_Q$ and $g_v$ shall be taken as 3.4. The background response $Q$ is given by

$$Q = \sqrt{\frac{1}{1+0.63\left(\frac{B+h}{L_{\bar{z}}}\right)^{0.63}}}$$

where $B$ and $h$ are defined in Section 26.3 and $L_{\bar{z}}$ is the integral length scale of turbulence at the equivalent height given by

$$L_{\bar{z}} = \ell\left(\frac{\bar{z}}{33}\right)^{\bar{\varepsilon}}$$

In SI: $L_{\bar{z}} = \ell\left(\frac{\bar{z}}{10}\right)^{\bar{\varepsilon}}$

in which $\ell$ and $\bar{\varepsilon}$ are constants listed in Table 26.9-1.

$R$, the resonant response factor, is given by

$$R = \sqrt{\frac{1}{\beta}R_nR_hR_B(0.53+0.47R_L)}$$

$$R_n = \frac{7.47N_1}{(1+10.3N_1)^{5/3}}$$

$$N_1 = \frac{n_1L_{\bar{z}}}{\bar{V}_{\bar{z}}}$$

$$R_\ell = \frac{1}{\eta} - \frac{1}{2\eta^2}\left(1-e^{-2\eta}\right) \quad \text{for} \quad \eta > 0$$

$$R_\ell = 1 \quad \text{for} \quad \eta = 0$$

where the subscript $\ell$ in Eqs. 26.9-15 shall be taken as $h$, $B$, and $L$, respectively, where $h$, $B$, and $L$ are defined in Section 26.3.

$n_1$ = fundamental natural frequency
$R_f = R_h$ setting $\eta = 4.6n_1h/\bar{V}_{\bar{z}}$
$R_f = R_B$ setting $\eta = 4.6n_1B/\bar{V}_{\bar{z}}$
$R_f = R_L$ setting $\eta = 15.4n_1L/\bar{V}_{\bar{z}}$
$\beta$ = damping ratio, percent of critical (i.e. for 2% use 0.02 in the equation)
$\bar{V}_{\bar{z}}$ = mean hourly wind speed (ft/s) at height $\bar{z}$

$$\bar{V}_{\bar{z}} = \bar{b}\left(\frac{\bar{z}}{33}\right)^{\bar{\alpha}}\left(\frac{88}{60}\right)V$$

In SI: $\bar{V}_{\bar{z}} = \bar{b}\left(\frac{\bar{z}}{10}\right)^{\bar{\alpha}} V$

, where $\bar{\alpha}$ and $\bar{b}$ are equal to 0.25 and 0.45 respectively. All calculation presented in table below:

Table 3-14. Gust effect calculation summary for left to right direction

| | |
|---|---|
| $\bar{V}_z$ | 20.02 m/s |
| $L_z$ | 108.75 |
| $n_1$ | 4.81 |
| $R_n$ | 0.05 |
| $\eta_h$ | 4.70 |
| $\eta_B$ | 4.15 |
| $\eta_L$ | 27.50 |
| $R_h$ | 0.19 |
| $R_B$ | 0.21 |
| $R_L$ | 0.04 |
| $R$ | 0.24 |
| $g_R$ | 4.03 |
| $I_z$ | 0.28 |
| Q | 0.86 |
| $G_f$ | 0.86 |

Velocity pressure exposure coefficients $K_z$ were calculated using the following formula:

For 15 ft. $\leq z \leq z_g$

$K_z = 2.01\ (z/z_g)^{2/\alpha}$

For $z < 15$ ft.

$K_z = 2.01\ (15/z_g)^{2/\alpha}$

, where $\alpha$ =7 and $z_g$ =365. 76 in SI units. The velocity pressure of the building is calculated by using the following formula:

[In SI: $q_z = 0.613 K_z K_{zt} K_d V^2$ (N/m$^2$); $V$ in m/s]

where

$K_d$ = wind directionality factor, see Section 26.6
$K_z$ = velocity pressure exposure coefficient, see Section 27.3.1
$K_{zt}$ = topographic factor defined, see Section 26.8.2
$V$ = basic wind speed, see Section 26.5

| Wall Pressure Coefficients, $C_p$ | | | |
|---|---|---|---|
| **Surface** | **L/B** | **$C_p$** | **Use With** |
| Windward Wall | All values | 0.8 | $q_z$ |
| Leeward Wall | 0-1 | -0.5 | $q_h$ |
| | 2 | -0.3 | |
| | ≥4 | -0.2 | |
| Side Wall | All values | -0.7 | $q_h$ |

Wall pressure coefficients were determined as $C_{pw}$= 0. 8 *and* $C_{pL}$= -0.3. After that, design wind pressure was estimated by using following formula:

$$p = qG_fC_p - q_i(GC_{pi}) \text{ (lb/ft}^2\text{)} \text{ (N/m}^2\text{)}$$

All calculation results including wind loads are presented in the table below:

Table 3-15. Wind load in left to right direction

| Floor | h | z | kz | q | P | Pext | F,kN |
|---|---|---|---|---|---|---|---|
| 7 | 3,3 | 23,1 | 0,913 | 799,659 | 549,608 | 792,592 | 55,78 |
| 6 | 3,3 | 19,8 | 0,874 | 765,204 | 525,927 | 768,911 | 51,76 |
| 5 | 3,3 | 16,5 | 0,829 | 726,363 | 499,232 | 742,216 | 49,97 |
| 4 | 3,3 | 13,2 | 0,778 | 681,499 | 468,396 | 711,381 | 47,89 |
| 3 | 3,3 | 9,9 | 0,717 | 627,724 | 431,436 | 674,421 | 45,40 |
| 2 | 3,3 | 6,6 | 0,638 | 559,058 | 384,242 | 627,227 | 42,22 |
| 1 | 3,3 | 3,3 | 0,524 | 458,615 | 315,207 | 558,192 | 37,58 |
| 0 | 3,3 | | | | | | |
| leeward | | | | | | | |
| | | | | 799.659 | | | |

Since, the values of B and L were switched, now B= 40.4 m and L= 20.4 m gust effect will be altered:

Table 3-16. Gust effect calculation summary for bottom to top direction

| | |
|---|---|
| $\overline{V}_z$ | 20.2 m/s |
| $L_z$ | 108.75 |
| $n_1$ | 4.81 |
| $R_n$ | 0.05 |
| $\eta_h$ | 4.70 |
| $\eta_B$ | 8.21 |
| $\eta_L$ | 13.89 |
| $R_h$ | 0.19 |
| $R_B$ | 0.11 |
| $R_L$ | 0.07 |
| $R$ | 0.18 |
| $g_R$ | 4.03 |
| $I_z$ | 0.28 |
| Q | 0.83 |
| $G_f$ | 0.83 |

Table 3-17. Wind load in bottom to top direction

| Floor | h | z | kz | q | P | Pext | F,kN |
|---|---|---|---|---|---|---|---|
| 7 | 3,3 | 23,1 | 0,913 | 799,659 | 532,979 | 768,612 | 107,129 |
| 6 | 3,3 | 19,8 | 0,874 | 765,204 | 510,014 | 745,647 | 99,410 |
| 5 | 3,3 | 16,5 | 0,829 | 726,363 | 484,127 | 719,760 | 95,958 |
| 4 | 3,3 | 13,2 | 0,778 | 681,499 | 454,225 | 689,857 | 91,972 |
| 3 | 3,3 | 9,9 | 0,717 | 627,724 | 418,383 | 654,016 | 87,193 |
| 2 | 3,3 | 6,6 | 0,638 | 559,058 | 372,616 | 608,249 | 81,092 |
| 1 | 3,3 | 3,3 | 0,524 | 458,615 | 305,670 | 541,303 | 72,167 |
| 0 | 3,3 | | | | | | |
| leeward | | | | | | | |
| | | | | 799.659 | | | |

Total stiffness = 28D

Frame 1, 2, 3, 4 = 7D, it will have 7/28 of total wind force.

Table 3-18. Left to right direction wind force per frame

| F,kN | Frame 1, 2, 3, 4 |
|---|---|
| 55,78 | 13,946 |
| 51,76 | 12,941 |
| 49,97 | 12,491 |
| 47,89 | 11,973 |
| 45,40 | 11,351 |
| 42,22 | 10,556 |
| 37,58 | 9,394 |

For bottom to top direction, total stiffness = 21D

Frame A-G = 3D, it will have 3/21 of total wind force.

*Table 3-19. Bottom to top direction wind force per frame*

| F,kN | Frame 1, 2, 3, 4 |
|---|---|
| 107,129 | 15,304 |
| 99,410 | 14,201 |
| 95,958 | 13,708 |
| 91,972 | 13,139 |
| 87,193 | 12,456 |
| 81,092 | 11,585 |
| 72,167 | 10,310 |

After the wind load was calculated, it is required to calculate the torsional moment from the wind loads. To calculate it, given equation is used:

$$T=Fx * Hx$$

$$T= Fy*Hy$$

Where:

T - Torsional moment, kN-m

Fx, Fy- wind load acting on frame, kN

Hx, Hy - Distance from the center of mass of the building, m

Values for torsional moments are given in tables 3-20 and 3-21.

Table 3-20. Torsional moment from left to right direction

| Floor | Fx, kN | Hx, m | T, kN-m |
|---|---|---|---|
| 7 | 55,78 | 20,35 | 1135,12 |
| 6 | 51,76 | 20,35 | 1053,32 |
| 5 | 49,97 | 20,35 | 1016,89 |
| 4 | 47,89 | 20,35 | 974,562 |
| 3 | 45,4 | 20,35 | 923,89 |
| 2 | 42,22 | 20,35 | 859,177 |

| | | | |
|---|---|---|---|
| 1 | 37,58 | 20,35 | 764,753 |

Table 3-21. Torsional moment from bottom to top direction

| Floor | Fx, kN | Hx, m | T, kN-m |
|---|---|---|---|
| 7 | 107,129 | 10,25 | 1098,07 |
| 6 | 99,41 | 10,25 | 1018,95 |
| 5 | 95,958 | 10,25 | 983,57 |
| 4 | 91,972 | 10,25 | 942,713 |
| 3 | 87,193 | 10,25 | 893,728 |
| 2 | 81,092 | 10,25 | 831,193 |
| 1 | 72,167 | 10,25 | 739,712 |

**3.6 Snow load**

According to ASCE 7-10, snow load on elevation from the ground of 1800 feet (548 meters) snow load is zero. Therefore, snow load was not considered during the analysis.

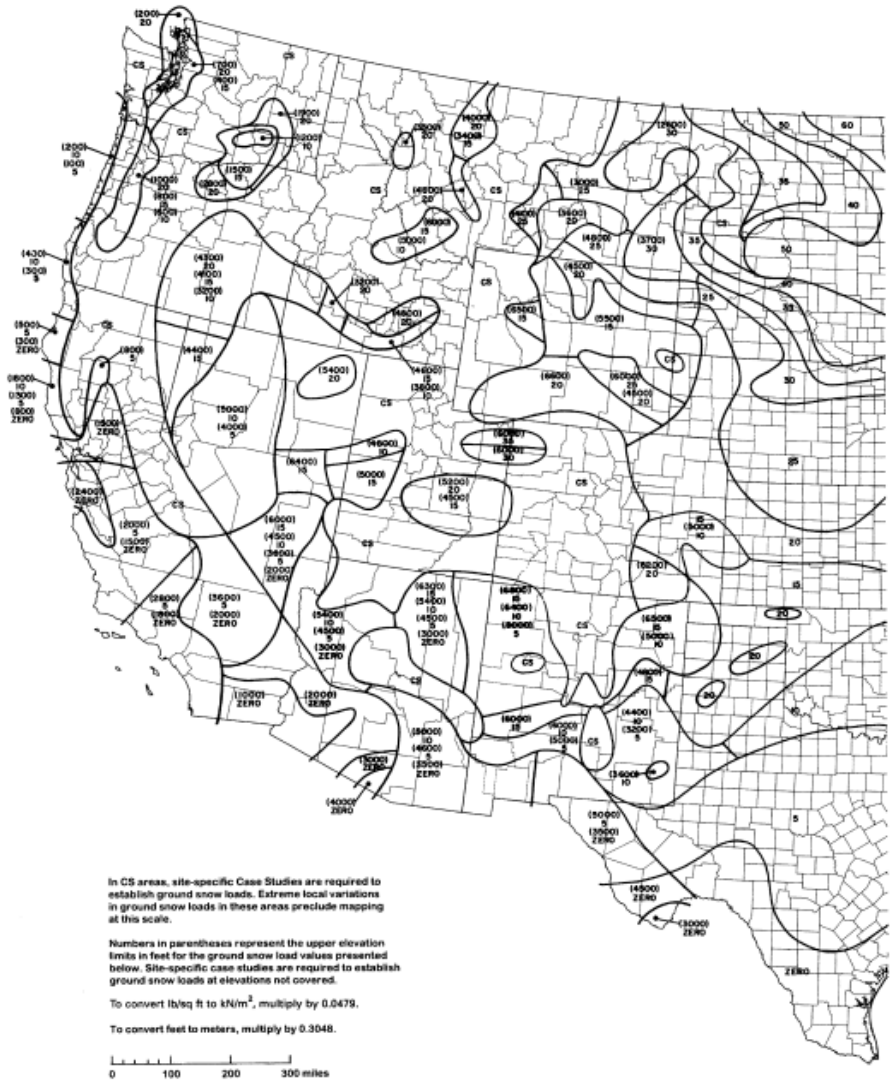


FIGURE 7-1 Ground Snow Loads, $P_g$, for the United States (Lb/Ft$^2$).

Figure 3-5. Ground Snow Loads, Pg, for the United States (Lb/Ft2 ). (ASCE 7-10)

### 3.7 Seismic load

To determine seismic load, initially it was required to define the category of the building site class of the soil. To determine the required values ASCE 7 hazard tool was used, values obtained are shown in the figure below.

Next, it is required to determine the values of Fa and Fv. They were determined using linear interpolation. Value of Ss is 1.15 and the value of S1 is 0.37 according to the ASCE 7-10. Final values of Fa and Fv are 1.04 and 1.67 respectively.

Table 3-22. Site coefficients Fa, Fv

CHAPTER 11 SEISMIC DESIGN CRITERIA

**Table 11.4-1 Site Coefficient, $F_a$**

| Site Class | Mapped Risk-Targeted Maximum Considered Earthquake ($MCE_R$) Spectral Response Acceleration Parameter at Short Period | | | | |
|---|---|---|---|---|---|
| | $S_S \le 0.25$ | $S_S = 0.5$ | $S_S = 0.75$ | $S_S = 1.0$ | $S_S \ge 1.25$ |
| A | 0.8 | 0.8 | 0.8 | 0.8 | 0.8 |
| B | 1.0 | 1.0 | 1.0 | 1.0 | 1.0 |
| C | 1.2 | 1.2 | 1.1 | 1.0 | 1.0 |
| D | 1.6 | 1.4 | 1.2 | 1.1 | 1.0 |
| E | 2.5 | 1.7 | 1.2 | 0.9 | 0.9 |
| F | See Section 11.4.7 | | | | |

Note: Use straight-line interpolation for intermediate values of $S_S$.

**Table 11.4-2 Site Coefficient, $F_v$**

| Site Class | Mapped Risk-Targeted Maximum Considered Earthquake ($MCE_R$) Spectral Response Acceleration Parameter at 1-s Period | | | | |
|---|---|---|---|---|---|
| | $S_1 \le 0.1$ | $S_1 = 0.2$ | $S_1 = 0.3$ | $S_1 = 0.4$ | $S_1 \ge 0.5$ |
| A | 0.8 | 0.8 | 0.8 | 0.8 | 0.8 |
| B | 1.0 | 1.0 | 1.0 | 1.0 | 1.0 |
| C | 1.7 | 1.6 | 1.5 | 1.4 | 1.3 |
| D | 2.4 | 2.0 | 1.8 | 1.6 | 1.5 |
| E | 3.5 | 3.2 | 2.8 | 2.4 | 2.4 |
| F | See Section 11.4.7 | | | | |

Note: Use straight-line interpolation for intermediate values of $S_1$.

Next it was required to find the values Sms, Sm1, Sds, and Sd1. Following equations were used:

$$S_{ms} = F_a * S_S = 1.15 * 1.04 = 1.196$$

$$S_{m1} = F_v * S_1 = 1.67 * 0.37 = 0.6179$$

$$S_{ds} = 2/3 * S_{ms} = 0.7973$$

$$S_{ds} = 2/3 * S_{m1} = 0.4119$$

$$T_0 = 0.2 * S_{d1}/S_{ds} = 0.5167$$

$T_L =$ 8 for California

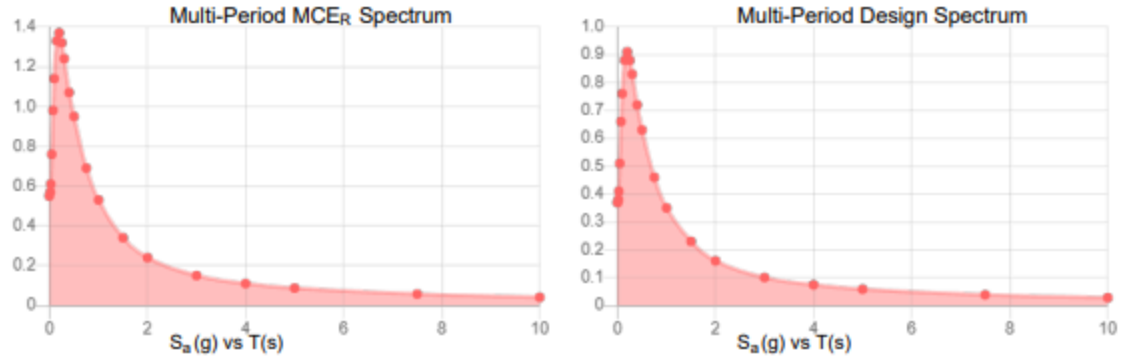





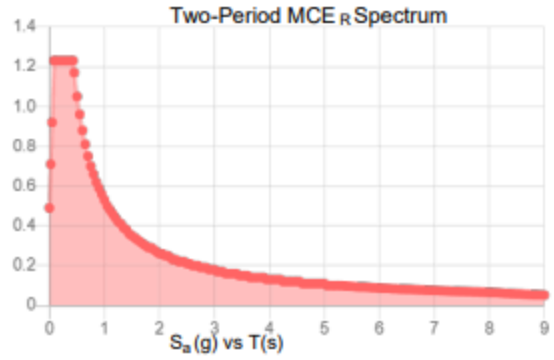


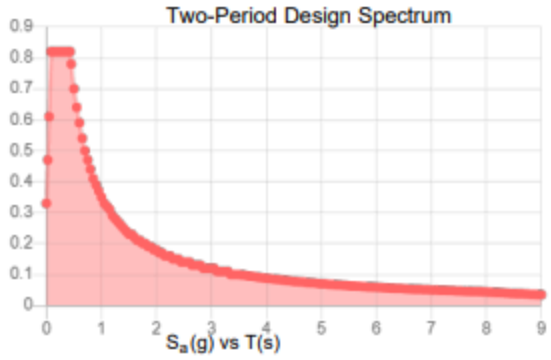


MCER Vertical Response Spectrum

Vertical ground motion data has not yet been made available by USGS.

Design Vertical Response Spectrum

Vertical ground motion data has not yet been made available by USGS.



Figure 3-6. Seismic analysis of the site class

According to the table 3-22, the risk category of the building was determined.
Risk category: D

Table 3-23. Seismic Design Category Based on Short Period Response Acceleration Parameter

| | Risk Category | |
|---|---|---|
| Value of $S_{DS}$ | I or II or III | IV |
| $S_{DS} < 0.167$ | A | A |
| $0.167 \leq S_{DS} < 0.33$ | B | C |
| $0.33 \leq S_{DS} < 0.50$ | C | D |
| $0.50 \leq S_{DS}$ | D | D |

Table 3-24. Seismic Design Category Based on 1-S Period Response Acceleration Parameter

| | Risk Category | |
|---|---|---|
| Value of $S_{D1}$ | I or II or III | IV |
| $S_{D1} < 0.067$ | A | A |
| $0.067 \leq S_{D1} < 0.133$ | B | C |
| $0.133 \leq S_{D1} < 0.20$ | C | D |
| $0.20 \leq S_{D1}$ | D | D |

Next, it was required to determine the base shear V. Equation used is provided in the figure 3-7

**12.8.1 Seismic Base Shear**

The seismic base shear, $V$, in a given direction shall be determined in accordance with the following equation:

$$V = C_s W \qquad (12.8\text{-}1)$$

where

$C_s$ = the seismic response coefficient determined in accordance with Section 12.8.1.1
$W$ = the effective seismic weight per Section 12.7.2

***12.8.1.1 Calculation of Seismic Response Coefficient***

The seismic response coefficient, $C_s$, shall be determined in accordance with Eq. 12.8-2.

$$C_s = \frac{S_{DS}}{\left(\frac{R}{I_e}\right)} \qquad (12.8\text{-}2)$$

where

$S_{DS}$ = the design spectral response acceleration parameter in the short period range as determined from Section 11.4.4 or 11.4.7
$R$ = the response modification factor in Table 12.2-1
$I_e$ = the importance factor determined in accordance with Section 11.5.1

The value of $C_s$ computed in accordance with Eq. 12.8-2 need not exceed the following:

$$C_s = \frac{S_{D1}}{T\left(\frac{R}{I_e}\right)} \quad \text{for} \quad T \le T_L \qquad (12.8\text{-}3)$$

$$C_s = \frac{S_{D1}T_L}{T^2\left(\frac{R}{I_e}\right)} \quad \text{for} \quad T > T_L \qquad (12.8\text{-}4)$$

$C_s$ shall not be less than

$$C_s = 0.044 S_{DS} I_e \ge 0.01 \qquad (12.8\text{-}5)$$

In addition, for structures located where $S_1$ is equal to or greater than $0.6g$, $C_s$ shall not be less than

$$C_s = 0.5 S_1/(R/I_e) \qquad (12.8\text{-}6)$$

where $I_e$ and $R$ are as defined in Section 12.8.1.1 and

$S_{D1}$ = the design spectral response acceleration parameter at a period of 1.0 s, as determined from Section 11.4.4 or 11.4.7
$T$ = the fundamental period of the structure(s) determined in Section 12.8.2
$T_L$ = long-period transition period(s) determined in Section 11.4.5
$S_1$ = the mapped maximum considered earthquake spectral response acceleration parameter determined in accordance with Section 11.4.1 or 11.4.7

Figure 3-7. Equations for base shear

According to ASCE 7-10 Table 12.2-1 Design Coefficients and Factors for Seismic Force-Resisting Systems:
Part C: Moment-Resisting frames - Special reinforced concrete moment frames:
R = 8;
Ω = 3.

After all of the calculations mentioned above, values of *Cs* and *V* are 0.0700315 and 2547.81 kN respectively. Lateral force *Fx* was calculated according to the equations shown in figure 3-8. Values are represented in the table 3-25.

**12.8.3 Vertical Distribution of Seismic Forces**

The lateral seismic force ($F_x$) (kip or kN) induced at any level shall be determined from the following equations:

$$F_x = C_{vx} V \qquad (12.8\text{-}11)$$

and

$$C_{vx} = \frac{w_x h_x^k}{\sum_{i=1}^{n} w_i h_i^k} \qquad (12.8\text{-}12)$$

where

$C_{vx}$ = vertical distribution factor
$V$ = total design lateral force or shear at the base of the structure (kip or kN)
$w_i$ and $w_x$ = the portion of the total effective seismic weight of the structure ($W$) located or assigned to Level $i$ or $x$
$h_i$ and $h_x$ = the height (ft or m) from the base to Level $i$ or $x$
$k$ = an exponent related to the structure period as follows:
for structures having a period of 0.5 s or less, $k = 1$
for structures having a period of 2.5 s or more, $k = 2$

Figure 3-8. Lateral force equation

Table 3-25. Lateral forces calculation

| Level | Wx, kN | hx, m | Wxhx^k | Cvx | Fx, kN |
|---|---|---|---|---|---|
| 1 | 4968 | 1 | 5179 | 0,00093 | 2,50 |
| 2 | 4823 | 4,3 | 92967,7 | 0,01661 | 44,96 |
| 3 | 4552 | 7,6 | 284352 | 0,0508 | 137,50 |
| 4 | 4552 | 10,9 | 584902 | 0,10449 | 282,84 |
| 5 | 4552 | 14,2 | 992674 | 0,17734 | 480,03 |
| 6 | 4552 | 17,5 | 1507669 | 0,26934 | 729,07 |
| 7 | 4552 | 20,8 | 2129887 | 0,3805 | 1029,95 |
| roof | 3830 | 24,1 | 2224502 | 0,3974 | 1075,71 |
| Sum | 36381 | | 5597630 | | 2706,86 |

## 3.8 Structural analysis

### 3.8.1 Analytical models development in software

After all of the calculations, it was required to create an analytical model using SAP 2000. Analytical model is represented in figure. First it was required to assign all loads calculated manually. Forces are: dead load, live load, roof live load, wind load, seismic load. After all the loads were assigned, to determine the ultimate load, load combinations provided in ACI 318M-14 were used. Load combinations are provided in Table 7. According to the ultimate load, software provided the required reinforcement for beams, columns and slabs.

Table 3-26. Load combinations

| Load combination | Equation | Primary load |
|---|---|---|
| $U = 1.4D$ | (5.3.1a) | $D$ |
| $U = 1.2D + 1.6L + 0.5(L_r \text{ or } S \text{ or } R)$ | (5.3.1b) | $L$ |
| $U = 1.2D + 1.6(L_r \text{ or } S \text{ or } R) + (1.0L \text{ or } 0.5W)$ | (5.3.1c) | $L_r$ or $S$ or $R$ |
| $U = 1.2D + 1.0W + 1.0L + 0.5(L_r \text{ or } S \text{ or } R)$ | (5.3.1d) | $W$ |
| $U = 1.2D + 1.0E + 1.0L + 0.2S$ | (5.3.1e) | $E$ |
| $U = 0.9D + 1.0W$ | (5.3.1f) | $W$ |
| $U = 0.9D + 1.0E$ | (5.3.1g) | $E$ |

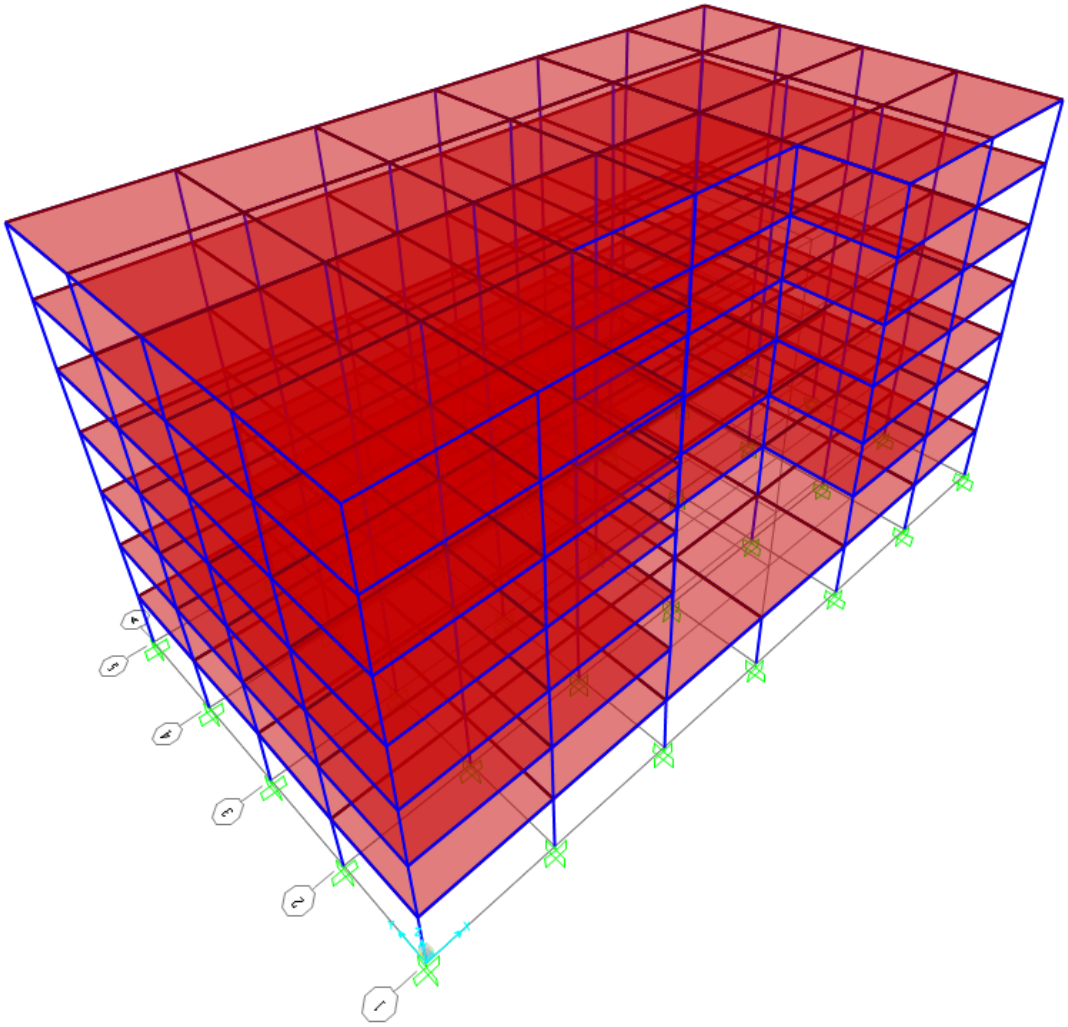

Figure 3-9. SAP2000 model

Initially all of the section properties were defined and all of the loads were assigned. There were 3 types of frame sections: column, short span beam and long span beam. SAP 2000 used to design the reinforcement of the frames for different load combinations. Figures 3-10, 3-11 and 3-12 demonstrate  given frames in SAP 2000.

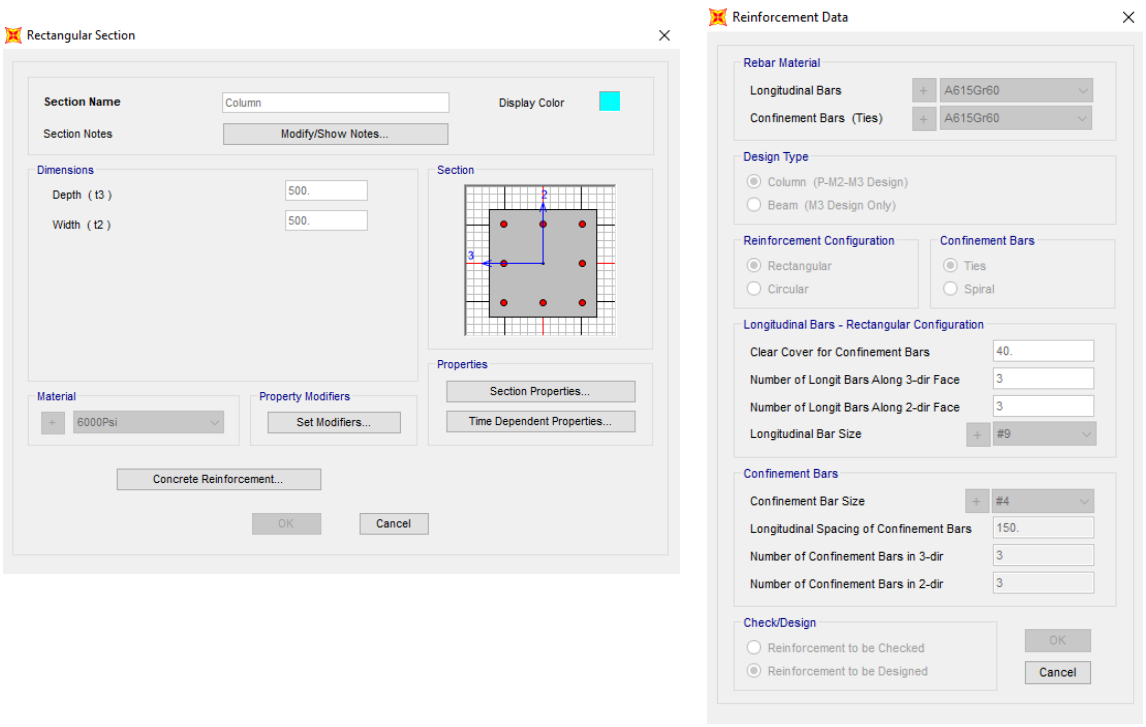


Figure 3-10. Column frame in SAP 2000

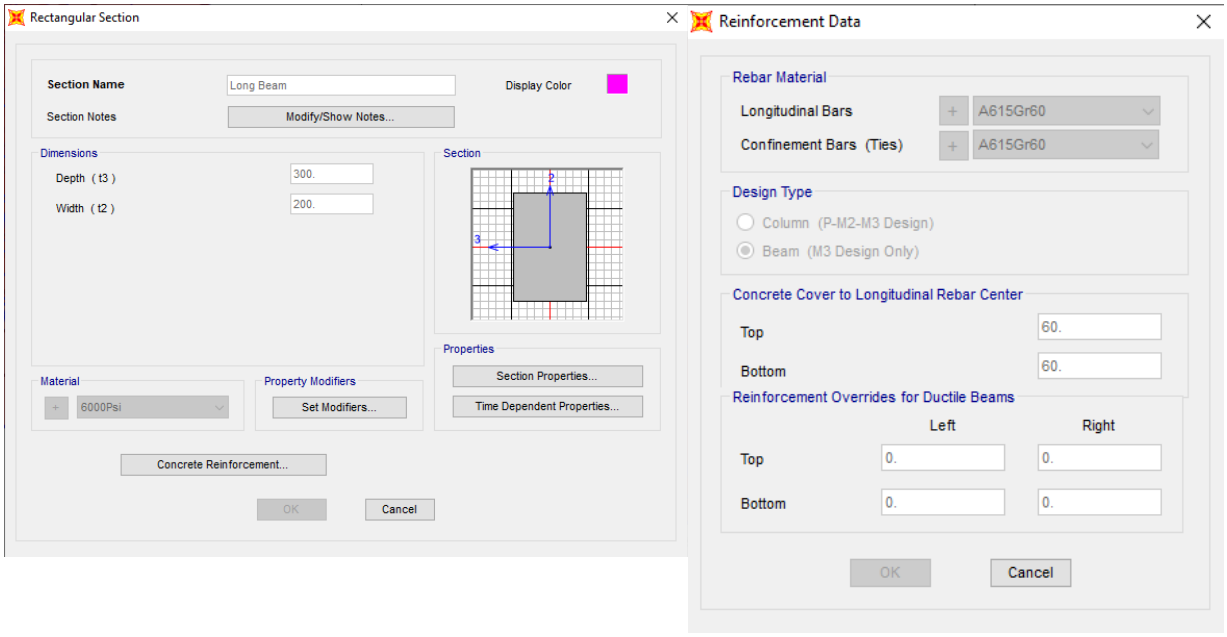


Figure 3-10. Long span frame in SAP 2000

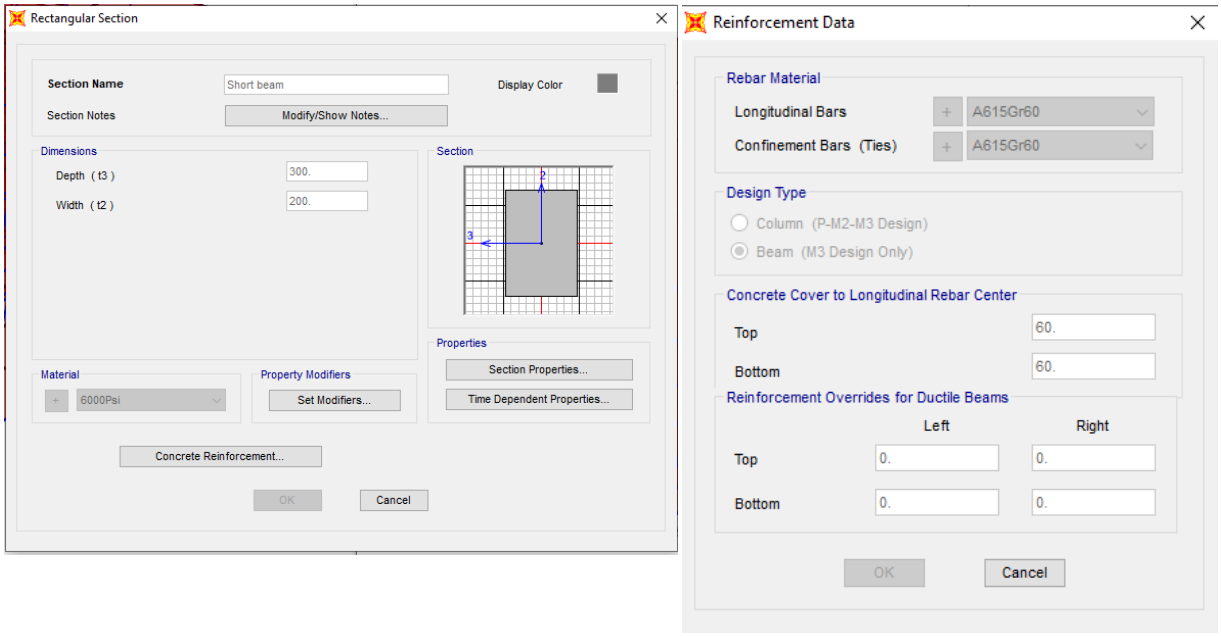


Figure 3-11. Short span frame in SAP 2000

After the frames were defined, load patterns were assigned. There are dead loads, live loads, wind loads and earthquake loads in the building. Seismic load is not considered in California as it was mentioned above.

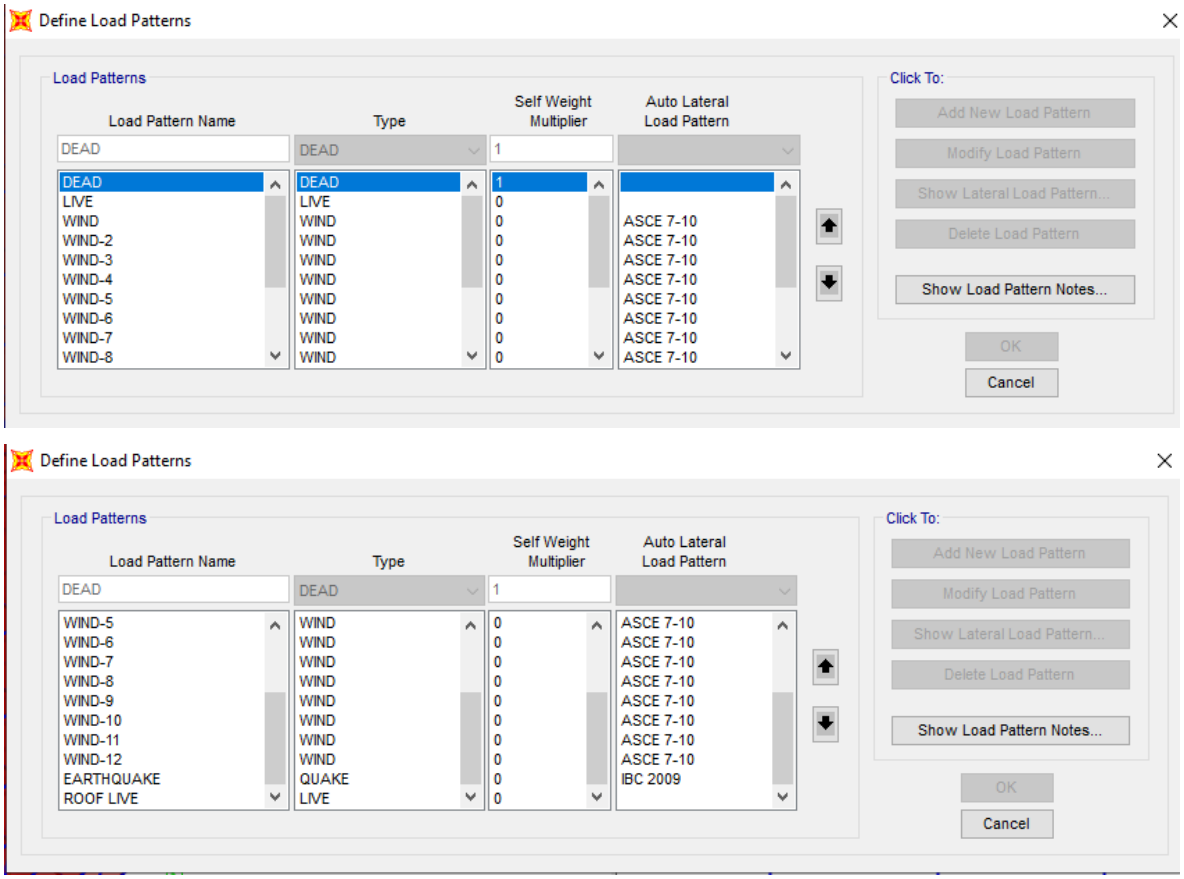


Figure 3-12 Load patterns.

### 3.8.2 Lateral drift

After all of the calculations, it was required to compare lateral drift provided by the SAP2000 and hand calculations. Figure 3-13 demonstrates the graph of drift calculated by SAP2000 and hand calculations. It can be seen that SAP2000 shows less drift for each floor, but mostly two of the drifts have the same pattern in the lateral drift.

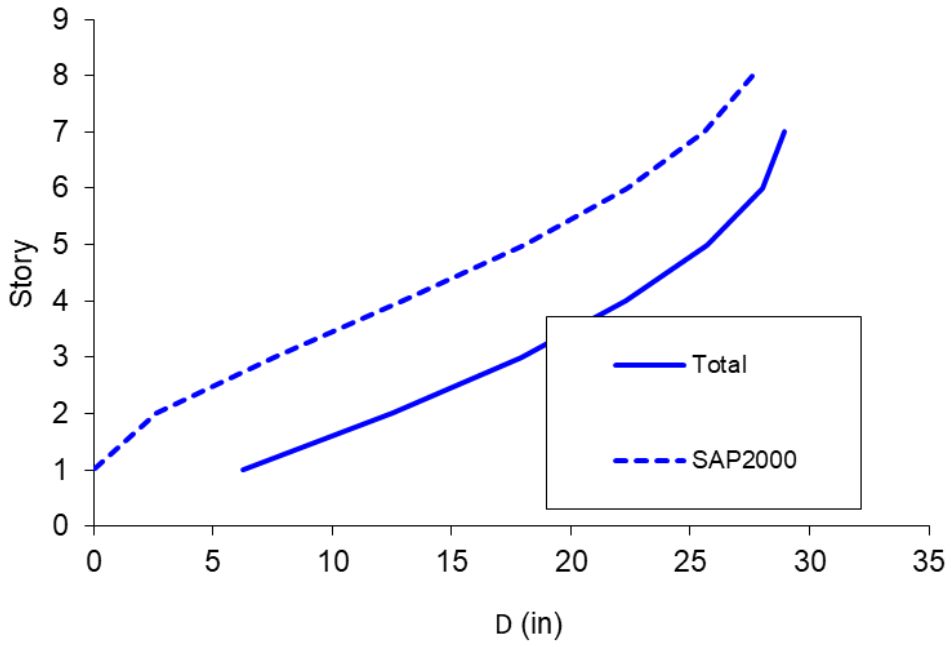


Figure 3-13. Lateral drift comparison.

## 3.9 Structural member design (size or check reinforcement)

### 3.9.1 Member size estimation

#### 3.9.1.1 Beam size

It was decided to use two-end continuous beams, because they have higher stiffness in seismic zones. According to ACI 318-14, minimum depth of the concrete beam is l/21, and minimum width of the beam is d/1.5. Beam size estimation is provided for short and long span

Where:

L- span [mm];

d - depth of the beam [mm].

Table 3-27. Beam size estimation.

| Beam sizing | | |
|---|---|---|
| Span length,mm | Depth (l/21), mm | Width (d/1,5), mm |
| 6700 | 295 | 197 |
| 6000 | 243 | 162 |

After estimation it was decided to use a beam with depth and width equal to 300 mm and 200 mm respectively for both long and short spans.

### 3.9.1.2 Slab thickness

Since the ratio of longer span to shorter is less than 2, a two-way slab system is used. Therefore, it is required to use the ACI 318-14 table to determine the slab thickness.

Table 3-28. Minimum thickness of non-prestressed two-way slabs.

**Table 8.3.1.2—Minimum thickness of nonprestressed two-way slabs with beams spanning between supports on all sides**

| $\alpha_{fm}$[1] | Minimum $h$, mm | | |
|---|---|---|---|
| $\alpha_{fm} \le 0.2$ | 8.3.1.1 applies | | (a) |
| $0.2 < \alpha_{fm} \le 2.0$ | Greater of: | $\dfrac{\ell_n\left(0.8+\dfrac{f_y}{1400}\right)}{36+5\beta\left(\alpha_{fm}-0.2\right)}$ | (b)[2],[3] |
| | | 125 | (c) |
| $\alpha_{fm} > 2.0$ | Greater of: | $\dfrac{\ell_n\left(0.8+\dfrac{f_y}{1400}\right)}{36+9\beta}$ | (d)[2],[3] |
| | | 90 | (e) |

[1] $\alpha_{fm}$ is the average value of $\alpha_f$ for all beams on edges of a panel and $\alpha_f$ shall be calculated in accordance with 8.10.2.7.

[2] $\ell_n$ is the clear span in the long direction, measured face-to-face of beams (mm).

[3] $\beta$ is the ratio of clear spans in long to short directions of slab.

To calculate the value of $\alpha_{fm}$, following equation is used (ACI 318M-14):

> **8.10.2.7** For a panel with beams between supports on all sides, Eq. (8.10.2.7a) shall be satisfied for beams in the two perpendicular directions.
>
> $$0.2 \le \frac{\alpha_{f1}\ell_2^2}{\alpha_{f2}\ell_1^2} \le 5.0 \qquad (8.10.2.7a)$$
>
> where $\alpha_{f1}$ and $\alpha_{f2}$ are calculated by:
>
> $$\alpha_f = \frac{E_{cb}I_b}{E_{cs}I_s} \qquad (8.10.2.7b)$$

For long spang value $\alpha_{f1} = 0.50$, and for short span $\alpha_{f2} = 0.30$. Therefore, value of $\alpha_{fm} = 0.78$. Thus it is required to use the greater value of row (b) or row (c). Using the equation provided in b, value of minimum thickness is 167.63 mm. Therefore, it was decided to use the 170 mm thickness slab.

### 3.9.1.3 Column size

According to the ACI 318 code formulas used to estimate the column size are presented below:

$$Wu = 1.2DL + 1.6LL$$

$$Pu < \varphi Pn$$

$$Pu = n * Wu * At$$

$$\varphi Pn = 0.8 * \varphi * (0.85 * fc' * Ac + fy * As)$$

In Capstone project I, preliminary design of the columns was done. Therefore, for each floor it was decided to use columns 500 mm x 500 mm. Columns do not change in dimensions on the floor to increase their resistance for the loads and prevent any cracking accidents.

## 3.10 Hand verification of SAP 2000 suggestions.

### 3.10.1 Long span beam design

It was required to check the reinforcement provided by SAP2000 software. Figure 3-29 shows hand verification of SAP 2000 suggestions for long span beam.

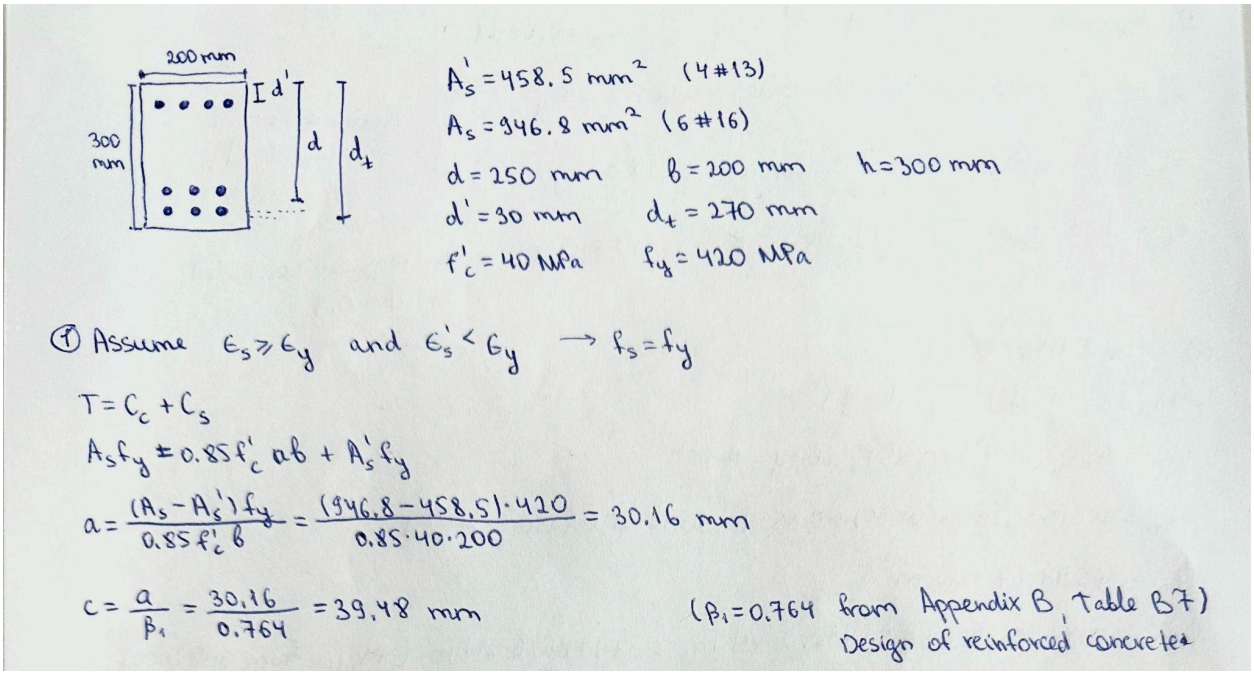

② $\epsilon_y = \frac{f_y}{E_s} = \frac{420}{200000} = 0.0021$

$\epsilon_s = \frac{d-c}{c} \cdot 0.003 = \frac{250-39.48}{39.48} \cdot 0.003 = 0.016 < \epsilon_y$

$\epsilon'_s = \frac{c-d'}{c} \cdot 0.003 = \frac{39.48-30}{39.48} \cdot 0.003 = 0.00072 < \epsilon_y$

$\epsilon_t = \frac{d_t-c}{c} \cdot 0.003 = \frac{270-39.48}{39.48} \cdot 0.003 = 0.0175 > \epsilon_y$

} Assumption is not verified.

③ Recalculate C:

$A_s f_y = 0.85 f'_c ab + A'_s \epsilon'_s E_s$

$A_s f_y = 0.85 f'_c b \beta_1 C + A'_s E_s \cdot 0.003 \cdot \frac{c-d'}{c} \quad | \cdot C$

$A'_s E_s C \cdot 0.003 - A_s f_y C - A'_s E_s d' \cdot 0.003 + 0.85 \cdot 0.764 \cdot f'_c \cdot b C^2 = 0$

$458.5 \cdot 200000 \cdot 0.003 C - 946.8 \cdot 420 C - 458.5 \cdot 200000 \cdot 30 \cdot 0.003 + 0.85 \cdot 0.764 \cdot 40 \cdot 200 \cdot C^2 = 0$

$5780 C^2 - 122556 C - 8253000 = 0$

$C = 49.85$ mm

④ Assume $\epsilon_s \geq \epsilon_y$ and $\epsilon'_s < \epsilon_y$, $\epsilon_y = 0.0021$

$\epsilon'_s = \frac{c-d'}{c} \cdot 0.003 = \frac{49.85-30}{49.85} \cdot 0.003 = 0.00119 < \epsilon_y$

$\epsilon_s = \frac{d-c}{c} \cdot 0.003 = \frac{250-49.85}{49.85} \cdot 0.003 = 0.012 > \epsilon_y$

} assumption is verified.

$\epsilon_t = \frac{d_t-c}{c} \cdot 0.003 = \frac{270-49.85}{49.85} \cdot 0.003 = 0.013 > 0.005 \rightarrow$ Tension controlled.

$\phi = 0.9$

⑤ $+G \sum M_n = 0$

$-M_n + C_s (d-d') + C_c (d - \frac{a}{2}) = 0$

$M_n = A'_s f_y (d-d') + 0.85 f'_c ab (d - \frac{a}{2})$

$M_n = 458.5 \cdot 420 (250-30) + 0.85 \cdot 40 \cdot 30.16 \cdot 200 (250 - \frac{30.16}{2})$

$M_n = 90544.67$ kN·m

$\phi M_n = 0.9 \cdot 90544.67 = 81490.2$ kN·m $>$ 74786.6 kN·m ($M_{ult}$ from SAP2000)

⑥ Check minimum depth:

1) $d_{min} = \sqrt{\frac{M_u}{0.167\, b f_c'}} = \sqrt{\frac{74786.6 \cdot 10^3}{0.167 \cdot 200 \cdot 40}} = 236.6 \text{ mm} < d\ (285 \text{ mm})$

$d = 300 - 15 = 285$ mm

$M_u = 74786.6$ kN·m (from SAP2000)

2) $K = \frac{M_n}{b d^2 f_c'} = \frac{90544.67}{200 \cdot 285^2 \cdot 40} = 0.14$

lever arm, $z = d\left(0.5 + \sqrt{0.25 - \frac{K}{1.134}}\right) = 243.88$ mm

3) $A_s = \frac{M_u}{0.85 f_y z} = \frac{74786.6 \cdot 10^3}{0.85 \cdot 420 \cdot 243.88} = 858.97 \text{ mm}^2$

SAP 2000 Assigned = 874. $mm^2$

Figure 3-14. Hand verification for long span beam

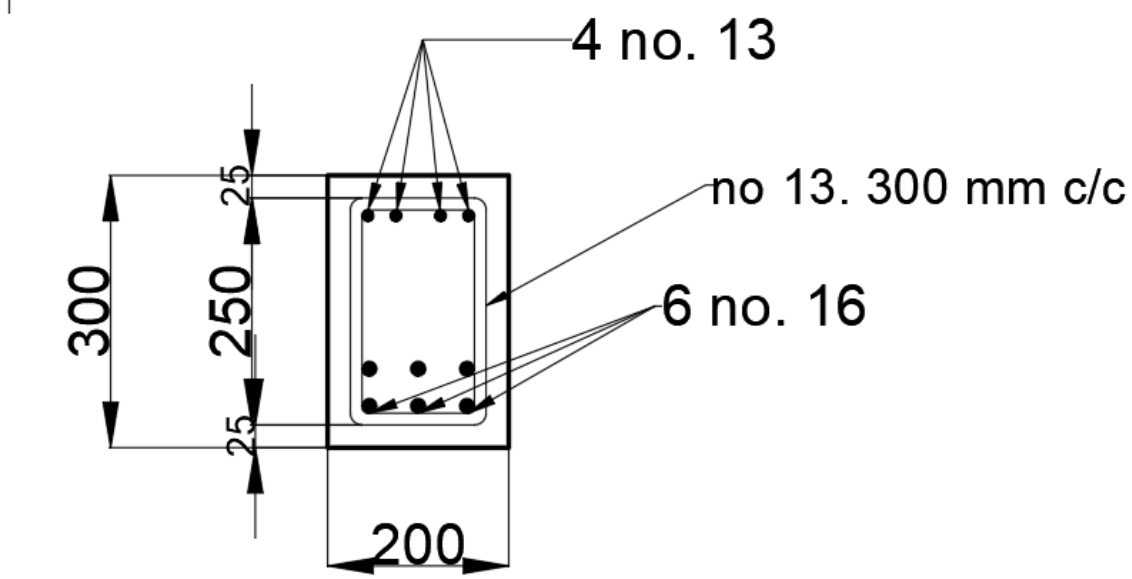

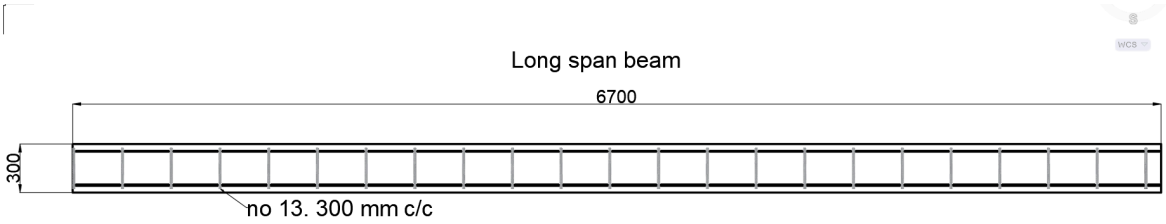


Figure 3-15 Structural detailing of the long span beam

### 3.10.2 Short span beam design

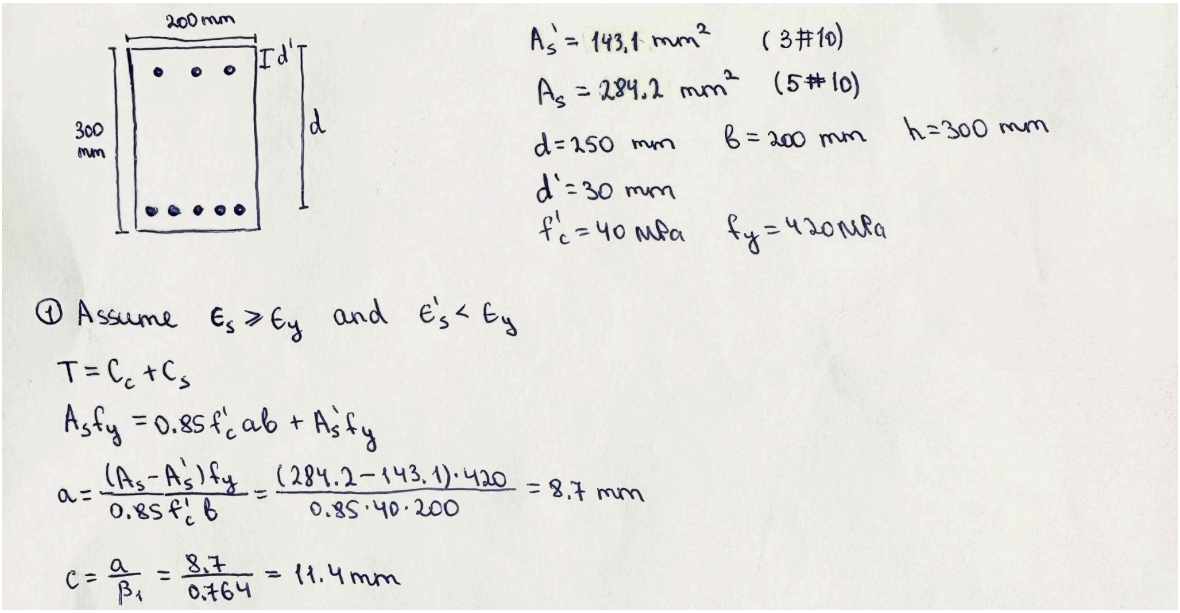

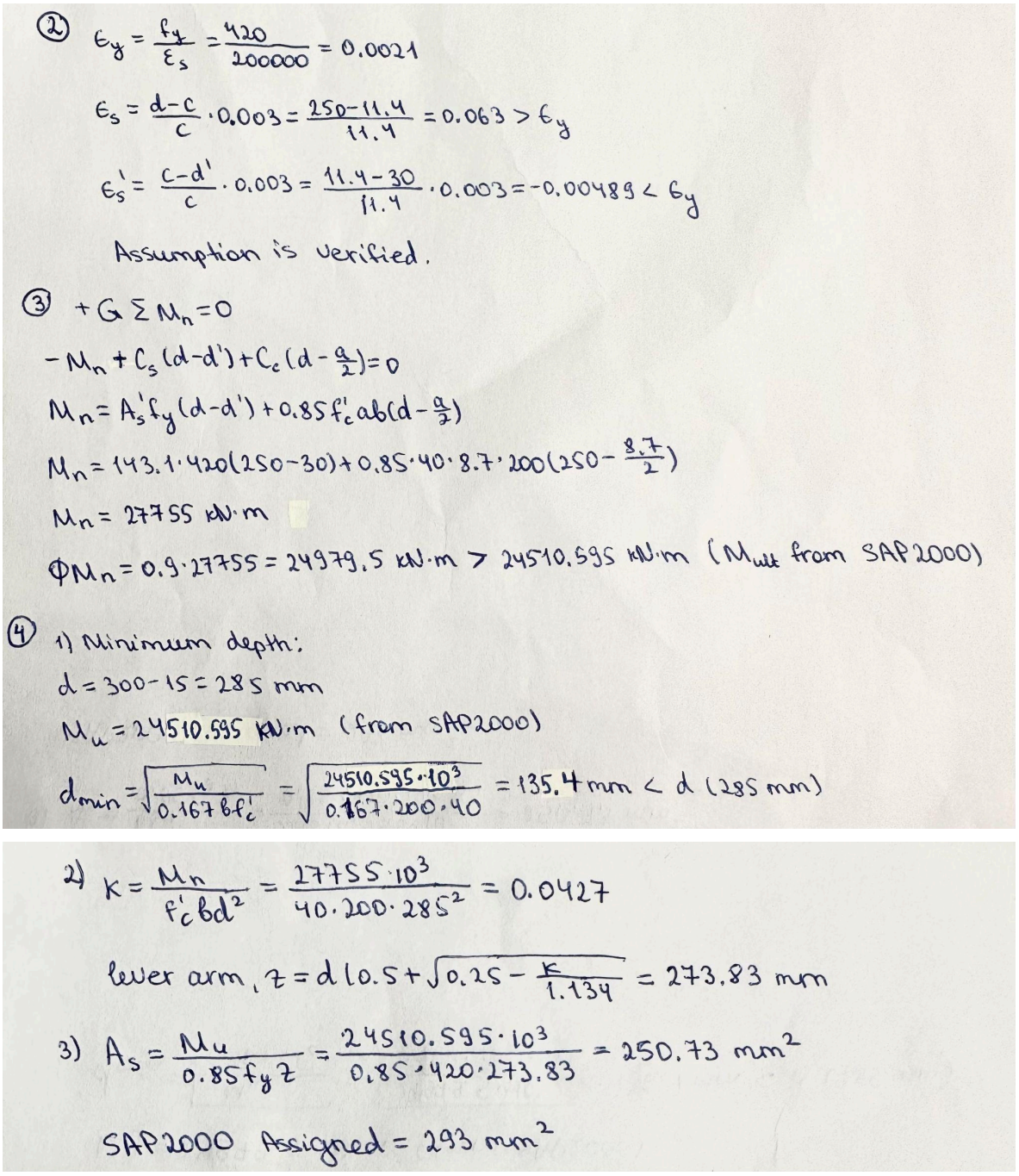


Figure 3-16. Hand verification of short span beam

### 3.10.3 Column design

To check the SAP2000 calculation, a column on the 4th floor was taken. Suggestions provided by the software are in table 3-29.

Table 3-29. Comparison of SAP2000 calculation and manual calculation

| | Size | SAP2000 suggested reinforcement area, mm2 | ⌀Pn, kN | Pu, SAP 2000, kN | Pu, hand calculations, kN |
|---|---|---|---|---|---|
| Column | 500mm x500mm | 10544 | 3464 kN | 4834 | 5329 |

It was decided to use the data provided by SAP 2000. Structural detailing of the column is provided in figure 3-17. According to ACI 315 (1999), spacing between reinforcement bars is less than 150 mm. Therefore ties should be on the edges.

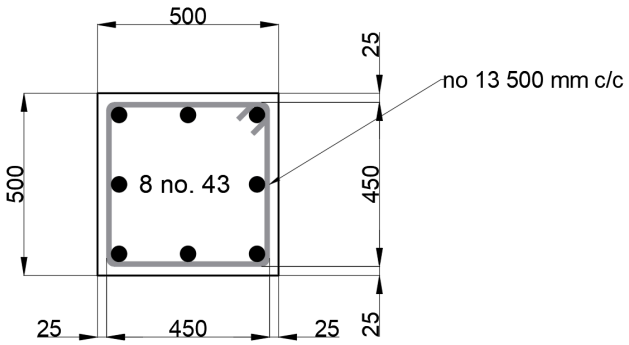

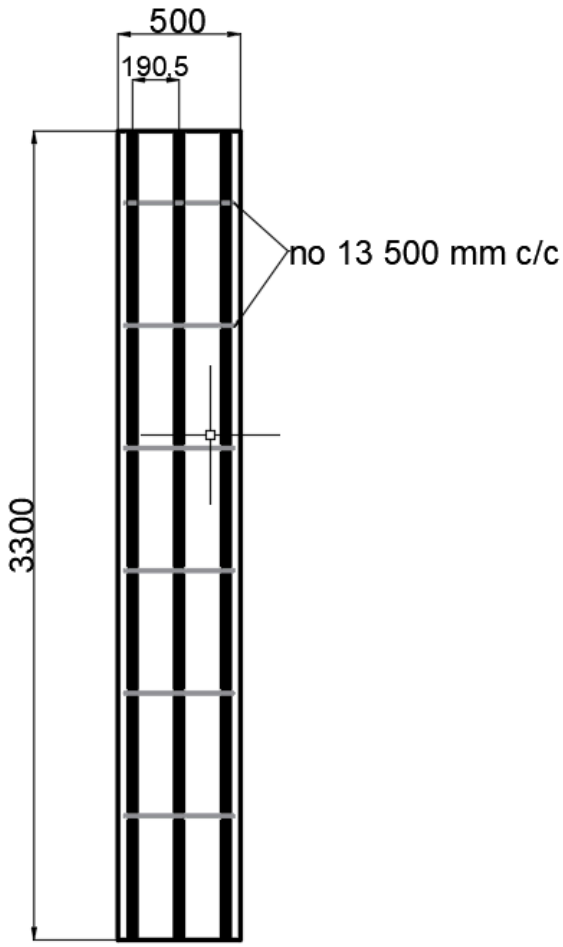


Figure 3-17. structural detailing of concrete column

### 3.10.4 Two-way slab design

Figure 3-18 demonstrates the calculation of a two-way slab. Design procedure was done for the interior panel. Table 3-30 shows the reinforcement for the slab and figure 3-19 represents the structural detailing.

b) Distribution of panel moments in transverse:

$$\frac{l_2}{l_1} = \frac{5}{6.7} = 0.75$$

$$\alpha_{f_1} = \alpha_s = \frac{\sum E I_b}{\sum E I_s} = \frac{\frac{0.2 \cdot 0.3^3}{12}}{\frac{6.7 \cdot 0.17^3}{12}} = 0.18 < 1$$

c) Column strip $= 0.75 M_n = -149.45$ kN·m

Middle strip $= 0.25 M_n = -49.82$ kN·m

(80%): Beam $= 0.8 \cdot (-149.45) = -119.56$ kN·m

(20%): Column strip $= 0.2 \cdot (-149.45) = -29.89$ kN·m

Middle strip $= -49.82$ kN·m

d) CS $= 0.6 M_p = 64.38$ kN·m

MS $= 0.4 M_p = 42.92$ kN·m

Beam $= 0.8 \cdot 64.38 = 51.5$ kN·m

CS $= 0.2 \cdot 64.38 = 12.89$ kN·m

MS $= 42.92$ kN·m

Design moment in short direction: $l_1 = 5$ m

a) $M_n = 0.65 M_{os} = 141.92$ kN·m

$M_p = 0.35 M_{os} = 76.42$ kN·m

b) $\frac{l_2}{l_1} = \frac{6.7}{5} = 1.34$

$$\alpha_{f_2} = \alpha_s = \frac{\sum E I_b}{\sum E I_s} = \frac{\frac{0.2 \cdot 0.3^3}{12}}{\frac{5 \cdot 0.17^3}{12}} = 0.22 < 1$$

$$\alpha_{f_2} \frac{l_2}{l_1} = 1.34 \cdot 0.22 = 0.29 < 1$$

c) CS $= 0.75 M_n = 106.44$ kN·m

MS $= 0.25 M_n = 35.48$ kN·m

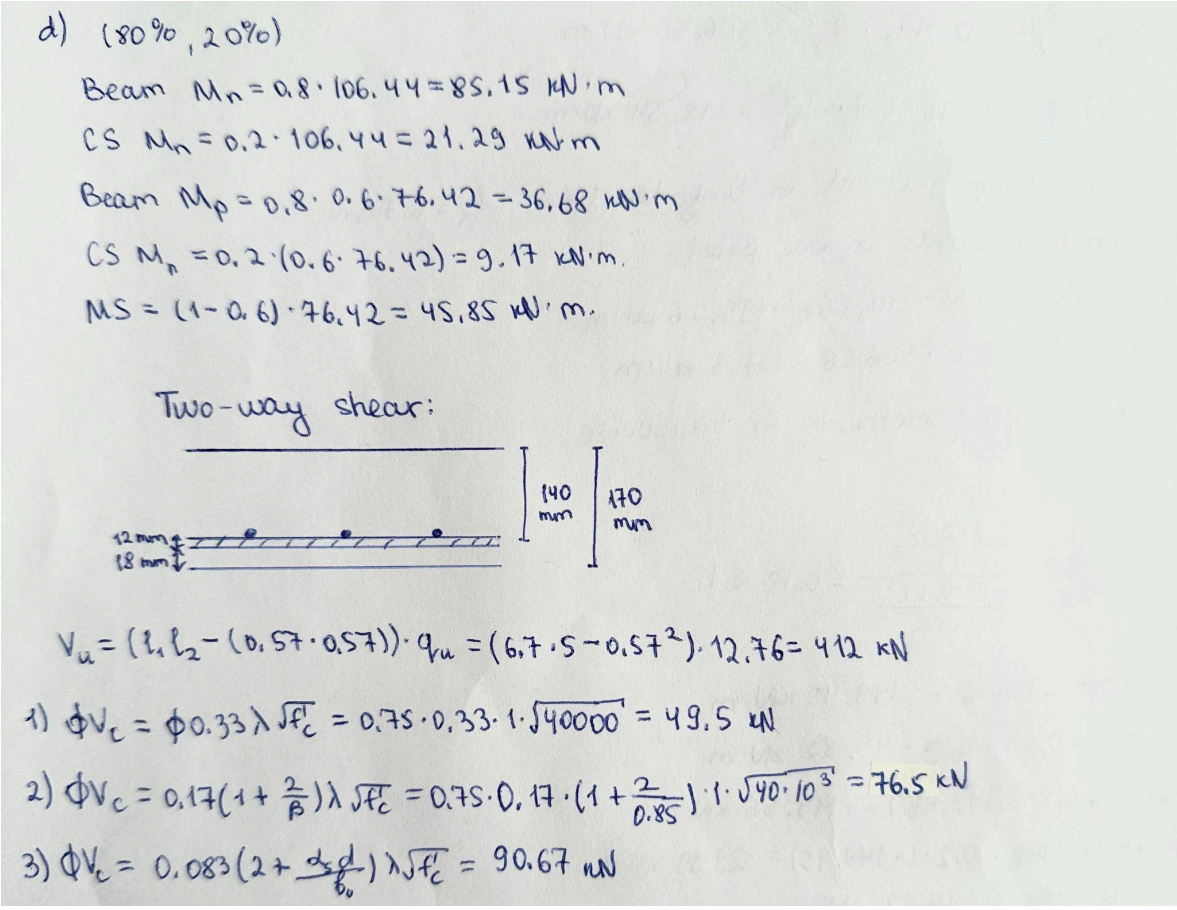


Figure 3-18. Interior panel two-way slab design

Table 3-30 Reinforcement of two way slab

| | Column strip | | Middle Strip | |
|---|---|---|---|---|
| Long direction | (-ve) moment | (+ve) moment | (-ve) moment | (+ve) moment |
| Mu (kN*m) | 29,89 | 12,89 | 49,82 | 42,92 |
| Width strip (mm) | 3350 | 3350 | 3350 | 3350 |
| d (m) | 0,14 | 0,14 | 0,14 | 0,14 |
| b (m) | 0,17 | 0,17 | 0,17 | 0,17 |
| Ru=Mu/ϕbd2 (kN/m2) | 9850,06 | 4247,82 | 16417,86 | 14144,01 |
| Steel ration ρ | 0,03 | 0,01 | 0,07 | 0,05 |
| As = ρbd (mm2) | 677,17 | 257,98 | 1570,14 | 1136,97 |
| Min As = | 428,4 | 428,4 | 428,4 | 428,4 |
| Bars | no. 13 spacing 190 mm c/c | no. 10 spacing 165 mm c/c | no. 19 spacing 180 mm c/c | no. 19 spacing 250 mm c/c |
| Short Direction | | | | |
| Mu (kN*m) | 21,29 | 9,17 | 35,48 | 45,85 |
| Width of strip (mm) | 2500 | 2500 | 2500 | 2500 |
| d (mm) | 0,14 | 0,14 | 0,14 | 0,14 |
| b (mm) | 0,17 | 0,17 | 0,17 | 0,17 |
| Ru=Mu/ϕbd2 (kN/m2) | 7015,98 | 3021,91 | 11692,21 | 15109,57 |
| Steel ration ρ | 0,02 | 0,01 | 0,04 | 0,05 |
| As = ρbd (mm2) | 450,16 | 179,61 | 850,10 | 1284,18 |
| Min As = | 428,4 | 428,4 | 428,4 | 428,4 |
| Bars | no. 10 spacing 150 mm c/c | no. 10 spacing 165 mm c/c | no. 13 spacing 150 mm c/c | no. 16 spacing 165 mm c/c |

Two-Way Slab (Interior Panel)

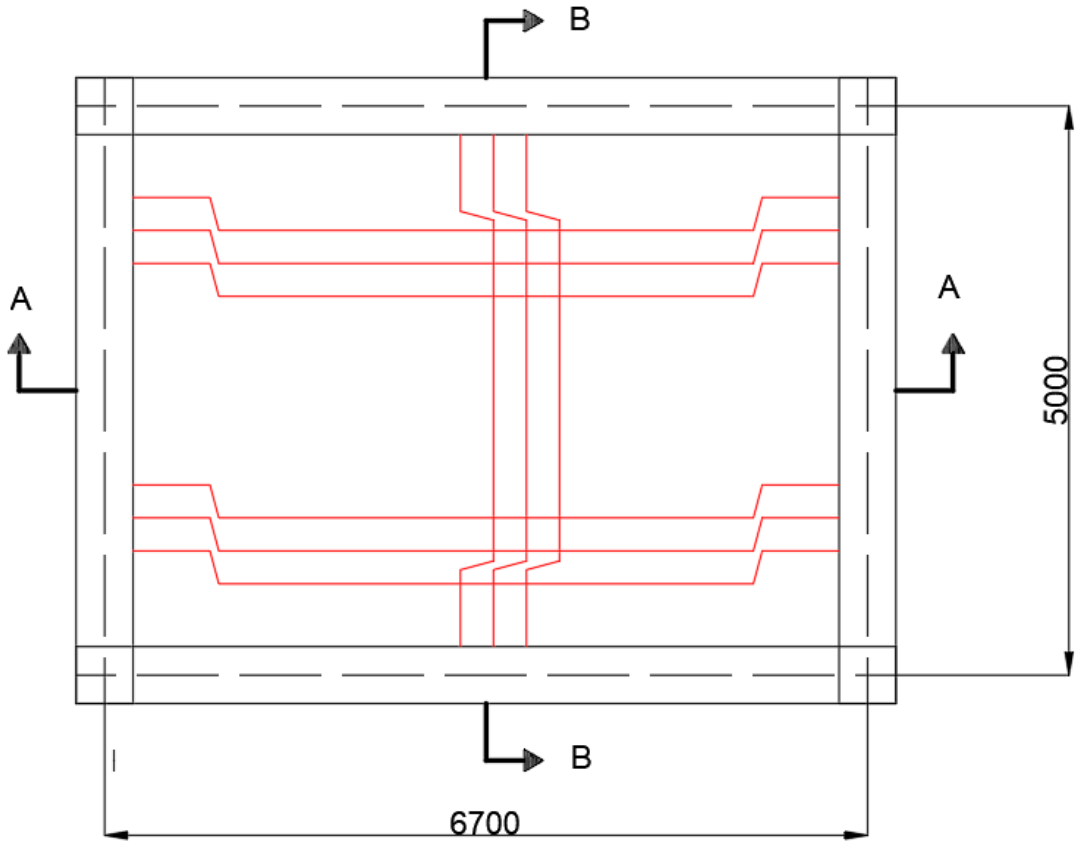


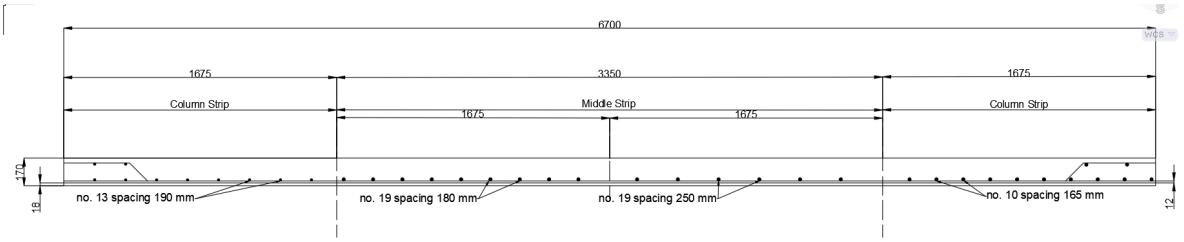


Section AA

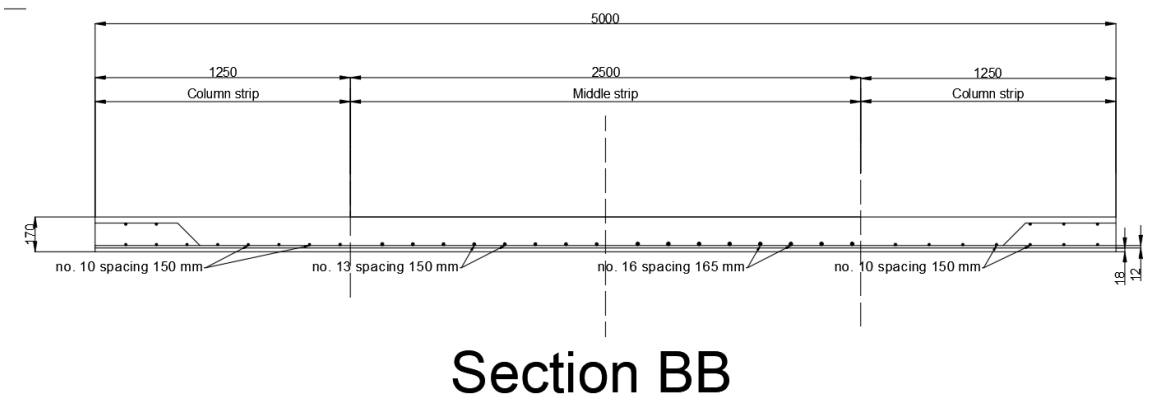


Figure 3-19. Structural detailing of interior panel

## 3.11 Structural serviceability design

### 3.11.1 Vertical deflection

To check vertical deflection, it is first required to calculate the instantaneous short term dead load deflection. Equation is following:

$$\delta_D = \frac{5wl^4}{384E_c I_e}$$

From hand calculations in the Figure 3-20, the value of instantaneous short deflection for dead load is equal to 2.25 m. Next, the short term deflection for live load and dead load was determined. Deflection for live load and dead load $\delta_{D+L}$ is equal to 2.58 m.

To determine long term deflection, following equation is used (ACI 318M-14):

$$\lambda_\Delta = \frac{\xi}{1+50p'} = \frac{2}{1+0} = 2$$

$\xi$ = 2 (according to Table 24.2.4.1.3—Time-dependent factor for sustained loads, ACI 318M-14)

Long term deflection will be the product of $\delta_{D+L}$ and $\lambda_\Delta$, therefore it is equal to 5.16 m.

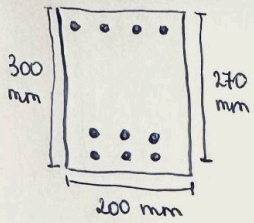


$L = 6.7$ m

$DL = 4.25$ kN/m²

$LL = 4.79$ kN/m²

Major beam

① Short-term Dead load deflection:

$$I_g = \frac{0.2 \cdot 0.3^3}{12} = 4.5 \cdot 10^{-4} \text{ m}^4$$

$$f_r = 7.5\lambda\sqrt{f'_c} = 7.5\sqrt{40000} = 1500 \text{ kN/m}^2$$

$$M_{cr} = \frac{f_r I_g}{y_t} = \frac{1500 \cdot 4.5 \cdot 10^{-4}}{0.15} = 4.5 \text{ kN·m}$$

$$M_a = \frac{q_D L^2}{8} = \frac{4.25 \cdot 6.7^2}{8} = 23.85 \text{ kN·m}$$

$$E_c = 4700\sqrt{f'_c} = 4700\sqrt{40000} = 94 \cdot 10^4 \text{ kN/m}^2$$

$$I_e = \left(\frac{M_{cr}}{M_a}\right)^3 \cdot I_g + \left(1 - \left(\frac{M_{cr}}{M_a}\right)^3\right) \cdot I_{cr}$$

$$n = \frac{E_s}{E_c} = \frac{20 \cdot 10^4}{94 \cdot 10^4} = 0.21$$

$$100x^2 = (270 - x) \cdot 946.7 \cdot 0.21$$

$$x = 22.2 \text{ mm} = 0.022 \text{ m}$$

$$I_{cr} = \frac{0.2 \cdot 0.022^3}{3} + 0.21 \cdot 0.946 \cdot 10^{-3} \cdot 0.2478 = 5 \cdot 10^{-5} \text{ m}^4$$

$$I_e = \left(\frac{4.5}{23.85}\right)^3 \cdot 4.5 \cdot 10^{-4} + \left(1 - \left(\frac{4.5}{23.85}\right)^3\right) \cdot 5 \cdot 10^{-5} = 5.27 \cdot 10^{-5} \text{ m}^4$$

$$\delta_D = \frac{5wl^4}{384 E_c I_e} = \frac{5 \cdot 4.25 \cdot 6.7^4}{384 \cdot 94 \cdot 10^4 \cdot 5.27 \cdot 10^{-5}} = 2.25 \text{ m}$$

② Short-term deflection for Dead + Live load:

$$M_a = \frac{4.79 \cdot 6.7^2}{8} = 26.88 \text{ kN·m}$$

$$I_e = \left(\frac{4.5}{26.88}\right)^3 \cdot 4.5 \cdot 10^{-4} + \left(1 - \left(\frac{4.5}{26.88}\right)^3\right) \cdot 5 \cdot 10^{-5} = 5.19 \cdot 10^{-5} \text{ m}^4$$

$$\delta_{D+L} = \frac{5 \cdot 4.79 \cdot 6.7^4}{384 \cdot 94 \cdot 10^4 \cdot 5.19 \cdot 10^{-5}} = 2.58 \text{ m}$$

③ Deflection for full Live load:

$$\delta_L = \delta_{D+L} - \delta_D = 2.58 - 2.25 = 0.33 \text{ m}$$

Figure 3-20. Deflection calculation for major beam

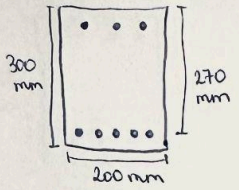


$L = 6.7\ m$

$DL = 4.25\ kN/m^2$

$LL = 4.79\ kN/m^2$

Minor beam

① Short-term dead load deflection:

$$I_g = \frac{0.2 \cdot 0.3^3}{12} = 4.5 \cdot 10^{-4}\ m^4$$

$$f_r = 7.5\lambda\sqrt{f'_c} = 1500\ kN/m^2$$

$$M_{cr} = \frac{f_r I_g}{y_t} = \frac{1500 \cdot 4.5 \cdot 10^{-4}}{0.15} = 4.5\ kN \cdot m$$

$$M_a = \frac{q_D L^2}{8} = \frac{4.25 \cdot 6.7^2}{8} = 23.85\ kN \cdot m$$

$$E_c = 4700\sqrt{f'_c} = 94 \cdot 10^4\ kN/m^2$$

$$I_e = \left(\frac{M_{cr}}{M_a}\right)^3 \cdot I_g + \left(1 - \left(\frac{M_{cr}}{M_a}\right)^3\right) \cdot I_{cr}$$

$n = 0.21$

$100x^2 = (270 - x) \cdot 284.2 \cdot 0.21$

$x = 12.4\ mm = 0.0124\ m$

$$I_{cr} = \frac{0.2 \cdot 0.0124^3}{3} + 0.21 \cdot 0.2842 \cdot 10^{-3} \cdot 0.2576 = 1.55 \cdot 10^{-5}\ m^4$$

$$\delta_D = \frac{5wl^4}{384 E_c I_e} = \frac{5 \cdot 4.25 \cdot 6.7^4}{384 \cdot 94 \cdot 10^4 \cdot}$$

$$I_e = \left(\frac{4.5}{23.85}\right)^3 \cdot 4.5 \cdot 10^{-4} + \left(1 - \left(\frac{4.5}{23.85}\right)^3\right) \cdot 1.55 \cdot 10^{-5} = 1.84 \cdot 10^{-5}\ m^4$$

$$\delta_D = \frac{5wl^4}{384 E_c I_e} = \frac{5 \cdot 4.25 \cdot 6.7^4}{384 \cdot 94 \cdot 10^4 \cdot 1.84 \cdot 10^{-5}} = 6.45\ m$$

② Short-term deflection for Dead + Live load:

$$M_a = \frac{4.79 \cdot 6.7^2}{8} = 26.88\ kN \cdot m$$

$$I_e = \left(\frac{4.5}{26.88}\right)^3 \cdot 4.5 \cdot 10^{-4} + \left(1 - \left(\frac{4.5}{26.88}\right)^3\right) \cdot 1.55 \cdot 10^{-5} = 1.75 \cdot 10^{-5}\ m^4$$

$$\delta_{D+L} = \frac{5 \cdot 4.79 \cdot 6.7^4}{384 \cdot 94 \cdot 10^4 \cdot 1.75 \cdot 10^{-5}} = 7.64\ m$$

③ Deflection for full live load:

$$\delta_L = \delta_{D+L} - \delta_D = 7.64 - 6.45 = 1.19\ m.$$

Figure 3-21. Deflection calculation for minor beam

### 3.11.2 Crack width

To determine the crack width, the following formula was used:

$$w = 0.0113\beta_h f_s \sqrt[3]{d_c A}$$

Where

$w$ = the estimated crack width

$\beta_h$ = ratio of the distance to the neutral axis from the extreme tension concrete fiber to the distance from the neutral axis to the centroid of the tensile steel

$f_s$ = steel stress

$d_c$ = the cover of the outermost bar

$A$ = the effective tension area of concrete around the main reinforcement

Calculation of crack width:

The value of $\beta_h$ is assumed to be 1.20, so that when the expression is applied to a beam, reasonable results are obtained.

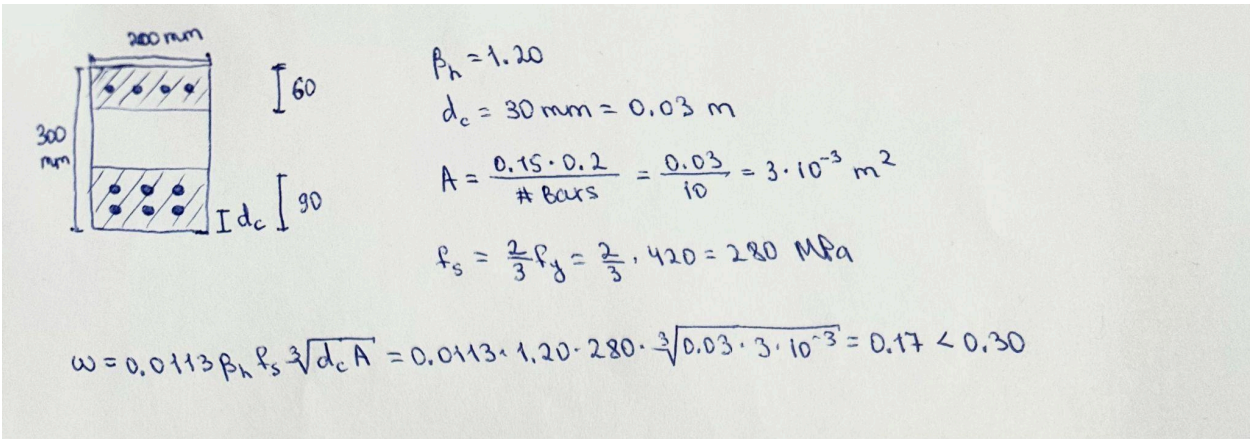


Figure 3-22. Crack width calculation

The following figure shows the reasonable crack widths for different exposure conditions.

| Exposure Condition | Permissible Crack Widths (in.) | (mm) |
|---|---|---|
| Dry air or protective membrane | 0.016 | 0.41 |
| Humidity, Moist air, soil | 0.012 | 0.30 |
| Deicing chemicals | 0.007 | 0.18 |
| Seawater and seawater spray, wetting and drying | 0.006 | 0.15 |
| Water-retaining structures | 0.004 | 0.10 |

*Source*: Reproduced with permission from the American Concrete Institute.

Figure 3-23. Guide to reasonable crack widths

In our case, it is Humidity, Moist air, soil. The result obtained from hand calculation is 0.17 mm, which is less than the permissible crack width of 0.30 mm.

## 3.12 Joint design

Due to the fact that the building is located in a seismic zone, it was decided to use the joint design type 2. Joint design is conducted with use of ACI 352R-02. Two types of joints are created: interior and corner joints.

### 3.12.1 Interior joint design

Interior joint design is made for the column in the middle of the building. Figure 3-24 demonstrates the connection between column and joints. Figure 3-25 shows the calculation of the joint design. Figure 3-26 shows the joint design of the beam and column.

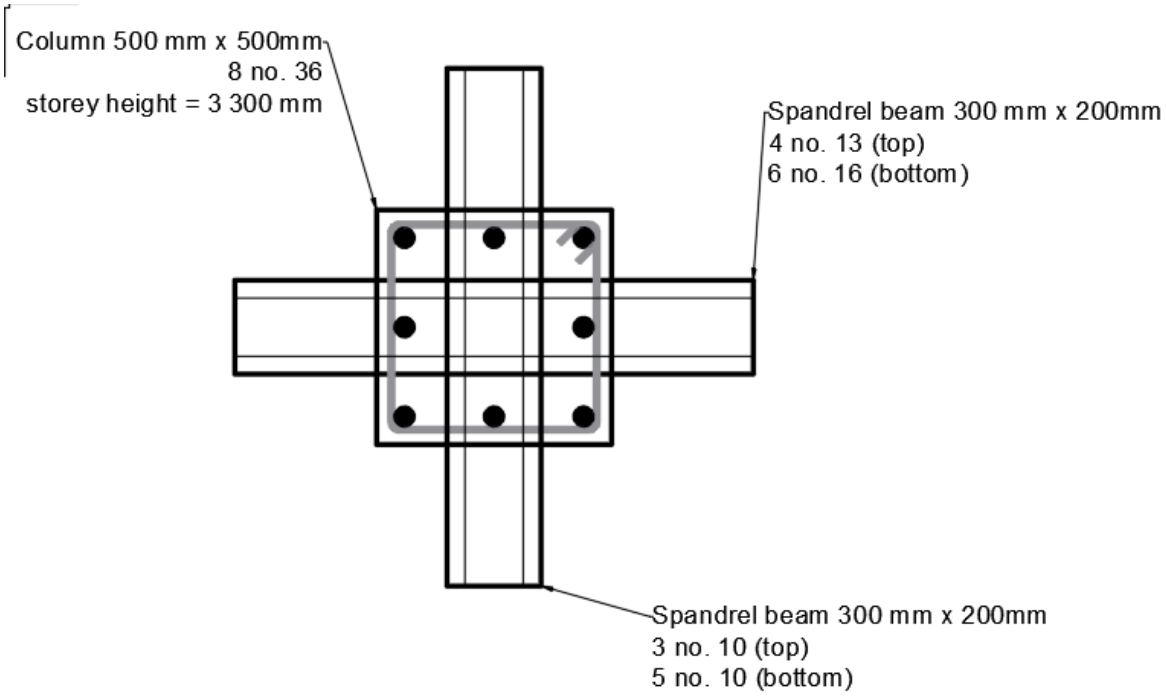


Figure 3-24. Interior joint

Interior & joint

$A_{sh}$ = 4 legs = $4 \cdot 129 = 516\ mm^2$

$s_h \leq \begin{cases} b_c/4 = 500/4 = 125mm \\ 6d_b = 6 \cdot 4\ 3mm = 258mm \\ 150\ mm \end{cases}$

$$A_{sh} = \frac{0,3 \cdot s_h b_c'' f_c'}{f_{yh}} \left(\frac{A_g}{A_c} - 1\right) > A_{sh} = 0,09 \frac{s_h b_c'' f_c'}{f_{yh}}$$

$$A_{sh} = \frac{0,3 \cdot 125 \cdot 430 \cdot 40}{420} \cdot \left(\frac{500^2}{430^2} - 1\right) = 376,48\ 540 mm^2$$

$$A_{sh} = \frac{0,09 \cdot 125 \cdot 430 \cdot 40}{420} = 460\ mm^2$$

$540 > 460$ (OK)

Required $A_{sh}$ :=

$A_{sh} = 0,5 \cdot 540 = 270 < 516$ (ok)

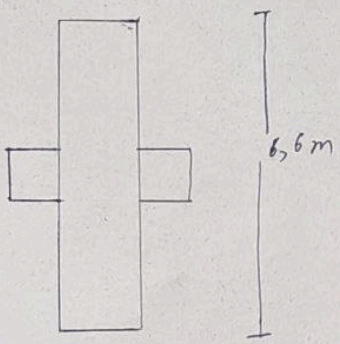


$$M_{pr,B} = A_s \alpha f_y \left(d - \frac{a}{2}\right)$$

$$a = \frac{A_s \alpha f_y}{0,85 f_c' b}$$

For (+ve)

$$a = \frac{A_s \alpha f_y}{0,85 f_c' b} = \frac{284 \cdot 125 \cdot 420}{0,85 \cdot 40 \cdot 200}$$

$= 21mm$

$M_{pr,1} = 284 \cdot 1,25 \cdot 420 \cdot (300 - \frac{21}{2}) =$

$= 43164\ kN \cdot mm$

For (-)ve

$$a = \frac{143,1 \cdot 1,25 \cdot 420}{0,85 \cdot 40 \cdot 200} = 11,05\ mm$$

$$M_{pr2} = 143,1 \cdot 1,25 \cdot 420 \cdot (300 - \frac{11,05}{2}) = 22123\ kN \cdot mm$$

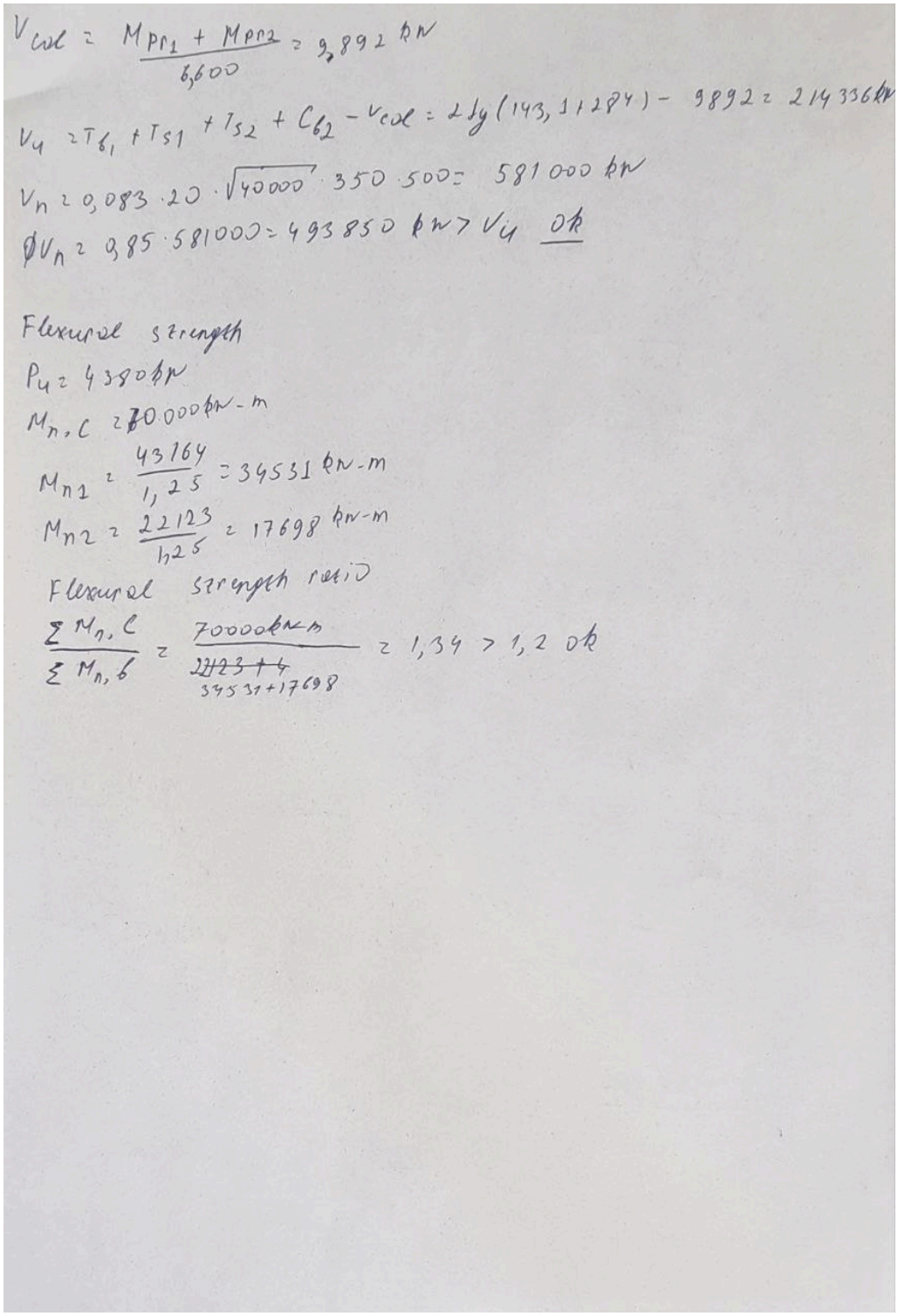


Figure 3-25. Interior column joint design

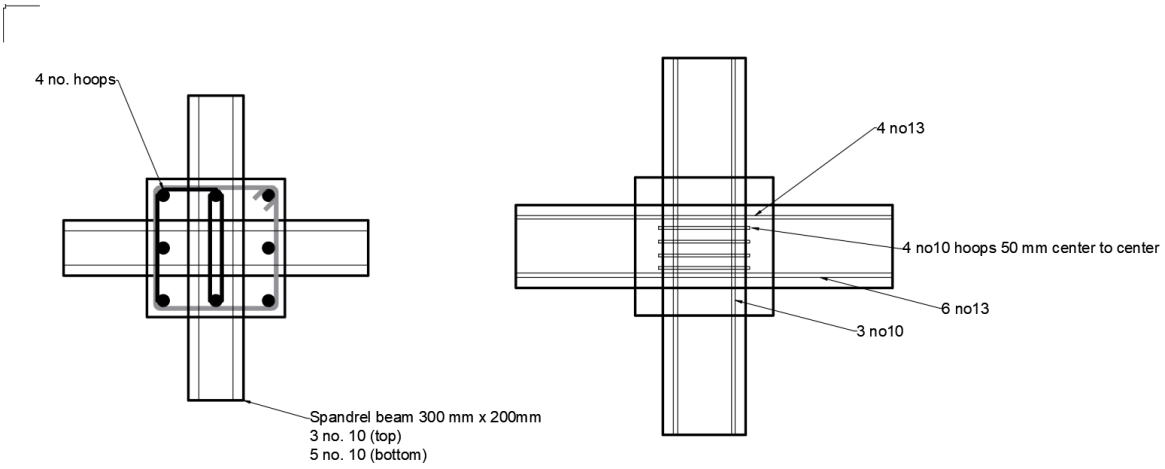


Figure 3-26. Interior joint design.

### 3.12.1 Corner joint design

Corner joint design is made for the column in the middle of the building. Figure 3-27 demonstrates the connection between column and joints, N-S direction is the long span beam and W-E direction is short beam span. Figure 3-28 shows the calculation of the joint design. Figure 3-29 shows the joint design of the beam and column.

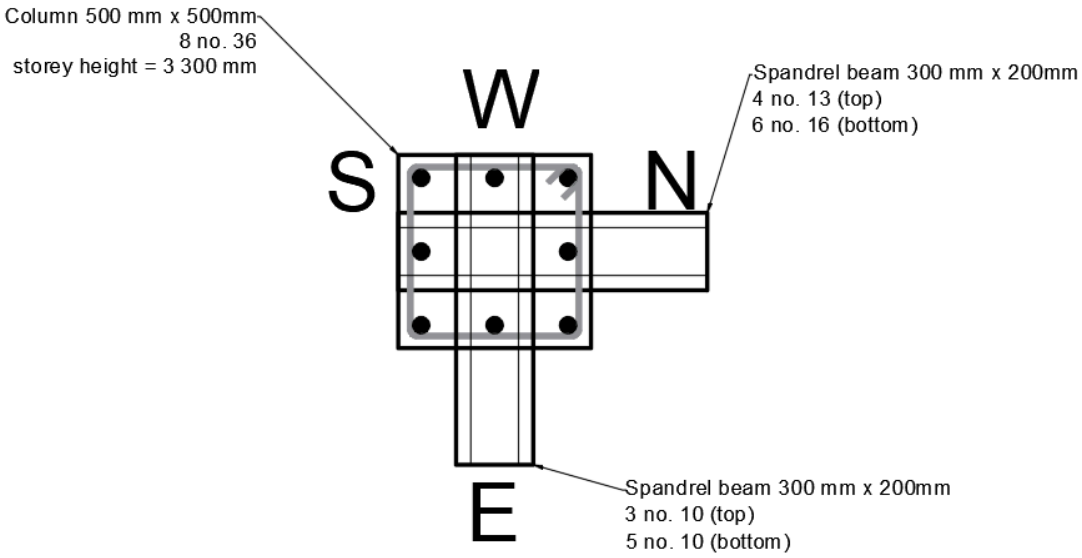


Figure 3-27. Corner column connection

Corner joint

$$A_{sh} = 0,3 \cdot \frac{125 \cdot 430 \cdot 40}{420} \cdot \left(\frac{500^2}{450^2} - 1\right) = 540\,mm^2$$

$$A_{sh} = \frac{0,09 \cdot 125 \cdot 430 \cdot 40}{420} = 460\,mm^2$$

$540 > 460$ (ok)

N-S

$$M_{pr,N-S} = [458,5 + 946,8] \cdot 1,25 \cdot 420 = 737782\,kN$$

E-W

$$M_{pr,E-W} = [143,2 + 284,2] \cdot 1,25 \cdot 420 = 224385\,kN$$

Column shear

$$V_{col;N-S} = \frac{M_{pr,N-S}}{6,6} = 111,785\,kN\text{-}m$$

$$V_{col,E-W} = \frac{M_{pr,E-W}}{6,6} = 34,000\,kN\text{-}m$$

$$V_{u\,N-S} = 626,15$$

$$V_{u\,E-W} = (143,2 + 284,2) \cdot 1,25 \cdot 420k - 38 = 186,39$$

$$V_n = \gamma \cdot \sqrt{f'_c}\, b_j\, h_c$$

N-S

$$b_j \leq \begin{cases} \frac{b_c + b_b}{2} = 350mm \\ b_b + \varepsilon \frac{m \cdot h_c}{2} = 700mm \\ b_c = 500mm \end{cases}$$

$$\phi V_n = 0,85 \cdot 12 \cdot \sqrt{40000} \cdot 350 \cdot 500 = 35700$$

$$\phi V_n > V_u$$

E-W

$$\phi V_n = 0,85 \cdot 12 \cdot \sqrt{40000} \cdot 350 \cdot 500 = 35700$$

$$\phi V_n > V_u$$

Figure 3-28. Joint design calculation

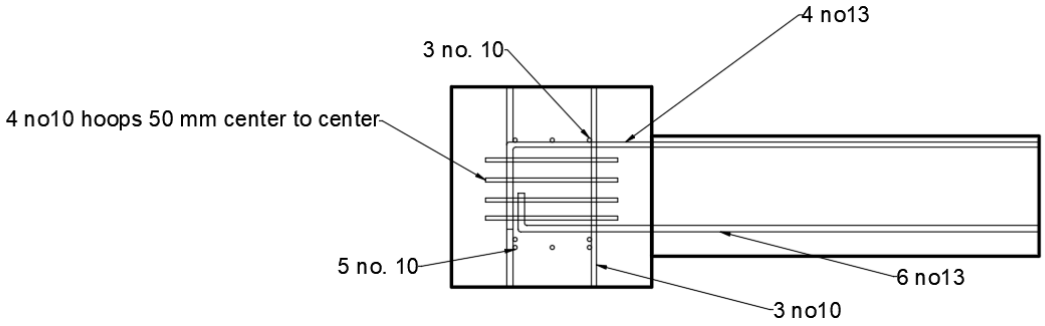


Figure 3-29. Joint design

# 4. GEOTECHNICAL DESIGN

The site description and soil profile, which provides the characteristics of the soil strata with reasoning, were incorporated in the geotechnical design of Capstone. The examination of liquefaction is carried out because sand layers persist. The effectiveness and bearing capability of various foundations have been examined. A pile foundation's level of settling was also examined.

## 4.1 Site description

The characteristics of the soil was fully tested by SOUTHERN CALIFORNIA GEOTECHNICAL, INC. by the request of government agencies. In order to provide criteria for designing the structure foundations, structure floor slabs, and parking lot pavements, along with site preparation recommendations and construction considerations for the proposed development, the scope of services included a visual site reconnaissance, subsurface exploration, field and laboratory testing, and geotechnical engineering analysis. This analysis also includes a site-specific liquefaction evaluation based on the location of the subject site. The scope of this geotechnical investigation's services did not include evaluating the site's environmental elements.

Five (5) borings were progressed 15 to 50 feet below the site's current grade as part of the subsurface research for this project. As part of the liquefaction assessment, the 50-foot deep digging was progressed at the location. One of the staff members recorded every boring as it was being drilled. Hollow-stem augers were used to progress the borings by a drilling rig with limited access that was positioned on a track. During drilling, representative bulk and mostly undisturbed soil samples were collected. Using a split barrel "California Sampler" with a succession of one-inch-long, 2.416-inch-diameter metal rings, relatively undisturbed soil samples were collected.ASTM Test Method D-3550 details this sampling strategy. In general compliance with ASTM D-1586, in-situ samples were also collected utilizing a 1.4 inch inner diameter split spoon sampler. With a series of strikes from a 140-pound weight that drops 30 inches, both of these samplers are pushed into the earth. For further study, the blow counts collected while driving are recorded. To keep the bulk samples' natural moisture content, they were gathered in plastic bags. The largely undisturbed ring samples were put in plastic sleeves that had been formed, sealed, and brought to lab.

All borings were resulted with almost similar characteristics of soil and all borings have shown that soil has clayley and silty sand structure. The data from the deepest boring B1 is shown below. B1 is also the closest boring to the location of our building which is desirable to be

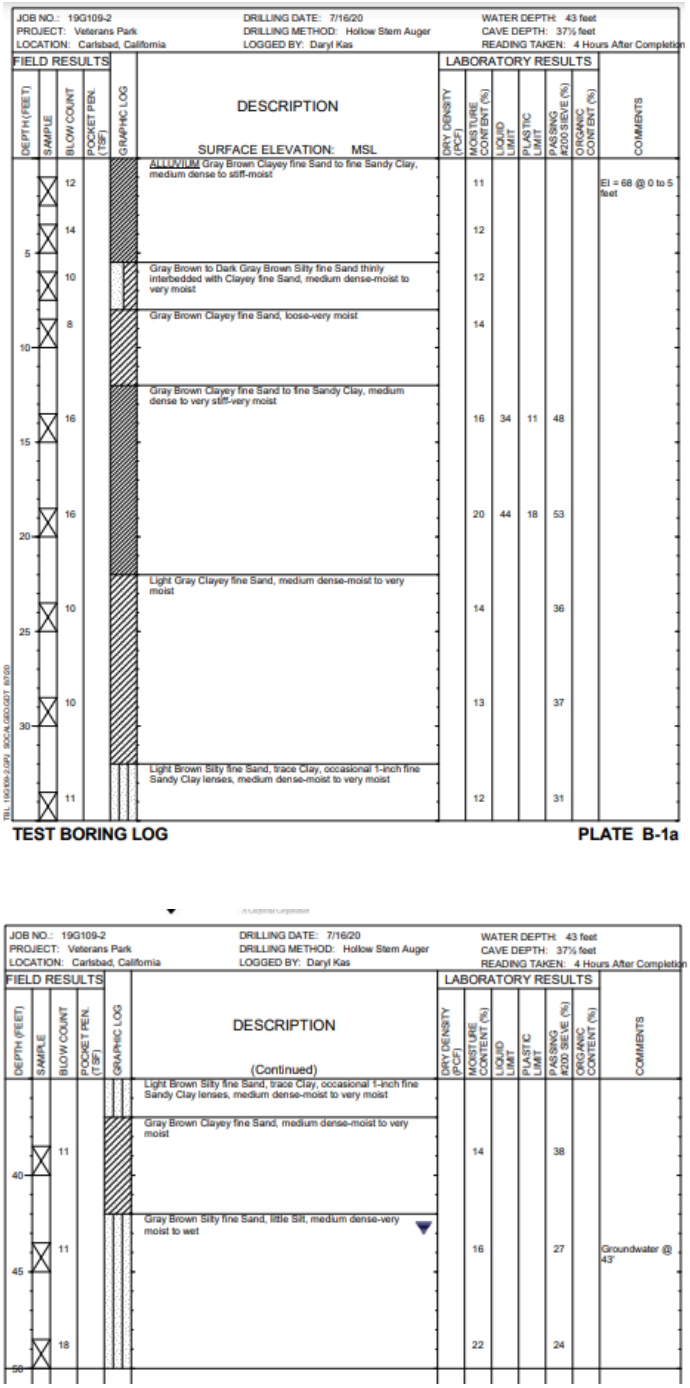


Figure 4-1. Soil profile with properties obtained from the boring

## 4.2 Soil Classification

The HARDENING SOIL MODEL - A PRACTICAL GUIDEBOOK Z Soil.PC

100701 report (2012) by Obrzud R. & Truty and the outcomes of field testing were utilized to determine the friction angles of soil layers. Swiss Standard SN 670 010b, Characteristic Coefficients of soils was used to identify cohesion. Layers upper 3.7 m will be excavated in order to build the basement, so the calculations will be carried out for layers under the basement. The table contained all the data that was required to determine the bearing capacity.

Table 4-1. Soil properties

| № | Soil layer | Soil Classification (USCS) | Depth (m) | Thickness (m) | Friction angle ϕ (deg) | Unit weight ($kN/m^3$) | Cohesion (kPa) | SPT N value |
|---|---|---|---|---|---|---|---|---|
| 2 | Light Gray Clayey fine Sand | SC | -7.00-9.75 | 2.75 | 30 | 18.87 | 11 | 30 |
| 3 | Light Brown Silty fine Sand | SM | -9.75-11.28 | 1.53 | 29 | 18.87 | 14 | 27 |
| 4 | Gray Brown Clayey fine Sand | SC | -11.28-12.80 | 1.52 | 31 | 18.87 | 11 | 30 |
| 5 | Gray Brown Silty fine Sand | SM | -12.80-15.24 | 2.44 | 28 | 18.87 | 14 | 29 |
| 6 | Bedrock | -- | -15.24-- | -- | | | | |

The determination of friction angle for each soil was performed using three methods described below. The results of each method were presented in the following table. Average value of all results was chosen as a friction angle.

Table 4-2. Summary of methods for calculating friction angles

| Method № | Equation | Reference |
|---|---|---|
| 1 | $\phi' = 27.5 + 9.2log[(N_1)_{60}]$ | Kulhawy and Chen, 2007 |
| 2 | $\phi' = \sqrt{20(N_1)_{60}} + 20$ | Hatanaka and Uchida, 1996 |
| 3 | $\phi' = tan^{-1}(\frac{N_{60}}{(12.2+20.3(\frac{\sigma'_{vo}}{p_a}))})^{0.34}$ | Schmertmann, 1975 |

Table 4-3. Results of effective friction angle correlation

| Soil layer № | N60 value | Overburden stress | y | delta z | (N1)60 | phi1 | phi2 | phi3 | phi ave |
|---|---|---|---|---|---|---|---|---|---|
| 1 | 13.0 | 57.36 | 18.87 | 3.05 | 17 | 38.8 | 38.4 | 38.4 | 38.5 |
| 2 | 10.0 | 57.55 | 18.87 | 3.04 | 13 | 37.7 | 36.1 | 36.5 | 36.8 |
| 3 | 10.0 | 28.87 | 18.87 | 1.53 | 13 | 37.7 | 36.1 | 35.4 | 36.4 |
| 4 | 18.0 | 28.68 | 18.87 | 1.52 | 24 | 40.2 | 41.9 | 40.5 | 40.9 |
| 5 | 5.0 | 46.04 | 18.87 | 2.44 | 7 | 35.3 | 31.8 | 33.2 | 33.4 |

**4.3 Liquefaction Analysis**

An analysis of the soil's liquefaction is the following study that is performed. When a solid soil behaves in a more viscous way due to liquefaction phenomenon, which causes

ground failure occurrence, the soil loses its strength and rigidity as a result of earthquake shaking or other abrupt loadings (Huang & Yu, 2013). It implies that the soil's ability to resist the weight of structures is declining because of time and natural circumstances, which leads buildings to sink and be demolished.

Using the SPT information obtained from field testing, the liquefaction of the project soil in the California region was evaluated. There are basic three steps in calculation of liquefaction potential (Duman et. al, 2015):

1. Calculation of Cyclic Stress Ratio (CSR).
2. Calculation of Cyclic Resistance Ratio (CRR).
3. Evaluate the liquefaction potential by calculation of the Factor of Safety against liquefaction.

**Calculation of Cyclic Stress Ratio (CSR)**

Cyclic Stress Ratio is calculated by using the following formula:

$$CSR = 0.65 \frac{a_{max}}{g} \frac{\sigma_{vo}}{\sigma'_{vo}} * r_d$$

,where $\alpha_{max}$ is the peak ground acceleration (PGA), g is an acceleration of gravity, $\sigma_{vo}$ is total vertical stress, $\sigma'_{vo}$ is effective vertical stress at depth which is the length of pipe, $r_d$ is a stress reduction factor.

According to the Peak Ground Acceleration Seismic Map, PGA value for Carlsbad, California is 0,3871 ($\alpha_{max}$).

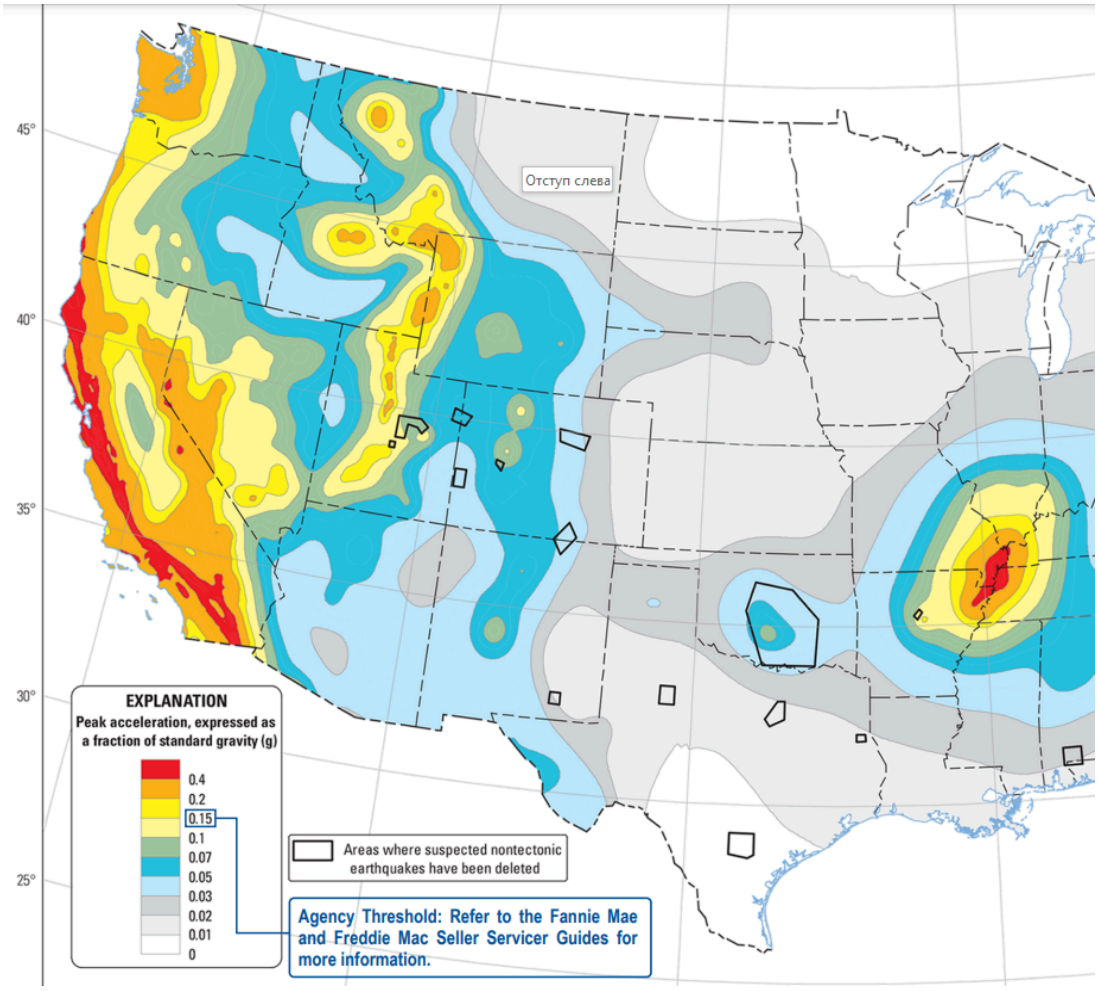


Figure 4-2. Peak Ground Acceleration Seismic Map

1) $\sigma_{vo} = \gamma_{ave} * z$ , where $\gamma_{ave} = 18.87\ kN/m^3$ and z = 11.5 m

,therefore, $\sigma_{vo} = 18.87 * 11.5 = 217{,}005\ kN/m^2$

2) $\sigma'_{vo} = (18.87 - 9.81) * 11.5 = 104{,}19\ kN/m^2$

According to Thomas F. Blake, stress reduction factor ($r_d$) when z=11.5m could be calculated by using the following formula:

$$r_d = \frac{1 - 0.4113(z)^{0.5} + 0.04052z + 0.001753(z)^{1.5}}{1 - 0.4177(z)^{0.5} + 0.05729z - 0.006205z^{1.5} + 0.00121z^2}$$

Thus,

$$r_d = \frac{1 - 0.4113(11.5)^{0.5} + 0.04052 * 11.5 + 0.001753(11.5)^{1.5}}{1 - 0.4177(11.5)^{0.5} + 0.05729 * 11.5 - 0.006205 * 11.5^{1.5} + 0.00121 * 11.5^2}$$

$r_d$= 0.8701557

Finally, Cyclic Stress Ratio is:

$$CSR = 0.65 \frac{0.3871}{9.81} \frac{217.005}{104.19} * 0.8701557 = 0.046445$$

**Calculation of Cyclic Resistance Ratio (CRR)**

In order to calculate Cyclic Resistance Ratio the following formula is used:

$$(N_1)_{60} = C_N * C_E * C_B * C_S * C_R * N$$

Firstly, N, SPT blow counts, is taken as 17.5 which is standardized value suggested factors given by Fear and Robertson (1996). To calculate $C_N$ the following equation is used:

$$C_N = \sqrt{\frac{P_a}{\sigma'_{vo}}} = \sqrt{\frac{100\ kPa}{104.19\ kN/m^2}} = 0.979 \leq 2$$

Energy correction factor that is depending on SPT equipment, $C_E$ is equal to 1.0 which is taken from the Table 4-4 :

Table 4-4. Energy correction factor

| *Country:* | *Hammer Type:* | *Hammer Release:* | ER | $C_E$ |
|---|---|---|---|---|
| United States | Safety | Rope and pulley | 60 | 1.00 |
| United States | Donut | Rope and pulley | 45 | 0.75 |
| Japan | Donut | Rope and pulley, special throw release | 67 | 1.12 |
| Japan | Donut | Free fall | 78 | 1.30 |

According to the table below correction factor of bore diameter (6 inch taken from site investigation), $C_B$ is 1.05.

Table 4-5. Correction factor

| *Diameter of Borehole:* | $C_B$ |
|---|---|
| 65 to 115 mm (2.5 to 4.5 inch) | 1.00 |
| 150 mm (6 inch) | 1.05 |
| 200 mm (8 inch) | 1.15 |

The next correction factor $C_S$ is taken as a standard sampler, 1.0. Final correction factor's value is taken as 1.0 and it is related to length of rod (z), as given in table below:

Table 4-6. Correction factor

- ***For $z \leq 3$ m:*** ***$C_R = 0.75$***
- ***For $3 < z < 9$ m:*** ***$C_R = (15 + z) / 24$***
- ***For $z \geq 9$ m:*** ***$C_R = 1.0$***

Thus,

$$(N_1)_{60} = 0.979 * 1 * 1.05 * 1 * 1 * 17.5 = 17.989125$$

The following step is calculation of cyclic resistance ratio (CRR) of soil for the earthquake magnitude of 7.5 (Idriss & Boulanger, 2010) by using following equation:

$$100 * CRR_{M=7.5} = \frac{95}{34-(N_1)_{60}} + \frac{(N_1)_{60}}{1.3} - \frac{1}{2}$$

$$CRR_{M=7.5} = \left(\frac{95}{34 - 17.989125} + \frac{17.989125}{1.3} - \frac{1}{2}\right)/100 = 0.1927125$$

After that, magnitude scaling factor, MSF, is calculated by choosing the equation from table below according to earthquake magnitude:

- **For $M_w < 7.0$:** $MSF = 10^{3.00} * M_w^{-3.46}$
- **For $M_w \geq 7.0$:** $MSF = 10^{2.24} * M_w^{-2.56}$

The second equation was taken to estimate MSF due to the magnitude of the earthquake, $M_w$, is equal to 7.5.

$$MSF = 10^{2.24} * 7.5^{-2.56} = 0.999639$$

And finally, CRR is estimated:

$$CRR = CRR_{M=7.5} * MSF = 0.1927125 * 0.999639 = 0.192643$$

**Factor of Safety against Liquefaction**

Factor of Safety (FS) against liquefaction is estimated by following equation:

$$FS = \frac{CRR}{CSR}$$

$$FS = \frac{0.192643}{0.046445} = 4.147$$

Final step of analysis is to identify severity index according to table below:

Table 4-7. Factor of Safety against Liquefaction

| Factor of Safety (FS) | Severity index |
|---|---|
| <1 | Very Critical |
| 1-2 | Critical |
| 2-3 | Low Critical |
| >3 | Non-Liquefiable |

From table 4-7 it is concluded that soil is Non-Liquefiable.

## 4.4 Foundation Design

As Foundation allows for the secure passage of loads from structures to the ground, they are essential structural components. There are primarily two categories of foundation: shallow and pile (deep). The primary distinction between these two types of foundations is that shallow foundations must withstand soil shear pressures whereas deep foundations must withstand horizontal forces like earthquake and wind loads. In general, Californian structures are built on pile foundations. But in this capstone, a foundation analysis will be carried out in terms of stability and budgetary constraints. Through the use of settlement and bearing capacity calculations, the stability of the foundation will be evaluated. The cost-effectiveness of a foundation is assessed by looking at the materials required, the installation costs, and other costs (equipment, workforce).

### 4.4.1 Shallow foundation:

A shallow foundation, which is typically referred to as footings, is positioned beneath the soil at a depth that is less than the foundation's breadth, and it shifts the vertical loads from a building to the ground's top layers. When the soil nearest to a surface has a suitable carrying capability, footings are typically not necessary. Furthermore, when the soil is stable or where sufficient soil treatment has been done, shallow foundations perform effectively. The overturning, sliding, and settling should be prevented and minimized by carefully planning the footings. Their dimensions and size are determined by the kind of construction and the weight of the loads that must be supported.Typically, a shallow foundation is built on a building site following ground excavation. Spread footing was chosen because it is affordable, suitable for any soil with sufficient bearing capability, and cost-effective. The square form of the footing is the one chosen.

**Bearing capacity for shallow foundation**

There are two ways to determine a shallow foundation's bearing capacity: two bearing capacities: Terzaghi's and General bearing capacity formulas (Das 2011). In the next Figure, bearing capacity will be estimated as II case since it is assumed that the shallow foundation is 3 m deep and that the groundwater table is located at 13.1064 m below the surface. As a result, the water table depth is more than the foundation depth.

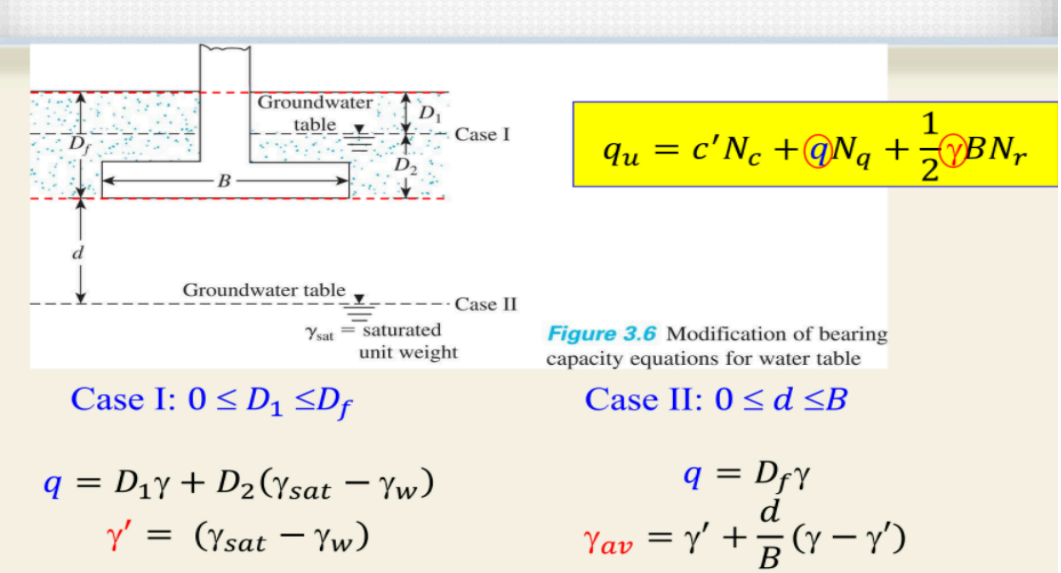


Figure 4-3. Bearing capacity equations according to water table level

$$q = \gamma D_f \quad (4.1)$$

The foundation will be square in design, its length and breadth must be equal. According to the standards stated in Figure, B is assumed to be 2m, and FS is considered to be 3.

| Standard | Admissible factor of safety | Note |
|---|---|---|
| Code for Design of Building Foundations (GB50007-2011) [18] | 2.0–3.0 | |
| Engineering and Design-Bearing Capacity of Soils, U.S. Army Corps of Engineers [21] | 2.0–4.0 | Factor for roadway or railway bridge foundations is 4.0 |

Figure 4-4. Standards for Factor of Safety of foundations

Silty Sand properties: $\gamma = 18.87\ kN/m^3$ $\varphi = 31^o$ $c' = 17$ $D_f = 3m$

1) **Terzaghi's Ultimate Bearing Capacity equation for square footing:**

$$q_u = 1.3c'N_c + qN_q + 0.4\gamma BN_\gamma \quad (4.2)$$

For $\varphi = 31^o$ from table___ in appendix__ $N_c = 40.41,\ N_q = 25.28,$

$N_\gamma = 22.65$

$$D_f = 3m \qquad \text{B=2m}$$

$$q_u = 1.3 * 17 * 40.41 + 18.87 * 3 * 25.28 + 0.4 * 18.87 * 2 * 22.65 = 2666.08\ kPa$$

$$Q_u = q_u A \quad (4.3)$$

$$Q_u = 2666.08 \times 2 \times 2 = 10664.32\ kN$$

$$Q_{all} = \frac{Q_u}{FS} \quad (4.4)$$

$Q_{all} = 3554\ kN < 5726\ kN$ (Vertical load), that is UNACCEPTABLE

1) **The General Bearing Capacity equation**

$$q_u = cN_c F_{cs} F_{cd} F_{ci} + qN_q F_{qs} F_{qd} F_{qi} + 0.5\gamma BN_\gamma F_{\gamma s} F_{\gamma d} F_{\gamma i} \quad (4.5)$$

For $\varphi = 31^o$ from table___ in appendix__ $N_c = 40.41,\ N_q = 25.28,$

$N_\gamma = 22.65$

$F_{cs} = 1 + (B/L) * (N_q/N_c)$=1.4171

$F_{qs} = 1 + (B/L)tan\varphi$=1.4006

$F_{\gamma s} = 1 - 0.4(B/L)$=0.73

For $D_f/B = 1.5 > 1$

$F_{cd} = F_{qd} - \frac{1-F_{qd}}{N_c tan\varphi} = 1.1321$ #

$F_{qd} = 1 + 2tan\varphi(1 - sin\varphi)^2 tan^{-1}(\frac{D_f}{B}) = 1.1251$

$F_{ci} = F_{qi} = F_{\gamma i} = 1$

$q_u = 17 \times 40.41 \times 1.4171 \times 1 \times 1.1321 + 18.87 \times 3 \times 25.28 \times 1.4006 \times 1.1251 \times 1 +$

$$+ 0.5 \times 18.87 \times 2 \times 22.65 \times 0.73 \times 1 \times 1 = 3668.29\, kN$$

$Q_u = 3668.29 \times 2 \times 2 = 14673\, kN$

$Q_{all} = 4891.1\, kN < 5726 kN$ (Vertical load), that is UNACCEPTABLE

In light of the fact that the permissible load in both Terzaghi's bearing capacity equation and The General bearing capacity equation was less than the vertical load, it can be said that the shallow foundation CANNOT support the whole vertical load of the structure. As a result, this foundation type is inappropriate. Since shallow foundations have already failed the stability criterion, their cost-effectiveness will not be examined.

### 4.4.2 Pile foundation

A pile foundation, also referred to as a deep foundation, is a long, cylindrical column made of reinforced concrete or steel that is buried in the ground to support a building and transmit vertical loads through water, weak, compressible soil layers, or bedrock using frictional resistance or end bearing. The width of piles is much smaller than their length. Deep foundations are utilized in the construction of high-rise buildings, water tanks, and bridges where there are excessively huge weights and concentrated loads since they can support more loads than spread footings can. The following circumstances necessitate the use of pile foundations:

- When the bedrock is at a decent depth below the surface and the upper soil layers are poor and highly compressible, they cannot support the loads from buildings.
- When lateral loads caused by wind, seismic loads, and ground pressures are applied to the building. Tall buildings, chimneys, earth-retaining structures, and transmission towers are all examples of this type of circumstance.
- When seasonal variations cause shrinkage and swelling in expansive or collapsible soils.
- When uplifting forces are seen in structures like transmission towers, offshore platforms, and situations where the basement is below the water table.
- In order to prevent loss of bearing capacity brought on by soil erosion at ground level, bridge abutments and piers must be built.

In our case we have the first and second case as the bedrock located at approximately 11.5 m deep and the soil is located in seismic zone. Moreover, most of the layers are sandy soils and the desirable decision is to set deep foundations that will stand straight on the bedrock.

Pile foundations are divided into the following categories based on a design function:

a) By creating friction pressures between the soil and the pile's entire surface, friction piles transfer load from the construction to the soil nearby, such as sand or hard clay. The majority of the bearing capacity is maintained by friction piles by shear stresses along the piles, which make them suitable for locations where bedrock or stiff strata are too deep.
b) The load of the structure is immediately transferred onto the strong layer or strata by end-bearing piles acting as a column. Typically, the bedrock or dense layer of soil is where the bottom end of the pile is situated.

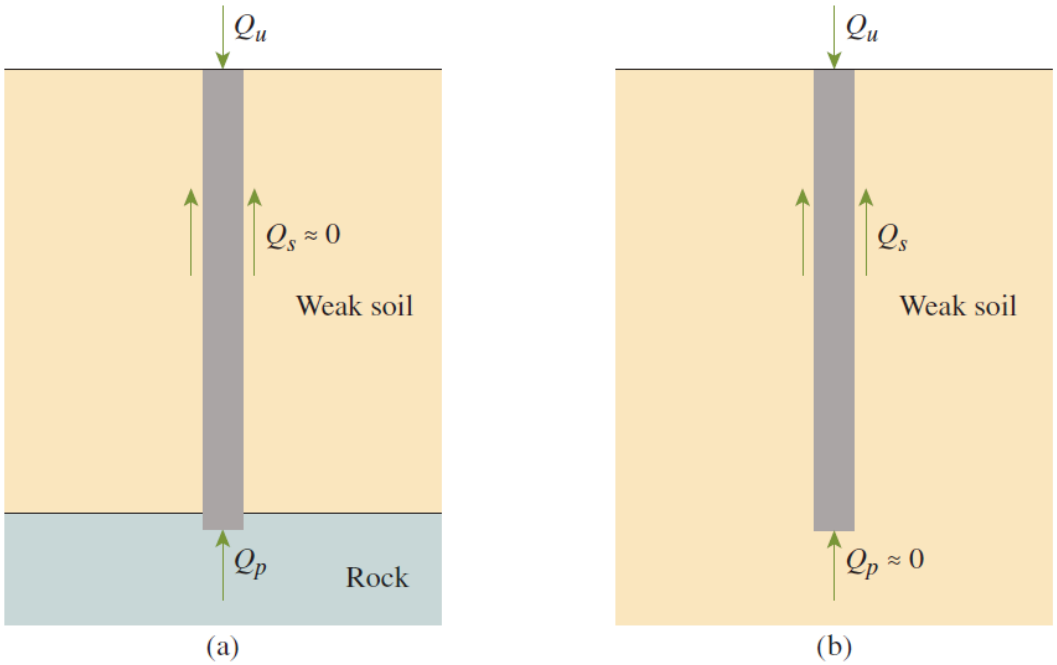


Figure 4-5. a) End-bearing piles. b) Friction piles

According to our soil profile it is desirable to use end bearing piles as the soil over bedrock is vulnerable to horizontal stresses and the foundation that stands alone can undergo horizontal motion.

Deep foundations are divided into driven and bored piles based on how they were constructed. The key distinction between them is that while driven piles are produced off-site under carefully controlled conditions, bored piles are poured on location. Because there is less vibration in metropolitan locations, bored piles are also preferable in cohesive soils to create friction piles. Additionally, bored piles are more cost-effective and offer greater capacities than driven piles, which is why bored piles were chosen for this capstone.

Pile foundations are divided into steel, concrete, timber, and composite piles in addition to based on the materials used in their construction. The materials in the table below were compared in order to choose the most appropriate type:

Table 4-8. Foundation materials in construction

| | Precast Prestressed Concrete | Cast-in-place Concrete | Steel | Composite | Timber |
|---|---|---|---|---|---|
| Length | 10-45 m | 5-15 m | 15-60 m | 9-20 m | 15-40 m |
| Load can be carried | 300-3000 kN | 200-500 kN | 300-1200 kN | 250-750 kN | 130-250 kN |
| Advantages | Saves time because there is little chance of a project delay. Effective from a financial standpoint. Greater longevity and less frequent maintenance. Quality control. There is less labor needed. | Comparably less expensive, able to withstand structural damage, high level of strength, readily extensible | Able to withstand heavy driving stresses, Installing it is simple and it can go through the stiff layers. Possess a high bearing capacity | -relatively affordable<br>-conserves time<br>-lowers the expense of excavation | Simple to install<br>Cost per pile length is lower |
| Disadvantages | - Difficult to carry to the site | -It is challenging to join | Relatively pricey high | It is challenging to ensure a | Diminished bearing capacity, |

| | | | | | |
|---|---|---|---|---|---|
| | - Expensive to purchase | pieces of concrete after pouring.<br>-More workers are needed. | likelihood of electrolysis and corrosion | joint between two different materials. | Possibly harmed by hard driving, Cannot be driven through dense soil layers |

Precast concrete will be the most appropriate material in terms of load range once all of the material's properties have been considered, since it has the highest load capacity compared to other materials and provides affordable options for huge structures. Its quality can be managed, and it can resist the seismic conditions of the California region. Moreover, Precast concrete requires less laborers.

Designing the pile cap is a further important step that needs to be addressed. It is decided to be square shaped because of some advantages:

- High frictional resistance on the top of pile
- Larger bending stresses
- Relatively low cost of manufacture

**Bearing capacity for deep foundation**

The bearing capacity of pile foundation ($Q_u$) is computed as a sum of load-carrying capacity ($Q_p$) and frictional resistance ($Q_s$).

$$Q_u = Q_p + Q_s \quad (4.5)$$

There are other ways to compute the Qu, including the Meyerhof's, Castello's, and Vesic's techniques, and it is determined to use the Meyerhof's Method after considering the presence data. For a more thorough foundation examination in Capstone II, more

techniques will be applied. The point bearing capacity Qp for the sand and clay layers will be determined independently using Meyerhof's approach.

**Calculation of Load-carrying capacity**

**Meyerhof's method for Sand:**

$$Q_p = A_p q_p = A_p q' N_q^* \quad (4.6)$$

where $A_p$ is area of pile tip,

$q_p$ is unit point resistance

$q'$ is effective vertical stress at the level of the pile tip

$N_q^*$ is the bearing capacity factors for piles

Nevertheless, $Q_p$ should not exceed the limiting value $A_p q_l$ meaning that:

$$Q_p = A_p q' N_q^* \leq A_p q_l \quad (4.7)$$

$$q_l = 0.5 p_a N_q^* tan\varphi' \quad (4.8)$$

Consequently,

$$Q_p = A_p q' N_q^* \leq 0.5 A_p p_a N_q^* tan\varphi' \quad (4.9)$$

**Meyerhof's method for clay:**

$$Q_p = 9 A_p c_u \approx N_c^* A_p c_u \quad (4.10)$$

where $c_u$ is an undrained cohesion of soil below the tip of pile, that is equal to two times of drained cohesion $c'$.

**Calculation of Frictional Resistance**

Skin friction will be determined separately for the sand and clay layers in order to assess point bearing capacity. The results of the Standard Penetration Test (SPT) were correlated with the friction resistance of sand. The average unit resistance fav can be calculated using average SPT values as indicated by Briaud et al.

$$f_{av} \approx 0.224 p_a (\overline{N_{60}})^{0.29} \quad (4.11)$$

where $p$ is a perimeter, L is a length of the pile and $(\overline{N_{60}})$ is an average value of SPT, $p_a$ is atmospheric pressure.

Followingly, skin friction of the sand is

$$Q_s = 0.224 p_a (\overline{N_{60}})^{0.29} pL \quad (4.12)$$

For clay layer, skin friction can be estimated applying α, β $and$ λ methods. From these methods, it is used the α method where unit skin resistance $f$ is given as

$$f = \alpha c_u \quad (4.13)$$

where α is an empirical adhesion factor and is in a range of 0-1. Hence, skin friction of clay is

$$Q_s = \sum f \Delta L p = \sum \alpha c_u \Delta L p \quad (4.13)$$

Assumptions were made in order to choose the ideal pile proportions. The assumption for the pile's length began at 7 meters with a 0.5-meter increment, while the assumption for the pile's breadth (measured as a square pile) began at 0.15 meters with a 0.05-meter increment. Qs and Qp were calculated independently for each pile's length and width before being added together. Allowable bearing capacity was then calculated. According to the permitted bearing capacity of the piles that must withstand the load from the structure, the most suitable pile length and width were chosen. The optimum options for length and width are 11.5m and 0.6m, respectively. Every trial was conducted using a Microsoft Excel file.

Consequently,

$$Q_p = 521,054\ kN \quad \text{and} \quad Q_s = 27532,9\ kN$$

$$Q_u = 28053,953\ kN$$

$$Q_{all} = \frac{Q_u}{FS} = \frac{4362,591\ kN}{3} = 9351,318\ kN > 1300 kN \text{ (Vertical load)}$$

As it is seen, this pile dimension can withstand the vertical load of 5726 kN. Therefore,in this Capstone we decided to work with pile foundation rather than shallow foundation.

### 4.4.3 Mat Foundation

**Design of the mat foundation**

To design the matt foundation first we have to look at the plan of the building which is given below.

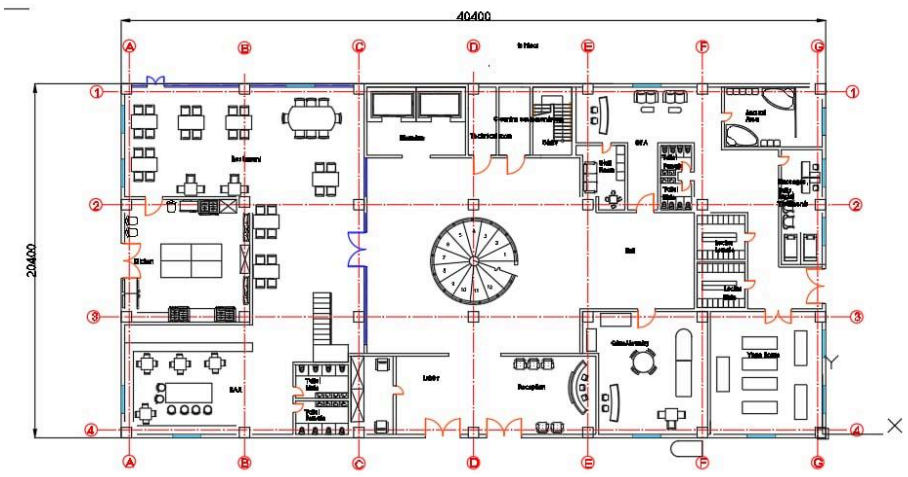


Figure 4-6. Design of the building

Here we can see the columns which are in 4x7 order. After identifying the column locations we are going to design the mat foundation.

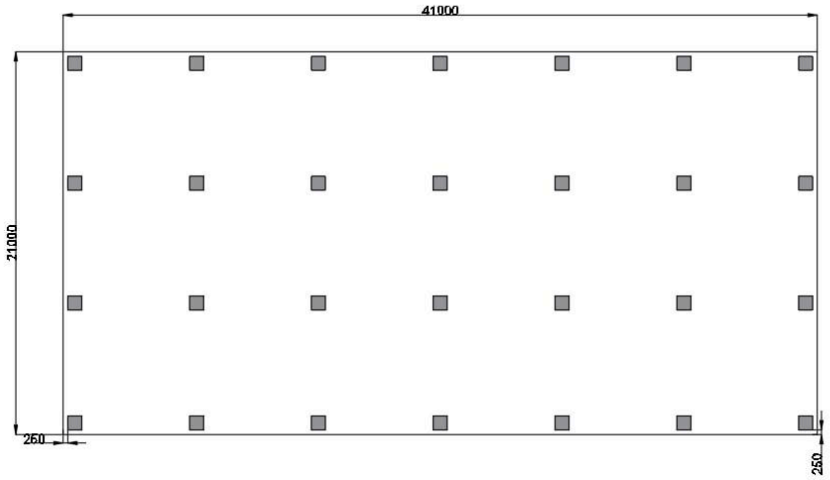

Figure 4-7. Rectangular shaped design of the Matt foundation

It was decided to be rectangular shape, 21x41 meters and the edges have 25 cm offset between footing and the body of the foundation.

**Bearing capacity**

Our first soil layer is saturated sandy clay with the depth of 3m. So the depth Df is selected to be 1.5 m and it is totally will be in this first layer. The formula of ultimate bearing capacity for clay taken from SI Principles of Foundation Engineering, 9th ed as shown below.

$$q_u = 5.14c_u\left(1 + 0.195\frac{B}{L}\right)\left(1 + 0.4\frac{D_f}{B}\right)$$

Where: Cu is undrained cohesion (17 kPa)

B is 21 m

L is 41 m

Df is 1.5 m

By substituting the needed values $q_u$ is equal to 98.85 kN per square meter. For the whole area $q_u = 98.85 * 41 * 21 = 85112.66\ kN$. By dividing it to safety factor of 3 it becomes 28370.89 kN which is less than our total load 160328 kN.

**General bearing capacity equation:**

$$q_u = cN_cF_{cs}F_{cd}F_{ci} + qN_qF_{qs}F_{qd}F_{qi} + 0.5\gamma BN_\gamma F_{\gamma s}F_{\gamma d}F_{\gamma i} \quad (4.5)$$

For $\varphi = 31^o$ from table___ in appendix__ $N_c = 40.41$, $N_q = 25.28$, $N_\gamma = 22.65$

Shape factors:

$F_{cs} = 1 + (B/L) * (N_q/N_c)$=1.3204

$F_{qs} = 1 + (B/L)tan\varphi$=1.3078

$F_{\gamma s} = 1 - 0.4(B/L)$=0.795

Depth factors:

For $D_f/B = 1.5 < 1$

$F_{cd}$=$F_{qd} - \frac{1-F_{qd}}{N_c tan\varphi} = 2.2015$

$F_{qd}$ =$1 + 2tan\varphi(1 - sin\varphi)^2 tan^{-1}(\frac{D_f}{B}) = 2.154$

Inclination for undrained case:

$F_{ci} = F_{qi} = F_{\gamma i} = 1$

$q_u = 17 \times 40.41 \times 1.3204 \times 1 \times 2.2015 + 18.87 \times 3 \times 25.28 \times 1.3078 \times 2.154 \times 1 +$

$+ 0.5 \times 18.87 \times 21 \times 22.65 \times 0.795 \times 1 \times 1 = 9596.11\ kN$

$Q_{all} = 9596.11/3 = 3198.7\ kN < 5726kN$ (Vertical load), that is UNACCEPTABLE

The both equations show that Mat foundation is inapplicable and the decision still be a pile foundation for this Capstone Project.

### 4.4.4 Pile Cap Design

Since using a single pile foundation was not an option, it was decided to employ a collection of heaps instead, necessitating the creation of a pile cap. Four heaps are picked as a group. The allocation of a set of piles must then be planned in order to ensure

maximum efficiency and support design loads. The AASHTO (2016) states that the spacing between heaps is equivalent to 2.5D, the pile head must reach into the pile cap for at least 12 inches (304,8 mm), and the minimum distance between the center of the pile and the pile cap edge is 9 inches (228.6 mm). Additionally, the piles' concrete covers should be at least 6 inches (152,4 mm) thick.

Relying on these specifications, the pile parameters were:

- Spacing between piles is 1200mm
- The distance from center of pile to pile cap edge is 500mm
- Length and width of the pile cap is 3000mm
- Pile cap height is 800mm
- Pile head extension into pile cap is 350mm

## 4.5 Axial and lateral bearing capacity

### 4.5.1 Axial bearing capacity design by GEO5 software

Previous manual calculations of axial bearing capacity must be validated by a particular software in order to ensure that the dimensions of the piles chosen are reliable and reasonable. For this purpose, the GEO5 software was used to define the soil strata beginning at the basement floor based on the soil profile and properties listed in Table 4-1. Figure 4-8 depicts a dialog window from the software containing parameters and soil profile.

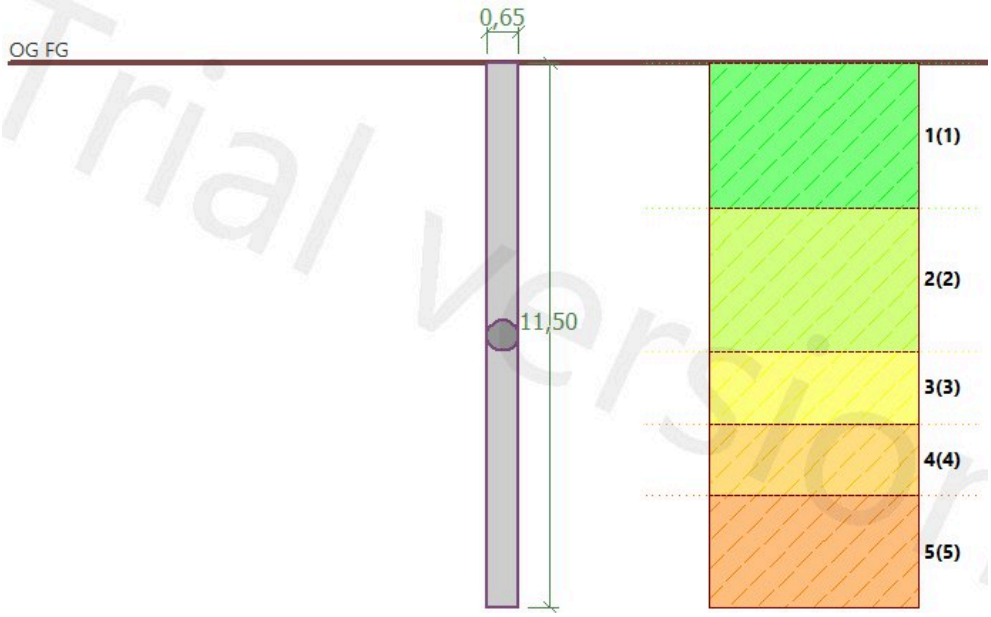


| No. | Soil name |
|---|---|
| 1 | 1 |
| 2 | 2 |
| 3 | 3 |
| 4 | 4 |
| 5 | 5 |
| 6 | 6 |

**1**

| | | |
|---|---|---|
| Unit weight : | $\gamma$ = | 18,87 kN/m$^3$ |
| Angle of internal friction : | $\varphi_{ef}$ = | 31,00 ° |
| Cohesion of soil : | $c_{ef}$ = | 17,00 kPa |
| Poisson's ratio : | $\nu$ = | 0,35 |
| Deformation modulus : | $E_{def}$ = | 5,00 MPa |
| Saturated unit weight : | $\gamma_{sat}$ = | 20,00 kN/m$^3$ |
| Angle of dispersion : | $\beta$ = | 12,00 ° |

Figure 4-8. Definition of soil profile and properties in GEO5

Bearing capacity was verified by using two methods: CSN 73 1002 and Effective Stress Method. These are the results of these procedures:

1) CSN 72 1002 METHOD

CSN 72 1002 METHOD requires that the soil type is defined first and to use a suitable modulus of elasticity of soil based on its characteristics. As it is seen from Figure 4-9, pile bearing capacity is satisfactory.

¥

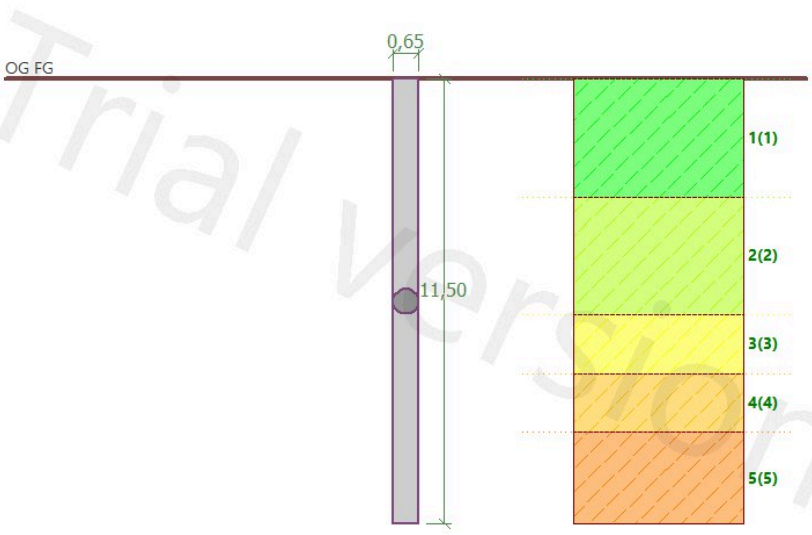


**Verification of pile vertical bearing capacity according to LS**
Analysis carried out with automatic selection of the most unfavourable load cases.

Verification of compressive pile:
Most unfavorable load case No. 1. (Load No. 1)
Pile skin bearing capacity $R_s$ = 1369,19 kN
Pile base bearing capacity $R_b$ = 1560,93 kN

Pile bearing capacity $R_c$ = 2930,12 kN
Ultimate vertical force $V_d$ = 1300,00 kN

$R_c$ = 2930,12 kN > 1300,00 kN = $V_d$

Pile bearing capacity is SATISFACTORY



Figure 4-9. Output of CSN 72 1002 METHOD

2) Effective Stress METHOD

Effective Stress was the second method for analyzing vertical load-bearing capacity. This method requires entering the coefficient of pile bearing capacity, $\beta_p$, and the coefficient of pile bearing capacity, $N_p$, which were chosen based on Table 4-8's recommendations.

Table 4-8. Range of coefficients *Np* and β*p* (Fellenius, 1991)

| Type of soil | $\varphi_{ef}$ | $N_p$ | $\beta$ |
|---|---|---|---|
| Clay | 25 - 30 | 3 - 30 | 0.23 - 0.40 |
| Silt | 28 - 34 | 20 - 40 | 0.27 - 0.50 |
| Sand | 32 - 40 | 30 - 150 | 0.30 - 0.60 |
| Gravel | 35 - 45 | 60 - 300 | 0.35 - 0.80 |

Result presented in Figure 4-10, shows that pile bearing capacity is satisfactory.

**Verification of bearing capacity : effective stress method**
Analysis carried out with automatic selection of the most unfavourable load cases.

Verification of compressive pile:
Most unfavorable load case No. 1. (Load No. 1)
Pile skin bearing capacity $R_s$ = 1056,56 kN
Pile base bearing capacity $R_b$ = 309,88 kN

Pile bearing capacity $R_c$ = 1366,44 kN
Ultimate vertical force $V_d$ = 1300,00 kN

$R_c$ = 1366,44 kN > 1300,00 kN = $V_d$

Pile bearing capacity is SATISFACTORY

Figure 4-10. Effective Stress Method for minimum coefficient of bearing capacity

Consequently, the bearing capacity was validated using both techniques in the GEO5 software. The selected dimensions (D=0.6m and L=11.5m) of the pile foundation are adequate to withstand the calculated axial forces from the 15-story residential structure.

### 4.5.2 Lateral load bearing capacity check by LPile

Lateral loading analysis is important for foundation design because foundations are typically required to resist lateral loads and moments in addition to axial loads. To maintain acceptable lateral forces, the designer must identify deflections and stresses in the proposed soil-pile system. In this section, the lateral bearing capacity will be determined using the software programs LPile and GEO5. This analysis involved determining the geotechnical stability of the soil adjacent to the piles against the designed loads, maximum forces acting on the piles, and horizontal displacement, but only after determining the horizontal subgrade reaction coefficient.In Excel VBA, LPile software was used to automate calculations based on a number of input parameters and assumptions. The subsequent assumptions were made:

- Loads and restraints on top node
- Constant soil stiffness in each element
- Constant elastic modulus and moment of inertia.
- Constant subdivision length

In the calculation, the length of each element was divided every 0.5 meters, and since the length of the pile was 11.5 meters, this resulted in a total of 23 elements. The parameters are depicted in Figure 4-11:

**Laterally loaded elastic piles on elastic foundation**

Using Excel VBA
Constant pile EI
Constant soil stiffness in each element
Constant subdivision length
Loads and restraints on top node

| | | |
|---|---|---|
| Description | Test 1 | |
| General parameters | | |
| Pile length | 11,5 | m |
| Elements | 23 | |
| $E_{pile}$ | 1,97E+05 | kPa |
| $I_{pile}$ | 8,76E-03 | $m^4$ |
| Element length | 0,5 | m |

Clear results

SOLVE

Top node moment restraint (0=fixed; 1=free)

| Node | θ |
|---|---|
| 1 | 1 |

Top node loads

| | Fh | M | Top node reaction | |
|---|---|---|---|---|
| Node | [kN] | [kNm] | | [kNm] |
| 1 | 100 | 0 | M | 0,0 |

Figure 4-11 LPile parameters

For calculations, it was necessary to calculate the crucial variable parameter "horizontal subgrade reaction coefficient" using the Broms (1964) method.
It idealizes the soil as a series of horizontal strata, so the linear analysis formula for the horizontal subgrade reaction is:

$$k_h = 0.65\left(\frac{E_s}{(1-\nu^2)}\right)\left(\frac{E_s B^4}{E_p I_p}\right)^{\frac{1}{12}}$$

where $E_s$ - Modulus of elasticity of the soil,
B - Lateral dimension of the pile,
$E_p I_p$ - Flexural rigidity of the pile,
ν - Poisson ratio (for sand ν ≅0.35).

The values for Ep and Poisson ratio were assumed based on the guidelines. Respectively horizontal subgrade reaction was calculated in Table 4-9.

Table 4-9: Results of calculation of $k_h$

| Soil Layer | Poisson ratio | $k_h$ , $kN/m^2$ |
|---|---|---|
| Sandy Clay | 0,35 | 8120 |
| Light Gray Clayey fine Sand | 0,35 | 11978 |
| Light Brown Silty fine Sand | 0,30 | 15023 |
| Gray Brown Clayey fine Sand | 0,35 | 13105 |
| Gray Brown Silty fine Sand | 0,30 | 15235 |

The results of the LPIle software were given in the followings:

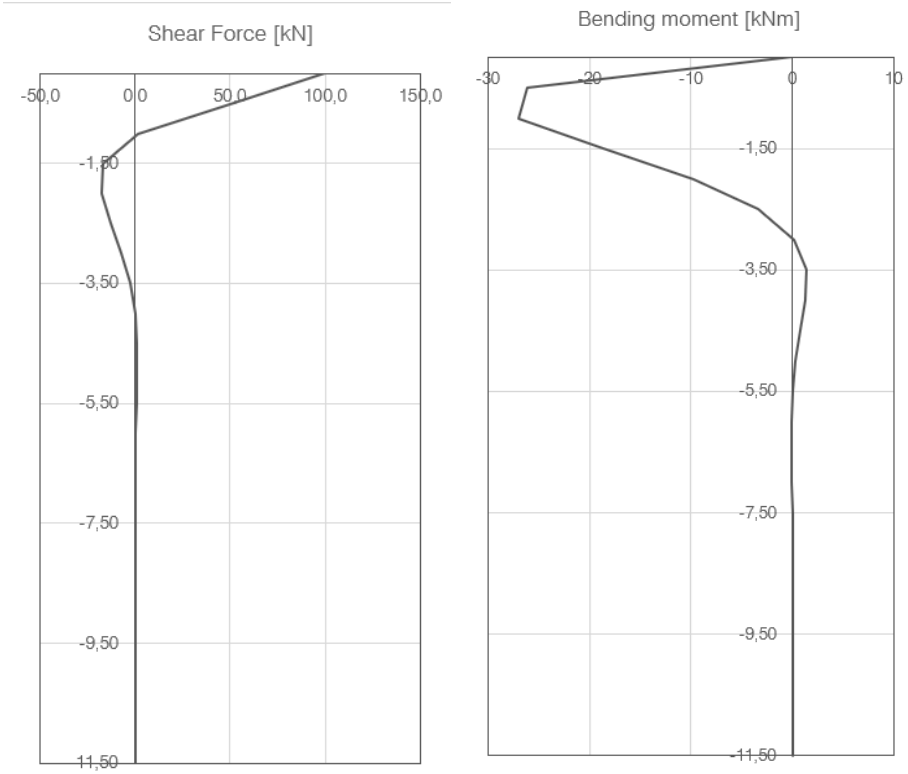


Figure 4-12. Shear force and bending moments diagram using LPile.

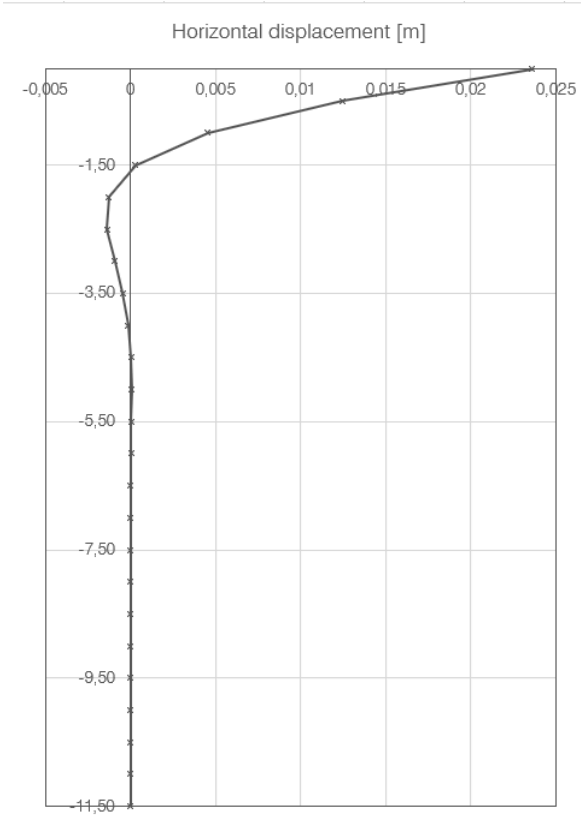


Pile displacement and rotation

| z | $u_x$ | θ |
|---|---|---|
| [m] | [m] | [rad] |
| 0,00 | 0,024 | -0,0235 |
| -0,50 | 0,012 | -0,0197 |
| -1,00 | 0,005 | -0,0120 |
| -1,50 | 0,000 | -0,0054 |
| -2,00 | -0,001 | -0,0013 |
| -2,50 | -0,001 | 0,0006 |
| -3,00 | -0,001 | 0,0011 |
| -3,50 | 0,000 | 0,0008 |
| -4,00 | 0,000 | 0,0005 |
| -4,50 | 0,000 | 0,0002 |
| -5,00 | 0,000 | 0,0000 |
| -5,50 | 0,000 | 0,0000 |
| -6,00 | 0,000 | 0,0000 |
| -6,50 | 0,000 | 0,0000 |
| -7,00 | 0,000 | 0,0000 |
| -7,50 | 0,000 | 0,0000 |
| -8,00 | 0,000 | 0,0000 |
| -8,50 | 0,000 | 0,0000 |
| -9,00 | 0,000 | 0,0000 |
| -9,50 | 0,000 | 0,0000 |
| -10,00 | 0,000 | 0,0000 |
| -10,50 | 0,000 | 0,0000 |
| -11,00 | 0,000 | 0,0000 |
| -11,50 | 0,000 | 0,0000 |

Figure 4-13. Horizontal displacement

From Figure 4-13, the horizontal displacement is equal to 24 mm which is under the limit of 25 mm. Thus, according to the LPile software the used pile dimensions are satisfactory.

### 4.5.3 Lateral load bearing capacity verified by GEO5 software

GEO5 was then utilized to examine the lateral loading. To test the lateral loads, the program applied all soil strata to the model. Figure 4-18 depicts the input parameters as follows: unsaturated and saturated unit weight of soil, deformation modulus, angle of friction and dispersion, and Poisson ratio.

| No. | Soil name |
|---|---|
| 1 | 1 |
| 2 | 2 |
| 3 | 3 |
| 4 | 4 |
| 5 | 5 |
| 6 | 6 |

**2**

| | | | |
|---|---|---|---|
| Unit weight : | $\gamma$ | = | 18,87 kN/m$^3$ |
| Angle of internal friction : | $\varphi_{ef}$ | = | 30,00 ° |
| Cohesion of soil : | $c_{ef}$ | = | 11,00 kPa |
| Poisson's ratio : | $\nu$ | = | 0,35 |
| Deformation modulus : | $E_{def}$ | = | 8,00 MPa |
| Saturated unit weight : | $\gamma_{sat}$ | = | 20,00 kN/m$^3$ |
| Angle of dispersion : | $\beta$ | = | 15,00 ° |

Figure 4-14. Soil type input parameters for GEO5

Then, the pile's loads and geometry were assigned. The length of the pile is 11.5 meters and its diameter is 0.65 meters. The categories of loads to be assigned are vertical forces, horizontal forces, and the structure's bending moment. Consequently, in the "horizontal capacity" window of the program, the following output graphs were obtained:

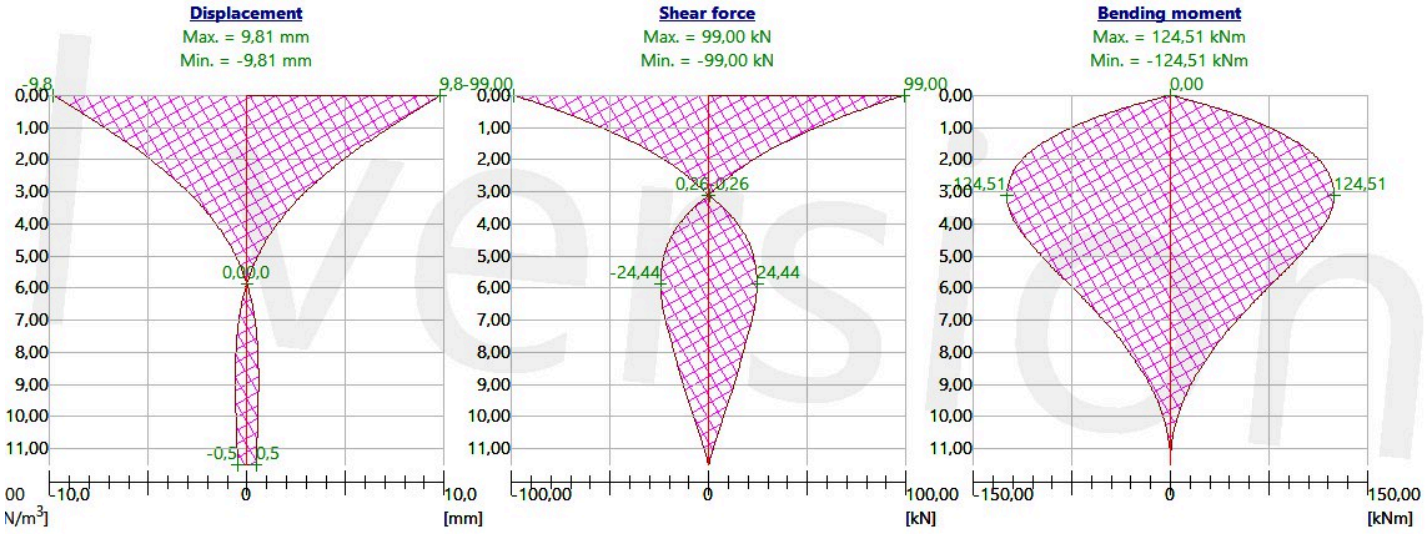

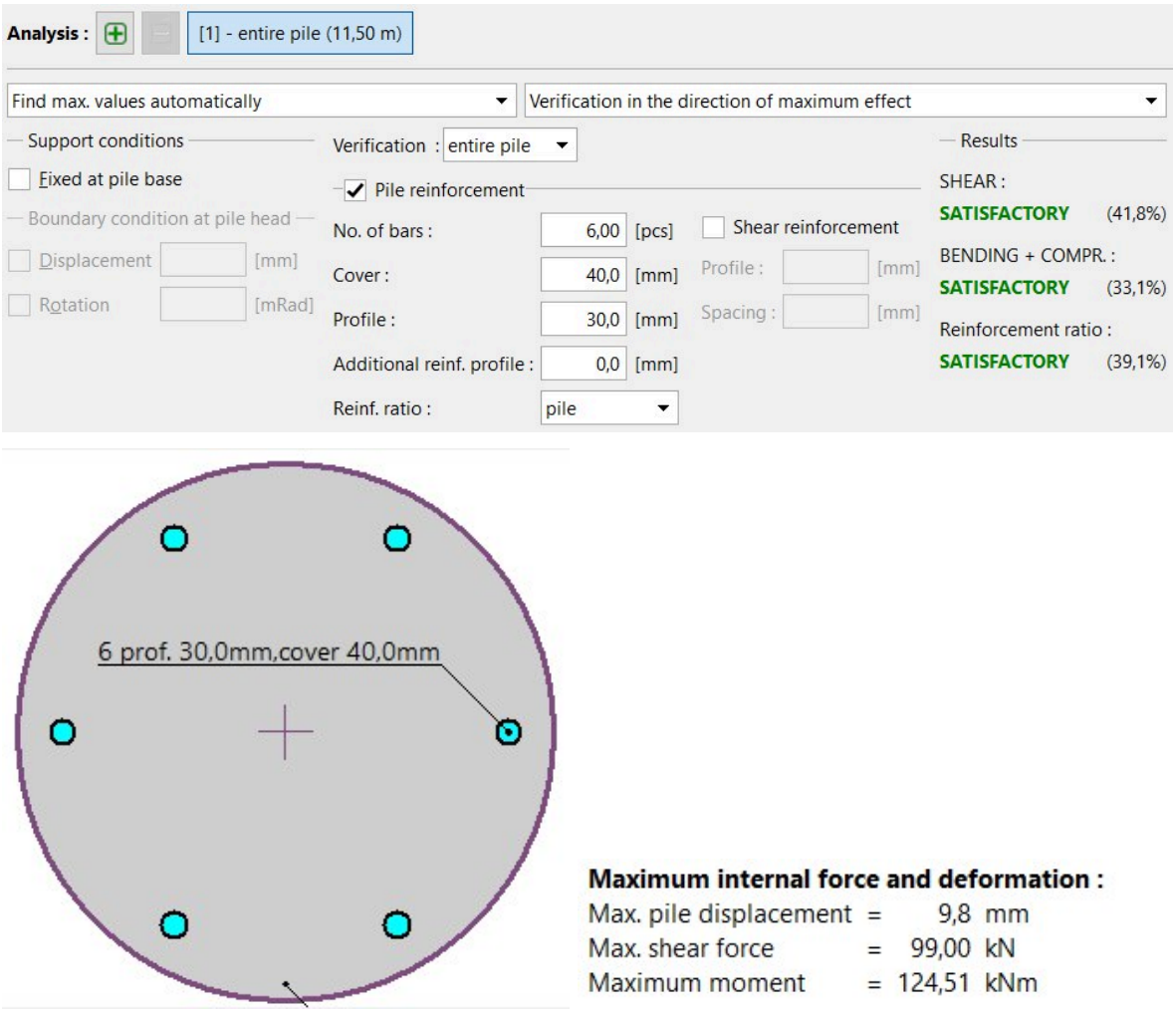


Figure 4-15. Output of GEO5 software

Figure 4-15 reveals that the greatest horizontal displacement was 9,8 mm, the maximum shear force was 99 kN, and the maximum bending moment was 141.93 kN. These outputs were adequate and comparable to the LPIle program's output. The 7.94 m lateral deformation is less than the limit of 25 mm (7.94 mm < 25 mm, acceptable). The foundation can therefore withstand the lateral loads that will be exerted by the structure and meet the serviceability requirements.

### 4.6 Plaxis 3D simulation

The Plaxis 3D program was used to simulate a model of one set of piles in order to evaluate the performance of the foundation. To calculate the load settlement at certain positions in the foundation, the piles were modeled using the volume piles approach. It should be noted that the foundation was subjected to vertical loads applied as a point load

and that the simplified form of the pile groups were modeled. The volume pile model is displayed below:

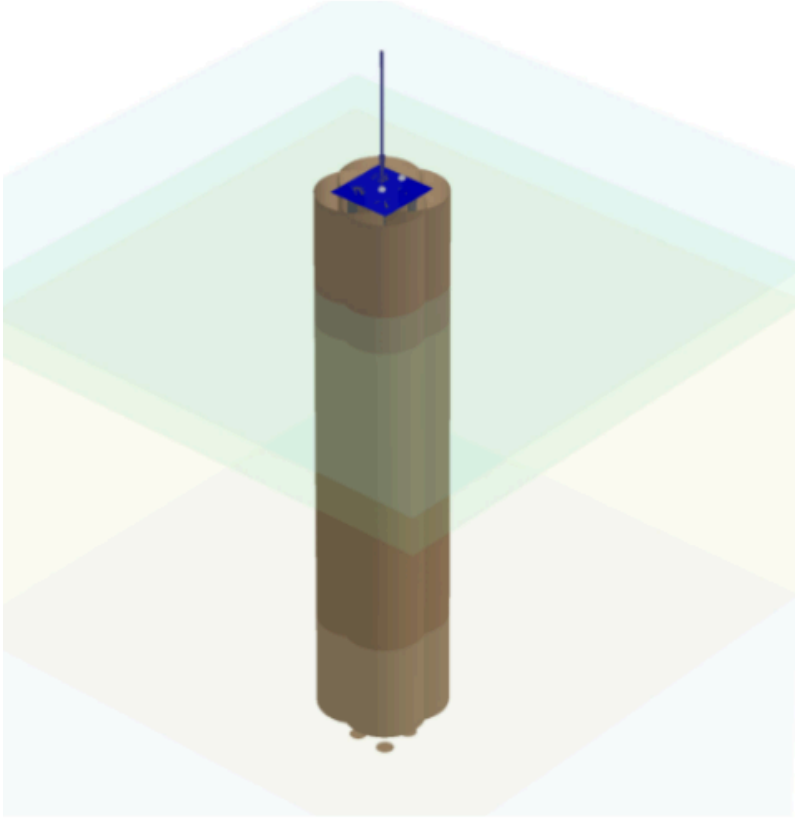

Figure 4-16. Model of Volume piles in Plaxis 3D

All five soil layers that were created using the Mohr-Coulomb soil model were included in the soil model. Table 4-1 and Table 4-9 were used to determine the soil characteristics Es, v,,, and cu. While leaving other soil properties at their preset values. Since executing the project simulation with a fine mesh required a lot of time, a medium mesh was used instead.

Simulation of the piles were done in 3 construction stages:

1) Initial phase. In this phase point loads, plates and interfaces are not activated

2) 1st Phase. The pile interfaces and plates are activated along with assigning the pile material.

3) 2nd Phase. The point load acting on the pile is activated.

So, the staged construction is completed and the next step is to add the investigated points. These investigated points are defined at the top of the piles in the mesh given in Figure 4-17.

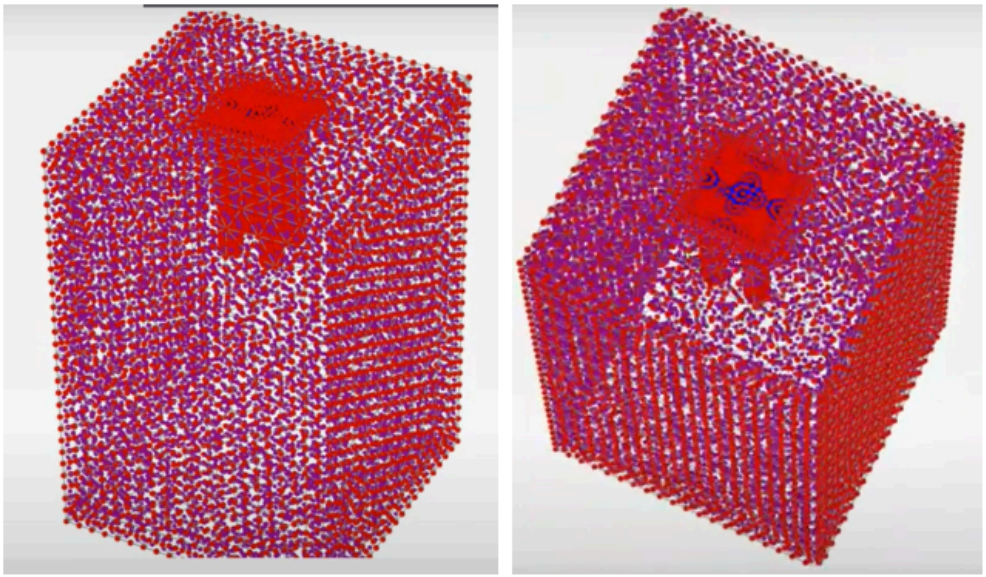

Figure 4-17. Investigated points in Plaxis 3D

As soon as the points to be investigated are established, the analysis may be performed and the phases calculated. The output of the volume piles is created as a deformed mesh in Figure 4-22 when the computation of phases is complete. The highest vertical deformation was 10.3 mm, which is less than the acceptable limit of 25 mm. The load settlement curve for certain sites at the top of piles is shown in Figure 4-23, and it is obvious from this graph that the vertical displacements are within the permissible range of 25 mm.

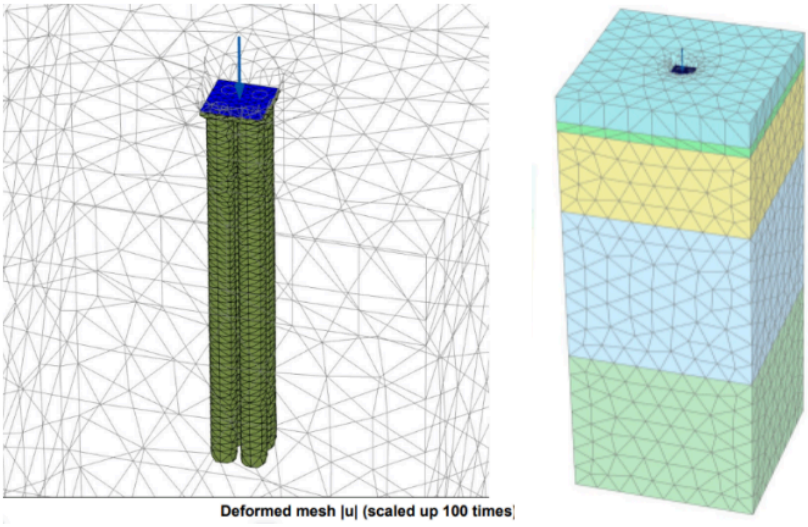


Figure 4-18. Deformed Mesh interface of volume piles in Plaxis 3D

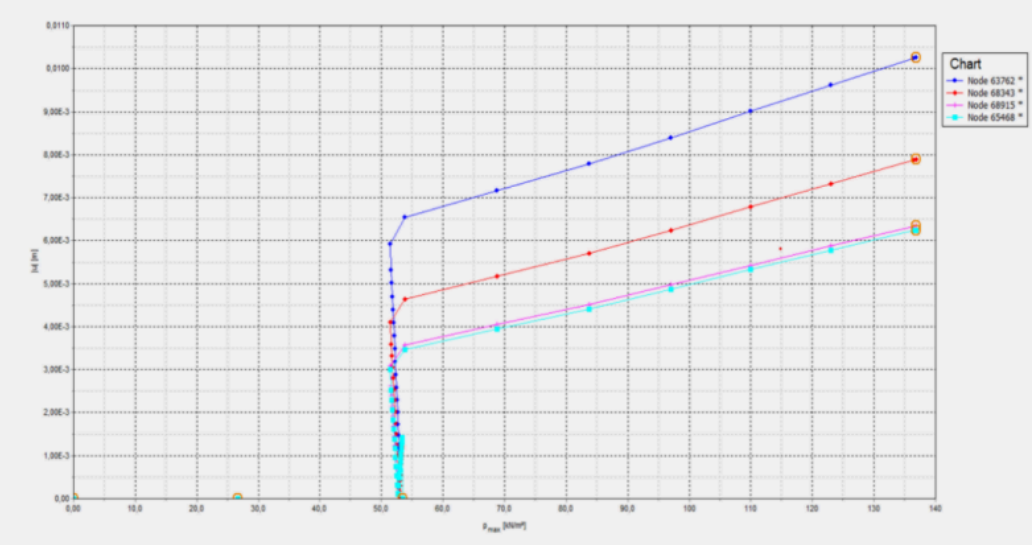


Figure 4-19. Load settlement chart for nodes at the top of the piles

## 4.7 Settlement of pile foundation

### 4.8.1 Elastic settlement

Initially, elastic settlement of pile foundation was estimated using the formula given in the book by Das (2019):

$$s_e = s_{e(1)} + s_{e(2)} + s_{e(3)}$$

Where,

$S_e(1)$ = elastic settlement of pile

$S_e(2)$ = settlement of pile caused by the load at the pile tip

$S_e(3)$ = settlement of pile caused by the load transmitted along the pile shaft

Elastic settlement of pile calculated using the formula below:

$$s_{e(1)} = \frac{(Q_{wp} + \xi Q_{ws}) * L}{A_p * E_p}$$

Where,

Load carried at pile tip under working load:

$$Q_{wp} = \frac{Q_p}{FS}$$

Load carried at pile skin resistance under working load:

$$Q_{ws} = \frac{Q_s}{FS}$$

Settlement of pile caused by the load at the pile tip determined by the following formula:

$$s_{e(2)} = \frac{(q_{wp} * B) * (1 - \mu_s^2) * I_{wp}}{E_s}$$

Where the influence factor was chosen as 0.9.

Settlement of pile caused by the load transmitted along the pile shaft can be determined by the following formula:

$$s_{e(3)} = \frac{(Q_{ws} * D)(1 - \mu_s^2) I_{ws}}{pLE_s}$$

$$I_{ws} = 2 + 0.35\sqrt{\frac{L}{D}}$$

All the calculations were done via Excel and can be seen in Table below.

| Qwp, Kn | Qws, Kn | Ep, Pa | e | Ap, m2 | Se(1), mm | μs | Es, kN/m2 | Se(2), mm | Se(3), mm | Se total |
|---|---|---|---|---|---|---|---|---|---|---|
| 236.4043333 | 29494.23333 | 21000000 | 0.67 | 0.81 | 0.00025016331 57 | 0.45 | 84600 | 0.00832006297 9 | 0.04129 95893 | 0.04986 981559 |

Table 4-10. Elastic settlement of pile

Total settlement of piles: $s$ =0.00025+0.00832+0.0413 = 0.04987 mm which is less than 25.4 mm specified by LRFD *e* (Paikowsky, 2004)

**Elastic settlement of group of piles**

Settlement of group of piles are designed under the same working load per pile and increases with the width of the group ($B$ ) and center to center spacing between piles (d). The method for *g* calculating the settlement was proposed by Vesic (1969):

$$s_{g(e)} = \sqrt{\frac{B_g}{D}} * s_e$$

Where Se is the settlement of each pile under the same working load, D is the width of each pile *e* in the group.

$s_{g(e)} = \sqrt{\frac{2275}{650}} * 0.04987 = 0.0935$ mm which is also less than the limit of 25.4 mm (LRFD)

Justification of settlement results by software:

### 4.7.2 Consolidation settlement

The calculation approach given by Das (2019) involves the steps given below:

Step 1. Simplify the pile group to a solid footing with a depth of 2L/3 (where L is the pile length). This means that the vertical uniaxial load *Q*g acts at a depth of 10.7m from the pile top.

Step 2. Find the effective stress increase (Δσ1' ) and effective overburden pressure (σ1' ) at every midlayer of clay stratum by the following formula:

$$\Delta\sigma_i^{'} = \frac{Q_g}{(B_g+z_i)*(L_g+z_i)}$$

Where $z$ = distance between 2L/3 from pile top and middle of soil layer, i.

$$\Delta\sigma_i^{'} = \frac{5488}{(2.275+101.9)*(2.275+101.9)} = 0.506\ \frac{kN}{m^2}$$

$$\sigma_1^{'} = 19 * 1 + 10 * 0.5 + (18.5 - 9.81) * 8.9 + (18.8 - 9.81) * 4.65 = 143.14\ \frac{kN}{m^2}$$

Step 3. Compression Index was determined using formula found by Nishida (1956):

$$C_c = 1.15 * (e_0 - 0.27)$$

Where : $e_0 = 0.7$ (initial void ratio)

$$C_c = 1.15 * (0.7 - 0.27) = 0.495$$

Step 4. Consolidation settlement of the pile group:

$$\Delta S_{c(g)} = \frac{C_c * H}{1+e_0} * \log log \left[\frac{\sigma_1^{'}+\Delta\sigma_1^{'}}{\sigma_1^{'}}\right]$$

Where, H is the thickness of the soil layer, i.

$$\Delta S_{c(g)} = \frac{0.495*41.8}{1+0.7} * \log log \left[\frac{143.14+0.506}{143.14}\right] = 18.65\ mm$$

Total consolidation settlement of the pile group is 18.65 mm.


Figure 4.20 Justification of settlement by software

## 4.8 Construction Procedure

According to the necessary size and purpose, a hammer is a piece of machinery used to install driven piles (Office of Research, Development, and Technology, Office of Infrastructure, RDT, 2006). Diesel hammers, hydraulic hammers, vibratory hammers, steam hammers, and drop forging hammers are the five primary types of commercially available hammers (Pile Driving Contractors Association, 2007).

A drop hammer method will be employed to drive the piles during installation. The most common impact driving technique is called a "drop hammer," and it uses a falling weight to produce the impact, which is then spread evenly over the top of the pile by a driving cap. According to "Pile Driving Installation Methods - Steel Piling Group", the hydraulic hammer is the sort of drop hammer that is now used the most. Drop hammers can be divided into two categories:

- Single-acting steam or compressed-air hammers
- Double-acting pile hammers

Sheet piling is the primary use for double-acting pile hammers. An acceptable choice for our precast reinforced concrete piles is a single-acting steam hammer. Huge weights in the form of cylinders are attached to single-acting steam or compressed air systems. The fixed piston rod is raised when steam or compressed air is supplied into the cylinder. The cylinder falls freely onto the pile helmet once the steam is cut off at the top of the stroke or at a lower height that the operator may choose (Mishra, n.d.). Preparing

concrete piles is the first step in the pile drive construction process. Because of uneven prestressing or improper concrete placement during casting, precast concrete piles should be straight and not cambered (Department of the Army Washington, DC, 1985).

The four fundamental procedures for creating and driving piles are as follows:

1. Positioning. With the hammer and cap, the pile driver is set up at the top of the leads (figure 4-7, 1).

2. The pile is often swung into the helmet, the pile line is braided around one-third of the way from the top, and the tip is inserted into the leads (figure 4-7, 2). A member of the handling crew can ascend the leads and use a tugline to assist in positioning the pile in the leads.

3. Centering. The pile cap and hammer are dropped to the top of the pile after being centered beneath the mound. After that, the cap is detachably attached to the hammer (figure 4-7, 3).

4. Driving. To push the pile, the hammer is raised and lowered (figure 4-7, 4). Once the pile is firmly in place, driving should be done gently by raising the hammer only a few inches at a time.The fall's height gradually increases up to a maximum of 6 feet. The punches should be delivered as rapidly as possible to keep the pile moving. In order to prevent the top of the pile from being destroyed, long drops should be avoided (Department of the Army Washington, DC, 1985).

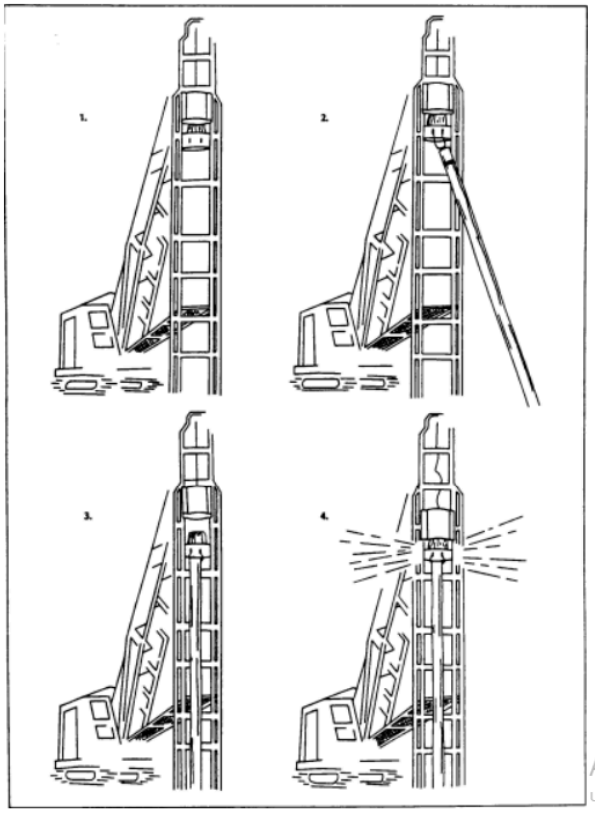

Figure 4-21. Basic steps in installing and driving the piles (Department of the Army Washington, DC, 1985)

### 4.9 Retaining wall design

Retaining walls are solid structures built and intended to hold soil laterally and withstand soil lateral pressure. It reduces the chance of the building collapsing, slippage, and erosion.

Retaining walls need to be built with stability in mind against tipping, sliding, water uplift, and too much foundation strain. They can be divided into two categories: traditional retaining walls and mechanically stabilized retaining walls. The traditional retaining walls, which come in 4 different varieties, were selected for this project. These types include:

- Gravity retaining walls
- Semigravity retaining walls
- Cantilever retaining walls
- Counterfort retaining walls

Among these conventional retaining walls, the most appropriate for the project is a cantilever wall in Figure 4-28 that is made of reinforced concrete. This retaining wall is economical up to 10m in height and acts like a vertical column fixed at the bottom (Das, 2019). Also, it is financially affordable and simple to construct.

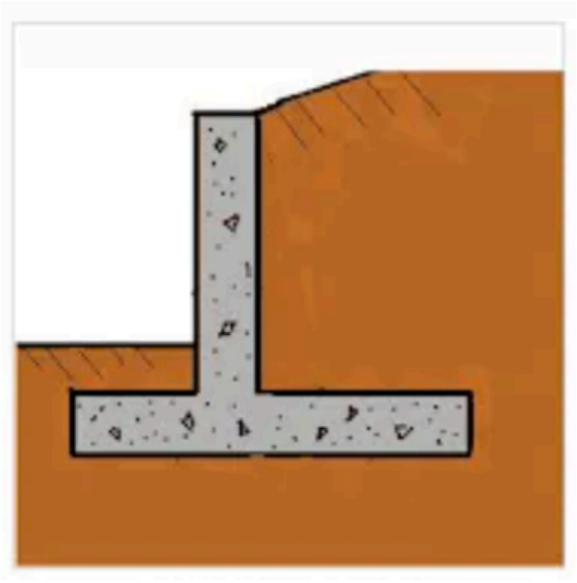

Figure 4-22. Cantilever retaining wall

The retaining wall was designed considering the different dimensions for the following parameters shown in Figure 4-29 and listed in Table 4-11.

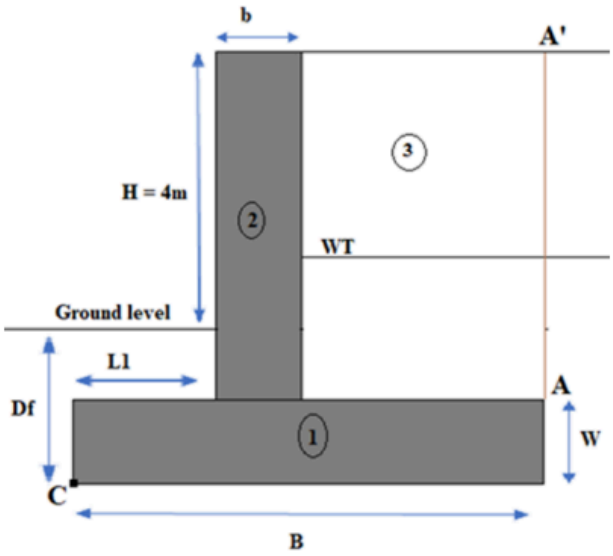


Figure 4-23. Dimensions of retaining wall

where

B - length of the retaining wall base,
L1-distance from the edge of retaining wall base to the slab,
b- width of the slab,
W- width of the retaining wall base.

Table 4-11. Various dimensions of Retaining wall

| Cases | B,m | L1, m | b, m | w, m |
|---|---|---|---|---|
| 1 | 2 | 0,4 | 0,5 | 0,3 |
| 2 | 2,5 | 0,6 | 0,6 | 0,5 |
| 3 | 3 | 0,7 | 0,6 | 0,8 |

For these cases, the stability of the retaining wall checked against overturning, sliding, and bearing capacity failure. The height of the retaining wall is constant for all cases, it is taken as H=4m and length of pile is 16 m, diameter is 0,6 m. The structure is placed 1,5 m below the ground meaning that the retaining wall is at a sand layer level. Thereby input parameters are:

- $\gamma = 19\ kN/M3$ (sand)
- $Df = 1.\ 5m$

- $c'$ = 0 for sand
- $\gamma\ conc$ = 23. 58 $kN/M3$
- $L$ = 16 $m$

### 4.10.1 Stability check against Overturning

To check stability for overturning, it is necessary to estimate the Rankine's active and passive earth pressure using the formula below:

$$P_p = \tfrac{1}{2}K_p\gamma_2 D^2 + 2c_2'\sqrt{K_p}D$$

where

$\gamma_2$ = unit weight of soil in front of the heel and under the base slab
$K_p$ = Rankine passive earth pressure coefficient = $\tan^2(45 + \phi_2'/2)$
$c_2'$, $\phi_2'$ = cohesion and effective soil friction angle, respectively

$$K_p = \tan^2\left(45 + \frac{\phi_2'}{2}\right)$$

$$P_a = \frac{1}{2}K_a\gamma H^2 - 2c'H\sqrt{K_a}$$

$$P_v = P_a \sin\alpha$$

$$P_h = P_a cos\alpha$$

To determine the Factor of Safety against overturning, it used the formula as given:

$$\text{FS}_{(\text{overturning})} = \frac{\Sigma M_R}{\Sigma M_o} \qquad (17.2)$$

where

$\Sigma M_o$ = sum of the moments of forces tending to overturn about point $C$
$\Sigma M_R$ = sum of the moments of forces tending to resist overturning about point $C$

The overturning moment is

$$\Sigma M_o = P_h(\tfrac{H'}{3})$$

Consequently, Factor of Safety against overturning is derived

$$FS_{(overturning)} = \frac{M_1 + M_2 + M_3 + M_4 + M_5 + M_6 + M_v}{P_a \cos\alpha (H'/3)}$$

The following tables prepared for determining the resisting moment and results for each cases were shown

Table 4-12. Calculation of FS against overturning for Case#1.

| Section | Area, m2 | V, (kN/m) | Mc, m | Mr, kN-m/m |
|---|---|---|---|---|
| 1 | 1,85 | 43,623 | 0,55 | 23,99265 |
| 2 | 0,6 | 14,148 | 1 | 14,148 |
| 3 | 4,07 | 77,33 | 1,4 | 108,262 |
| Total | | $\sum V$ =135,101 | | $\sum M_r$ =146,4027 |
| | | | **FS** | **2,905798 > 2** |

Table 4-13. Calculation of FS against overturning for Case#2

| Section | Area, m2 | V, (kN/m) | Mc, m | Mr, kN-m/m |
|---|---|---|---|---|
| 1 | 2,1 | 49,518 | 0,9 | 44,5662 |
| 2 | 1,25 | 29,475 | 1,25 | 36,84375 |
| 3 | 4,55 | 86,45 | 1,85 | 159,9325 |
| Total | = | $\sum V$ =165,443 | | $\sum M_r$ =241,3425 |
| | | | **FS** | **4,790163>2** |

Table 4-14. Calculation of FS against overturning for Case#3

| Section | Area, m2 | V, (kN/m) | Mc, m | Mr, kN-m/m |
|---|---|---|---|---|
| 1 | 1,92 | 45,2736 | 1 | 45,2736 |
| 2 | 2,4 | 56,592 | 1,5 | 84,888 |
| 3 | 8,64 | 164,16 | 2,65 | 435,024 |
| Total | | $\sum V$ =266,0256 | | $\sum M_r$ =565,1856 |
| | | | **FS** | **11,2178>2** |

Summarizing the computations for all 3 cases, it is evident from the above illustrated tables that dimensions of retaining wall are satisfactory as the factor of safety was more than the limit value of 2 set guidelines (Das, 2019).

### 4.10.2 Stability check against Sliding

In the next step, the stability of the retaining wall was checked for sliding along the base. The factor of safety against sliding expressed by the equation:

$$\mathrm{FS}_{(\mathrm{sliding})} = \frac{\Sigma F_{R'}}{\Sigma F_d}$$

where

$\Sigma F_{R'}$ = sum of the horizontal resisting forces

$\Sigma F_d$ = sum of the horizontal driving forces

Deriving this equation, Factor of Safety against sliding will be:

$$\mathrm{FS}_{(\mathrm{sliding})} = \frac{(\Sigma V)\tan(k_1\phi_2') + Bk_2c_2' + P_p}{P_a\cos\alpha}$$

Calculation results according to the formulas are illustrated in the following table:

Table 4-15. Calculation results for checking the sliding

| Case | $\sum V$, (kN/m) | $\sum F_d$, (kN/m) | $\sum F_r$, (kN/m) | **FS** |
|---|---|---|---|---|
| 1 | 135,101 | 37,7872 | 148,0257 | **3,917351>1,5** |
| 2 | 165,443 | 37,7872 | 161,9588 | **4,286075>1,5** |
| 3 | 266,0256 | 37,7872 | 208,1463 | **5,508381>1,5** |

As it is seen from Table 4-15, dimensions of all 3 cases are acceptable because the FS in each case was more than the limit of 1.5.

### 4.10.3 Stability check against Bearing capacity failure

Lastly the retaining wall was checked for stability against Bearing capacity failure. At this point, the base of the retaining wall was assumed to be a strip foundation subjected to a line load that could act eccentrically. Due to the presence of the eccentric line load, the distribution of pressure in soil is varied. So the linearly distribution of pressure under the wall base is expressed as:

$$q = \frac{\Sigma V}{A} + \frac{(\Sigma V)e}{I} y$$

where

$y$ = distance from the center where $q$ is computed ( the sign.

$A$ = base area per unit length = $B$

$I$ = moment of inertia per unit length = $B^3/12$

Using the formulas below,

$$e = \frac{B}{2} - \frac{\Sigma M_R - \Sigma M_o}{\Sigma V}$$

$$q_{\text{toe}} = \frac{\Sigma V}{B}\left(1 + \frac{6e}{B}\right)$$

$$q_u = c_2' N_c F_{cd} F_{ci} + q N_q F_{qd} F_{qi} + \frac{1}{2}\gamma_2 B' N_\gamma F_{\gamma d} F_{\gamma i}$$

It is derived the formula for Factor of Safety against the Bearing capacity failure, as follows:

$$\text{FS}_{(\text{bearing capacity})} = \frac{q_u}{q_{\max}}$$

Applying all the above mentioned formulas, it is determined the FS against bearing capacity failure and the results are shown in Table 4-16. So, as it is seen, the factors of safety of all 3 cases are larger than the limit of 3 (satisfactory). It means in each case the retaining wall is stable against bearing capacity failure

Table 4-16. Calculation results for checking the Bearing capacity failure

| Case | $\sum V$, (kN/m) | $\sum M_r$, kN-m/m | qtoe | qu | **FS** |
|---|---|---|---|---|---|
| 1 | 135,101 | 146,403 | 126,17 | 388,4995 | **3,079117>3** |
| 2 | 165,443 | 241,343 | 81,388 | 421,0556 | **5,17346>3** |
| 3 | 266,0256 | 565,186 | 11,499 | 478,3808 | **41,60188>3** |

In conclusion, from these trial dimension, it was selected the 2nd case with dimensions of:

- B=2,5m
- b=0,6m
- L1=0,6m
- w=0,5m
- H=4m

because it is the most sufficient one, as the FS against overturning, sliding and bearing capacity failure was in adequate range.

## 5. ENVIRONMENTAL DESIGN

1. Introduction

Globally, tourism is considered as an important part of economy and even considered as the main source of income in some countries. Even though there is no doubt about economic benefits of tourism, there are serious effect on environment that are underestimated by tourists. However, the industry should follow environmental and govermental policies in order to preserve a substantial economic activitty. Implementing a wastewater reuse system in hotel buildings has other various advantages such as ecosystem preservation, remaining compliant with the governing laws and policies, and long term financial advantage. Besides these benefits, water shortage issues and lack of proper irrigation system are addressed through implementation of wastewater system.

2. Literature review

2.1 EPA standards for reclaimed water.

There are different types of standards of controlling the amount of chemicals in effluent and reclaimed waters. As an example, Li et al. (2009), did the review for wastewater reuse standards of countries such as Germany, USA, China, Japan and Australia. However, on the other hand, the wastewater reuse standards of countries such as Jordan, Tunisia, USA and Japan were done by Yoonus and Al-Ghamdi (2020). All of the above mentioned standards are almost similar and the restrictions that were presented mostly based on the reuse purposes. These standards mostly focuses on restrictions of biochemical oxygen demand (BOD), Chemical oxygen demand (COD), total suspended solids (TSS), pH, NO3, total nitrogen (TN), turbidity, fecal coliforms and etc. In our case, for the Hotel design, the quality standards of reclaimed water presented by US Environmental Protection Agency (2012) were implemented. To be precise, standards focused on agricultural irrigation and reuse of grey water for urban purposes were used. The treatment regulations and purposes as the requirement of this standard are provided below in the form of Table 5-1.

Table 5-1. The average greywater content in hotels (Kobeyev et al., 2022)

| | High season | Max |
|---|---|---|
| Chemical oxygen demand (COD) [mg/L] | 145.1 ± 88.4 | 535.1 |
| 20-day biochemical oxygen demand ($BOD_{20}$) [mg/L] | 161.9 ± 105.5 | 360 |
| 5-day biochemical oxygen demand ($BOD_5$) [mg/L] | 145.4 ± 70.3 | 295 |
| Total organic carbon (TOC) [mg/L] | 42.2 ± 26.5 | 160.4 |
| Alkalinity [mg/L ($CaCO_3$)]] | 168.6 ± 15.8 | 227.4 |
| Conductivity, µs/cm | 767.4 ± 35.8 | 971.3 |
| pH | 6.9 ± 0.6 | 7.0 |
| Total suspended solids (TSS) [mg/L] | 43.4 ± 32.5 | 195.4 |
| Volatile suspended solids (VSS) [mg/L] | 38.5 ± 10.9 | 149.8 |
| Total nitrogen (TN) [mg/L] | 9.2 ± 4.7 | 25.5 |
| Total Kjeldahl nitrogen (TKN) [mg/L] | 9.2 ± 4.1 | 25.1 |
| $N\text{-}NH_4^+$ [mg/L] | 5.9 ± 3.2 | 14.4 |
| $P\text{-}PO_4^{3-}$ [mg/L] | 0.79.2 ± 4.71.4 | 6.7 |
| Total pathogen count [CFU/100 mL] | $1.5\times10^7$ | $4.1\times10^7$ |
| Total coliform count [CFU/100 mL] | $1.4\times10^6$ | $4.1\times10^6$ |
| E. coli [CFU/100 mL] | 0 | $1.1\times10^6$ |

Since in our project we used reclaimed wastewater from the hotel for restricted and unrestricted use purposes, the standards were used for unrestricted use, as it sets more stringent requirements and treats wastewater to a high level of purity.

Table 5-2. The US EPA standards of reclaimed greywater for restricted and unrestricted reuse.

| Category | Treatment Requirement | Applications after the treatment |
|---|---|---|
| Unrestricted reuse | BOD5: max. 10 mg/l<br>Faecal coliforms: max. 10/ml<br>Turbidity: max. 2 NTU<br>pH: 6-9<br>Residual chlorine: max. 1 mg/l Total | Toilet flushing, landscape irrigation, laundry, fire extinguishing, irrigation of crops, fruits and vegetables, street washing. |

| | | |
|---|---|---|
| | coliforms: max. 100/ml | |
| Restricted reuse | BOD5: max. 30 mg/l Detergent (anionic): max. 1 mg/l Faecal coliforms: max. 10/ml pH: 6-9 Residual chlorine: max. 1 mg/l Total coliforms: max. 100/ml TSS: max. 30 mg/l | Limited irrigation of landscape, subsurface irrigation of nonedible and edible crops, fruits and vegetables. |

## *3. Design of a Greywater treatment system*

There are three main classification of grey water treatment process such as biological, chemical and physical treatment technologies. During all processes, there should be a preatment step which leads to disinfection. According to Yoonus and Al-Ghamdi (2020), physical treatment technologies include primarily those which include adsorption by granular activated carbon, coarse filtration by sands and soils as well as fine filtration by membranes. Generally, this type of treatment clarifies the water from solids and reduces the content of organic pollutants. Three techniques are utilized to do this: Filters are used to separate the particles, contaminants are removed by chemically adhering them to the solid sand particles, and microbial organisms are used to break down the nutrients in grey water. The membrane filtration processes that operate under pressure, such as microfiltration, ultrafiltration, nanofiltration, and Reverse Osmosis (RO), are considered to be the most effective physical treatment procedures for grey water. Physical treatment techniques must be combined with other suitable technologies to successfully remove surfactants, organic debris, and nutrients from grey water. Chemical treatment, which includes a number of processes like coagulation, flocculation, photocatalytic oxidation, ion exchange, and others, is another choice for recycling grey water. The technologies that fall under the category of biological treatment are the most efficient for treating medium to high strength grey water. The Yoonus and Al-Ghamdi (2020) report mentions a number of technologies that fall under this category, including sequencing batch reactors (SBR), membrane bioreactors (MBR), rotating biological reactors (RBC), up-flow anaerobic sludge blanket (UASB), continuous flow sequencing reactors (CFSR), and others. These technologies' employment of microbes to remove organic debris is their defining feature. Grey water treatment generally benefits from the improved performance of biological treatment systems. GPS-X, created by Hydromantis Inc. (2021), the most cutting-edge and highly regarded software for designing, modeling, and optimizing wastewater treatment plants, was used to design the grey water treatment

plants. The layout of each plant and the selection of the most significant and delicate design criteria were typically required during the design phase for grey water treatment systems. With the least amount of money and area needed, good effluent quality was the goal of optimizing these characteristics (Figure 3-2). Coagulation and flocculation occur when water enters the grey water treatment system through an influent pipe. Coagulation and flocculation are accomplished using alum (Al(SO4)212H2O) and PACl solution (PAC-Al2(OH)nCl(6-n)), respectively. During these phases, colloidal particles and suspended solids agglomerate by attaching to one another and disperse. Following passage through the primary clarifier, the water enters an MBR tank with four connected reactors in sequence, where it is disinfected with chlorine before leaving the system through the effluent pipe. The flow of sludge also has a secondary cycle. The sludge goes through three different processes: a thickener to remove extra water, a digester to convert organic matter into carbon dioxide and methane gases, and a dewatering tank to solidify the slurry sludge by removing liquid. The water that is extracted from the sludge during this process is fed back into the main grey water treatment cycle, while the finished sludge that has gone through the thickener, digester, and dewatering tank is transported in a particular way to a sludge gallery for disposal.

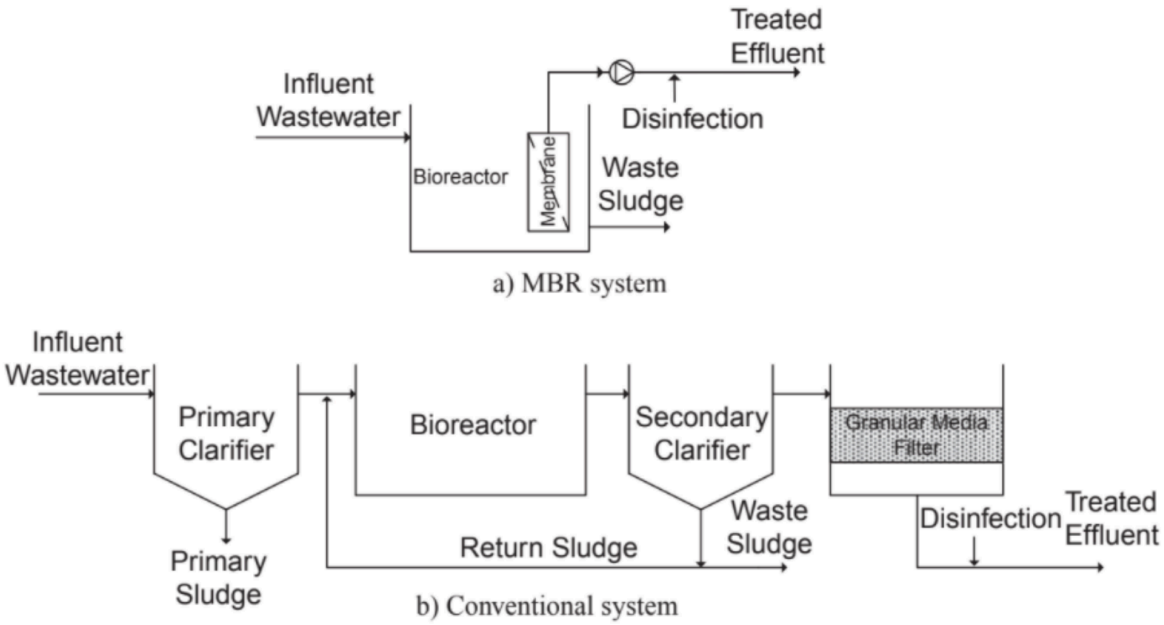


*Figure 5-1.* (a) MBR system and (b) Conventional activated sludge system (CAS)

The amount of hazardous content in an effluent has to be reduced to allowable limits to meet the water quality standards set by the U.S. Environmental Protection Agency (2012). A greywater treatment system has been designed to meet the requirements. Treatment steps consist of pre-treatment, aeration, membrane bioreactor, and disinfection by chlorination. All the steps are illustrated in Figure 5-2.

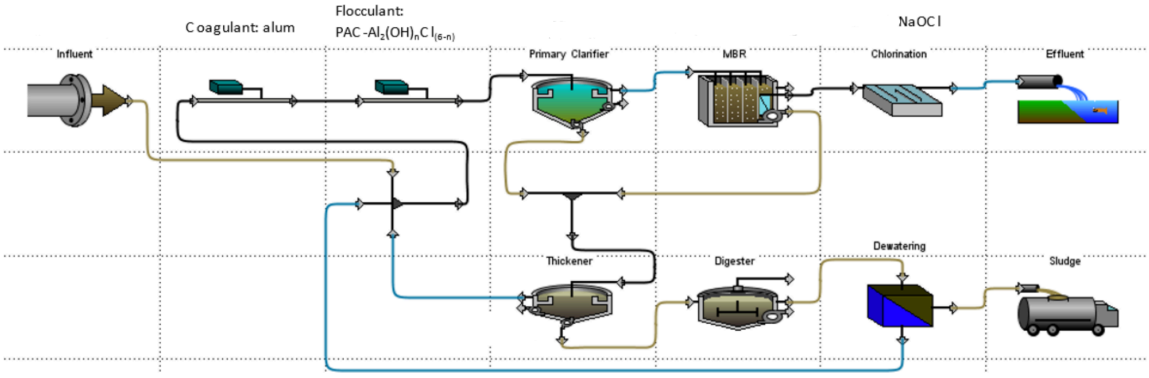


Figure 5-2. MBR plant layout modeled in th GPS-X software.

In the Table 5-3 below, there are initial greywater parameters and the parameters of the treated effluent.

**Table 5-3**. Greywater influent-effluent content before and after treatment (Kobeyev et al., 2022)

| | Before | After |
|---|---|---|
| $BOD_5$ [mg/L] | 295 | 4.77 |
| pH | 7.0 | 7.0 |
| TSS [mg/L] | 195.4 | 7.37 |
| Residual chloride [mg/L] | – | 0.956 |
| Total coliform [CFU/100 mL] | $4.1 \times 10^6$ | 9.061 |
| Total COD [mg/L] | 535.1 | 39.1 |
| Alkalinity [mg/L ($CaCO_3$)] | 227.4 | 14.73 |
| VSS/TSS | 0.767 | 0.775 |
| TKN [mg/L] | 25.1 | 5.58 |
| $N\text{-}NH_4^+$ [mg/L] | 14.4 | 3.29 |
| $P\text{-}PO_4^{3-}$ [mg/L] | 6.7 | 1.82 |

4. Design parameters

4.1 Volume of greywater generated in a month

All the average water demand values for different purposes are taken from Water Usage at St. Regis Resort Hotel:

Number of residents 340

Number of staff 20

**Total number of people = 360**

**Mid market hotel water consumption = 100 gal/day/room**

Number of people per room = 1.5

Demand per capita = 100 / 1.5 = 66.7 gal/capita/day

Flushing water per capita = 1.6 gal/flush x 4.8 flush/capita/day = 7.7 gal/capita/day

Average drinking water consumption = 0.5 gal/capita/day

Greywater generation per capita = 66.7 - 7.7 - 0.5 = 58.5 gal/capita/day

Greywater generated in one day = 58.5 gal/capita/day x 360 residents= 21 060 gal/day

Demand for flushing water per one day = 7.7 gal/capita/day x 360 residents = 2 772 gal/day

Irrigation demand = 0.5 acre x 43 600 sq ft/acre x 325 900 gal/acre = 7.1 x 10^9 gal

Greywater generated in one day fully covers toilet flushing demand. The remaining treated water can be used for territory irrigation purpose.

4.2 Screens

A pre-treatment step (screening) is required to remove coarse and fine solid particles from greywater in order to not damage treatment equipments following this step. Greywater goes through one channel of a dual channel with the same set of screens on each channel. A dual channel is required for the purpose of redundancy. Each channel consists of two screens: a coarse screen with openings of 20 mm and a fine screen with openings of 4 mm.

Approach velocity of water = 0.7 m/s

Screens are cleaned by a reciprocating rake. It is convenient in terms of maintenance since the moving parts of a reciprocating rake are not submerged into water. Another advantage is that it has low operating and maintenance costs.

4.3 Coagulation

Coagulation is necessary to gather suspended solids in water to form flocs. The design parameters for coagulation basin are as follows:

Mechanism of coagulation: sweep coagulation

Basin type: Continuous-flow Stirred Tank Reactor (CSTR)

Detention time: 7 s

G: 600 $s^{-1}$

Equivalent tank diameter: 16 cm

Water depth: 32 cm

Impeller type: Radial flow impeller

Impeller diameter: 5 cm

Water depth below impeller: 10 cm

Rotational power speed: 115 rpm

Motor power: 5 W

4.4 Flocculation

Flocculation is required to let the forming flocs of suspended solids to settle down. The design parameters for flocculation basin are given below:

Basin type: Rectangular tank with three compartments

Detention time: 30 min

G: 70 $s^{-1}$, 50 $s^{-1}$, $30^{-1}$

Water depth: 3 m

Volume of the basin: 0.9 $m^3$

Volume of each compartment: 0.3 $m^3$

Length and width of the compartment: 0.32 m

Water depth below impeller: 1 m

Impeller diameter: 0.1 m

Motor power: 5 W

Tip speed: 3 m/s

4.5 Settling tank

Settling is necessary to remove BOD5, suspended solids, and scum that are gathered in forms of flocs in the previous steps.

Sedimentation type: Type II

Basin type: Circular tank

Area: 3 $m^2$

Diameter: 2 m

Height including freeboard: 2.1 m

Detention time: 120 min

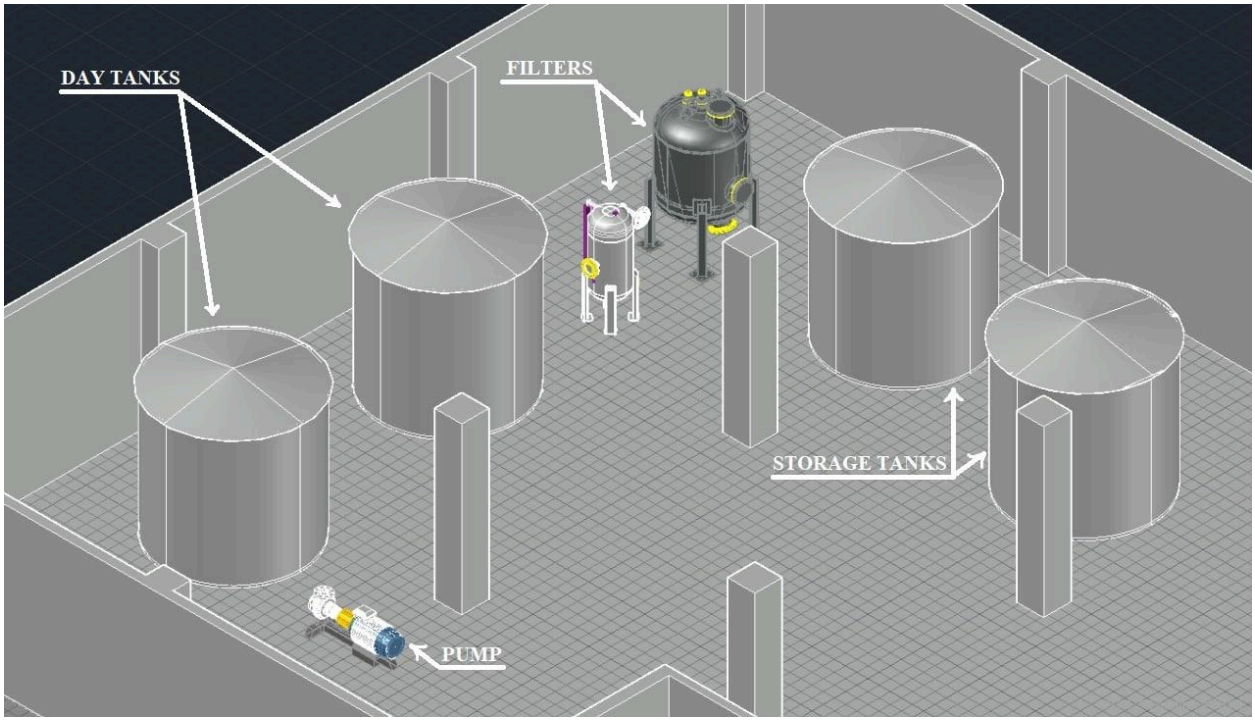


Figure 5-2. Design of storage tanks in the basement.

For redundancy purposes, each step of the system will have 2 identical elements. There will be two storage tanks for influent and two storage tanks for effluent use, presented in Figure 5-2 and Figure 5-3 . All the tanks and the filtration system will be located in the basement of the hotel since there is enough space. The outdoors of the hotel will not be occupied by the system, and the exterior aesthetics of the hotel will not be spoiled.

Figure 5-3. Side view of the system.

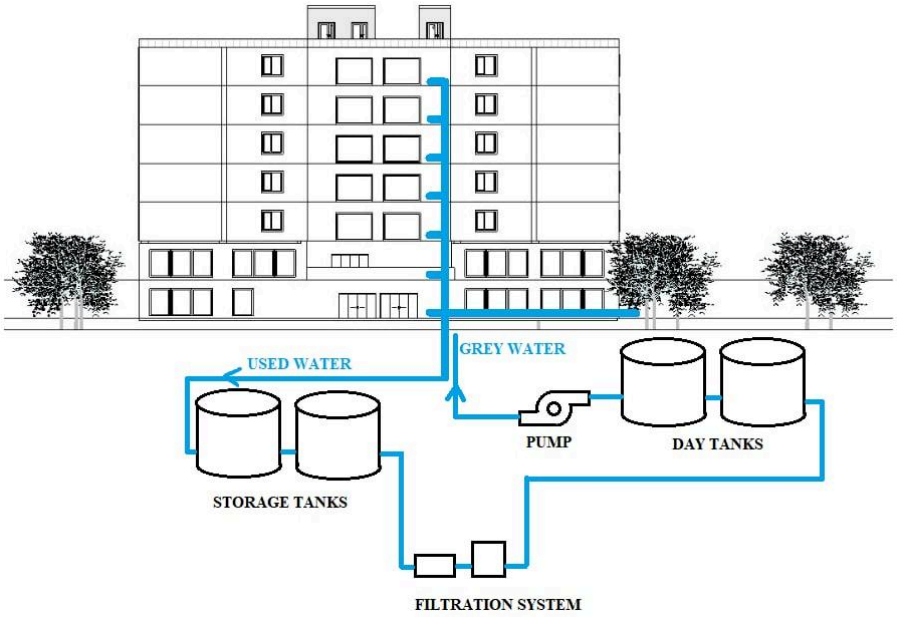


## 6. CONSTRUCTION MANAGEMENT DESIGN

Construction management is one of the most important processes of every building, because it calculates the cost of the project, arranges the scheduling of the building, makes all required assessments to ensure the safety of the building and makes planning processes. In addition to that, construction management helps to evaluate the profitability of the project, estimating all the equipment costs, operational costs, construction costs and make cost/benefit analysis.

Main objective of the construction management area are:

1. Project charter
2. Feasibility study
3. Cost/benefit analysis
4. Work breakdown structure
5. Scheduling
6. Risk management
7. Quality management

8. Procedure planning
9. Construction site planning

### 6.1 Project charter

Project charter is a construction management document that outlines the start and the end of the project, project scope, risks, assumptions, and stakeholders of the project.

<table>
<tr><td colspan="6">Project Charter</td></tr>
<tr><td>Project Title</td><td colspan="3">Design of Multi-story hotel in Carlsbad</td><td>Project Manager</td><td>Alikhan Serikbekov</td></tr>
<tr><td>Project start date</td><td>June 2023</td><td>Project end date</td><td>Feb 2025</td><td>Project sponsor</td><td>Nazarbayev University</td></tr>
<tr><td colspan="6">Business need</td></tr>
<tr><td colspan="6">a seven-story hotel in Carlsbad, California, that complies with building, safety, and sustainability standards while taking into account the area's moderate seismic activity</td></tr>
<tr><td colspan="3">Project scope</td><td colspan="3">Deliverables</td></tr>
<tr><td colspan="3">a rectangle building space of 40.4x20.4 m2 and 80 rooms, with restaurants, shops and gym.</td><td colspan="3">Seven-story hotel with 80 rooms, parking area, commercial areas</td></tr>
<tr><td colspan="3">Risks and issues</td><td colspan="3">Assumptions</td></tr>
<tr><td colspan="3">• Seismic zone<br>• Poor geological conditions because of its located near seashore<br>• Financial risks due to unexpected expenses<br>• Due to rise in price, cost of materials in the future may change</td><td colspan="3">• Project budget estimated by using average cost of materials<br>• Material sizes were chosen by iteration method till first best fit<br>• Time for the entire project was correlated estimating the time for each part of construction<br>• Other unseen circumstances were ignored</td></tr>
<tr><td colspan="6">Financials</td></tr>
<tr><td colspan="6">$70,758,002</td></tr>
</table>

<table>
<tr><td colspan="4">Milestone schedule</td></tr>
<tr><td colspan="2">Project construction milestone</td><td colspan="2">Target completion date</td></tr>
<tr><td colspan="2">Permission for the project</td><td colspan="2">July 2023</td></tr>
<tr><td colspan="2">Complete basement</td><td colspan="2">Mar 2024</td></tr>
<tr><td colspan="2">Complete structural system of the building</td><td colspan="2">Oct 2024</td></tr>
<tr><td colspan="2">Facade works</td><td colspan="2">Jun 2024</td></tr>
<tr><td colspan="2">Complete of the project</td><td colspan="2">Feb 2025</td></tr>
<tr><td colspan="2">Project team</td><td colspan="2">Approval/Review Committee</td></tr>
<tr><td>Project manager</td><td>Alikhan Serikbekov</td><td>Sponsor</td><td>Nazarbayev University</td></tr>
<tr><td rowspan="3">Team members</td><td rowspan="3">Zhaksylyk Olzhabekov<br>Darkhan Serikbay<br>Aruzhan Sibekova<br>Aidos Bolat<br>Damir Kiyashov<br>Diara Gazezova</td><td>Business Division Head</td><td>-</td></tr>
<tr><td>Business Unit Head</td><td>-</td></tr>
<tr><td>Finance Manager</td><td>-</td></tr>
</table>

Table 6-1. Project Charter

**6.2 Work Breakdown Structure**

Work Breakdown Structure is a construction management tool that focuses on decomposition of the project into small manageable parts. Multi-story hotel construction process can be divided into milestones given in Graph 6-2. Some of those sub-tasks also

divided into smaller tasks to ease the tracking of work that was done.

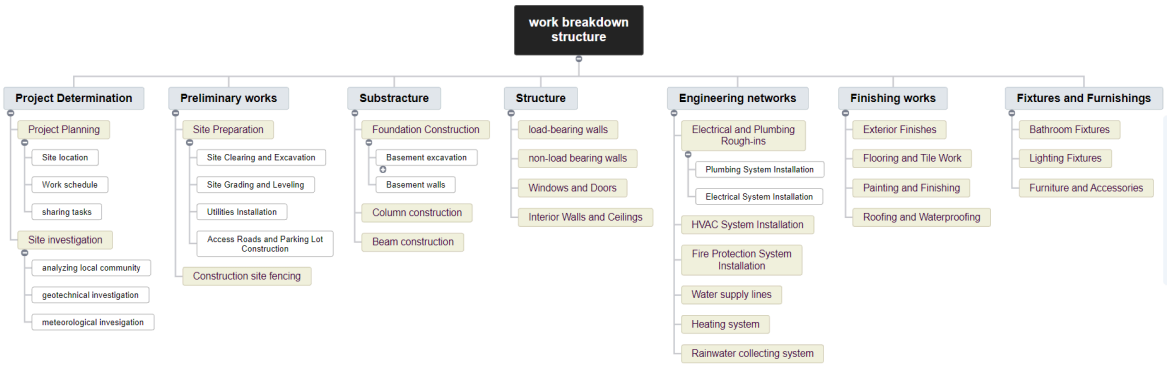


Graph 6-2. Work breakdown structure using PMBOK

### 6.3 Scheduling of the project

To make a professional plan, also known as gantt chart, for the project was conducted in computer-based engineering tool Primavera P6, which allows to create detailed gantt chart with all necessary parameters. As mentioned before, Primavera p6 is a very powerful project management software that is used by advanced users in top industries because of its features and benefits. It can help with organization of the project and decrease risks of losing data. Graph 6-3 contains the results retrieved from Primavera software.

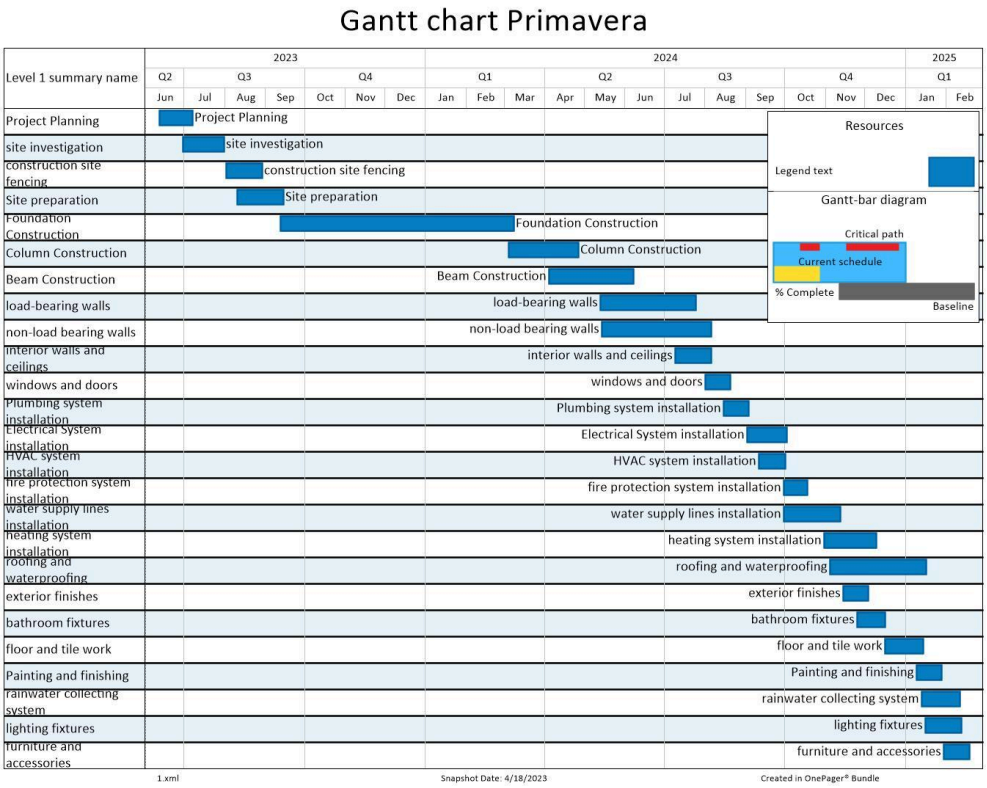


Graph 6-3. Scheduling of the project in Primavera P6

## 6.4 Cost estimation

Total cost estimation of the building was calculated using online tool RSMeans. For the year 2011, average cost per square foot for a seven-story building in the San Francisco region was $311.63. Total residential (floor) area was set to 140,000 square feet and story height to 10.82 ft (~3.3 m). Using all these values we estimated the cost of the building as $43,628,668. However this value is not working for the year 2022 because the average cost per square foot for a seven-story building in San Francisco changed significantly.

| | | | Quantity | % of Tota l | Cost per s.f. | Cost |
|---|---|---|---|---|---|---|
| **A** | | **Substructure** | | **2.25 %** | **$5.30** | **$741,766.70** |

| | | | | | | |
|---|---|---|---|---|---|---|
| B | | Shell | | 18.19 % | $42.79 | $5,989,991.46 |
| C | | Interiors | | 16.62 % | $39.09 | $5,473,024.07 |
| D | | Services | | 34.29 % | $80.66 | $11,292,346.28 |
| E | | Equipment & Furnishings | | 28.64 % | $67.36 | $9,430,168.10 |
| F | | Special Construction | | 0% | | |
| G | | Building Sitework | | 0% | | |
| | | SubTotal | | 100 % | $235.19 | $32,927,296.61 |
| | | Contractor Fees (GC,Overhead, Profit) | | 25.00 % | $58.80 | $8,231,824.15 |
| | | Architectural Fees | | 6.00 % | $17.64 | $2,469,547.25 |
| | | Total Building Cost | | | $311.63 | $43,628,668.01 |

Table 6-4a. Initial cost estimation using RSMeans website

To define real value for the year 2022, differences between the cost indices have to be investigated. Factors that are affecting the cost indices are labor rates and productivity, material prices and conditions in the marketplace (BCI, 2022). So the difference in cost indices between the years 2011 and 4th quarter of 2022 had shown 164% increase. Thus, the total cost of the building was raised to $70,758,002.

| | Quantity | % of Total | Cost per s.f. | Cost |
|---|---|---|---|---|
| SubTotal | | 100% | $385.80 | $54,013,742.71 |
| Contractor Fees (GC,Overhead,Profit) | | 25.00% | $96.46 | $13,503,435.68 |
| Architectural Fees | | 6.00% | $28.94 | $3,240,824.56 |
| User Fees | | 0.00% | $0.00 | $0.00 |
| Total Building Cost | | | $511.20 | $70,758,002.96 |

Table 6-4b. Correlated cost estimation for the year 2022

### 6.5 Profitability analysis

To analyze the payback period we assumed multiple things in our business. Firstly, occupancy of the hotel is assumed to be 70% all the time, because that is the average occupancy rate in California hotels. Price per person was also calculated analyzing the average prices for similar hotels nearby Los Angeles. To estimate the salary, we assumed to hire two housekeepers working 10 hours per day with hourly wage of $15, and two people as a receptionist working 12 hours per day each with hourly wage of $17. Carlsbad's Transient Occupancy Tax amount is 10% and an additional 2% from gross revenue is added to that, so we end up with 12% taxes in total. With all these assumptions, the payback period of the hotel is estimated to be 20 years. However as time goes those numbers would also change, thus more investigations on profitability will be needed in the future.

| | # of clients | occupancy | Ave Yearly Rate | Price per person | Revenue total | Salary | TOT+tax | Net profit | Cumulative profit |
|---|---|---|---|---|---|---|---|---|---|
| year 1 | 340 | 70.00% | 86870 | 110 | 9555700 | 7235760 | 12.00% | 1173256 | 1173256 |
| year 2 | 340 | 70.00% | 86870 | 110 | 9555700 | 7235760 | 12.00% | 1173256 | 2346512 |
| year 3 | 340 | 70.00% | 86870 | 120 | 10424400 | 7235760 | 12.00% | 1937712 | 4284224 |
| year 4 | 340 | 70.00% | 86870 | 120 | 10424400 | 7235760 | 12.00% | 1937712 | 6221936 |
| year 5 | 340 | 70.00% | 86870 | 130 | 11293100 | 7235760 | 12.00% | 2702168 | 8924104 |
| year 6 | 340 | 70.00% | 86870 | 130 | 11293100 | 7235760 | 12.00% | 2702168 | 11626272 |
| year 7 | 340 | 70.00% | 86870 | 140 | 12161800 | 7235760 | 12.00% | 3466624 | 15092896 |
| year 8 | 340 | 70.00% | 86870 | 150 | 13030500 | 7235760 | 12.00% | 4231080 | 19323976 |
| year 9 | 340 | 70.00% | 86870 | 150 | 13030500 | 7235760 | 12.00% | 4231080 | 23555056 |
| year 10 | 340 | 70.00% | 86870 | 150 | 13030500 | 7235760 | 12.00% | 4231080 | 27786136 |
| year 11 | 340 | 70.00% | 86870 | 150 | 13030500 | 7235760 | 12.00% | 4231080 | 32017216 |
| year 12 | 340 | 70.00% | 86870 | 150 | 13030500 | 7235760 | 12.00% | 4231080 | 36248296 |
| year 13 | 340 | 70.00% | 86870 | 150 | 13030500 | 7235760 | 12.00% | 4231080 | 40479376 |
| year 14 | 340 | 70.00% | 86870 | 150 | 13030500 | 7235760 | 12.00% | 4231080 | 44710456 |

| | | | | | | | | | |
|---|---|---|---|---|---|---|---|---|---|
| year 15 | 340 | 70.00% | 86870 | 150 | 13030500 | 7235760 | 12.00% | 4231080 | 48941536 |
| year 16 | 340 | 70.00% | 86870 | 150 | 13030500 | 7235760 | 12.00% | 4231080 | 53172616 |
| year 17 | 340 | 70.00% | 86870 | 150 | 13030500 | 7235760 | 12.00% | 4231080 | 57403696 |
| year 18 | 340 | 70.00% | 86870 | 150 | 13030500 | 7235760 | 12.00% | 4231080 | 61634776 |
| year 19 | 340 | 70.00% | 86870 | 150 | 13030500 | 7235760 | 12.00% | 4231080 | 65865856 |
| year 20 | 340 | 70.00% | 86870 | 150 | 13030500 | 7235760 | 12.00% | 4231080 | 70096936 |

Table 6-5. Profitability table

## 6.6 Risk management

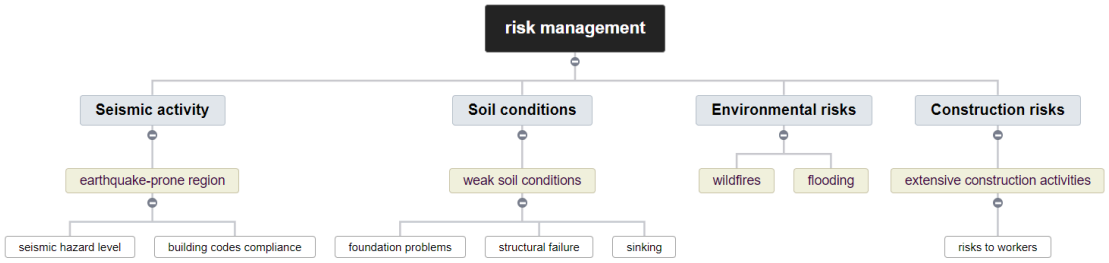


## 6.7 Construction site planning

Construction site planning is another important procedure to do while constructing a building. It allows effective use of the territory, design logical connections between buildings and gives overall visualization of the site. All the minor things like fences, trees, storage rooms and decorational elements should be presented in the construction site plan. Graph 6-10 represents the construction plan for this project.

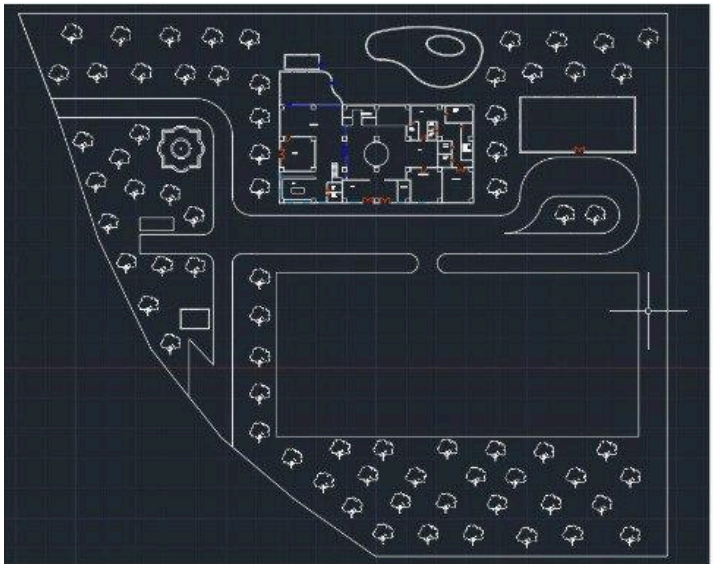

Graph 6-10. Construction site planning

## CONCLUSION

In summary, Capstone II developed the architectural and structural design of the structure after calculating the dead load, living load, snow load, and wind load. During the Capstone project we calculated lateral drifts and designed structural frames with the use of SAP2000 software. Moreover, joint design for structures was done to make the building more resistant to seismic drifts.

The soil profile and characteristics were examined for the geotechnical component. Analysis of foundation types, bearing capacity, and settling were all part of the foundation design process. Lateral bearing capacity and justifications with a software were computed for Capstone II, and a retaining wall was built.

The reuse of a grey water system collecting the water from kitchen, bathrooms, etc. without toilet flushing and drinking water, was designed in the project. In Capstone I the system preliminary design with description of whole processes and components were performed. To be precise, average daily use of greywater and holding tank sizes were calculated, and also locations of tanks and other system components were defined. The Capstone II covered cost analysis, the detailed design of the reactor and other crucial components of the system will be done.

Every business structure must first pay back its investment and benefit its managers. To specify the cost and timeplan for this project, the construction management part introduced several procedures that calculates all the benefits and expenses of this project, made a detailed schedule with manageable sub-parts, and conducted risk and quality management.

## REFERENCES


ACI Committee 318. (2014). *Building code requirements for structural concrete : (ACI 318-14)*. Farmington Hills, MI :American Concrete Institute.

American Concrete Institute. (2002). *ACI 352R-02: Recommendations for design of slab-column connections in monolithic reinforced concrete structures*. Farmington Hills, MI: American Concrete Institute

ASCE/SEI 7-10. *Minimum Design Loads for Buildings and Other Structures*. ASCE, 2010. ISBN: 978-0-7844-1085-1.

International Code Council. (2009). *International building code 2009*. ISBN: 978-1-58001-725-1.

Broms, B. B. (1964) : "Lateral resistance of piles in cohesive soils," Proc. ASCE, Vol. 90, No. SM 2, pp. 27-63.

Das, B.M. and N Sivakugan (2019). *Principles of foundation engineering*. Boston, Ma: Cengage Learning.

Fellenius B.H. 199. Piled Foundations. In Fang, H.-. Y (Ed), Foundation Engineering Design (pp. 511-535). Retrieved from https://www.fellenius.net/papers/133%20Foundation%20Engineering%20Handbook%20Chapter%2013.pdf

Nishida, Y. (1956). A Brief Note on the Compression Index of Soil. *Journal of the Soil Mechanics and Foundations Division*, 82(3).

Paikowsky, S. (2004). *Load and Resistance Factor Design (LRFD) for Deep Foundations*. Washington, D.C: TRANSPORTATION RESEARCH BOARD.

Braja M. (2019) *Principles of Foundation Engineering.* NY. Boston. USA: Cengage Inc.

Huang, Y., & Yu, M. (2013). Review of soil liquefaction characteristics during major earthquakes of the twenty-first century. *Natural hazards*, *65*(3), 2375-2384.

Li, F., Wichmann, K. and Otterpohl, R. (2009), “Review of the technological approaches for grey water treatment and reuses”, Science of The Total Environment, Vol. 407 No. 11, pp. 3439-3449, doi: 10. 1016/j.scitotenv.2009.02.004.

Duman, E. S., Ikizler, S. B., & Angin, Z. E. K. A. İ. (2015). Evaluation of soil liquefaction potential index based on SPT data in the Erzincan, Eastern Turkey. *Arabian Journal of Geosciences*, *8*(7), 5269-5283.

Robertson, P. K., Sego, D. C., Chan, D., Morgenstren, N. R., Fear, C. E., Hoffman, B., ... & List, B. R. (1996). CANLEX Phase III full scale flow liquefaction test: planning, objectives and conclusions.

Building Cost Index (BCI) (2022). Retrieved from https://www.turnerconstruction.com/cost-index.

Idriss, I. M., & Boulanger, R. W. (2010). SPT-based liquefaction triggering procedures. *Rep. UCD/CGM-10*, *2*, 4-13.

Kobeyev et al., 2022. *The hotel construction and reuse of greywater.* Environmental Engineering.

US Environmental Protection Agency (2012), "2012 guidelines for water reuse", in Nancy, S., Eric, P. and Lek, K. (Eds), 2nd ed., US Agency for International Development, Washington, DC, available at: https://www.epa.gov/sites/production/files/2019-08/documents/2012-guidelines-water-reuse.pdf.

Yoonus, H. and Al-Ghamdi, S.G. (2020), "Environmental performance of building integrated grey water reuse systems based on life-cycle assessment: a systematic and bibliographic analysis", Science of The Total Environment, Vol. 712, April, p. 136535, doi: 10.1016/j.scitotenv.2020.136535.

*LEED certification for new buildings | U.S. Green Building Council*. (n.d.). https://www.usgbc.org/leed/rating-systems/new-buildings#:~:text=LEED%20for%20Building%20Design%20and%20Construction%20(LEED%20BD%2BC),sustainability%20feature%2C%20maximizing%20the%20benefits.